UNIVERSITY OF CALIFORNIA, SAN DIEGO

Marine megafauna in environmental extremes: distribution and oceanic dispersal of polar and tropical tetrapods

A dissertation submitted in partial satisfaction of the requirements for the degree Doctor of Philosophy

in

Oceanography

by

Geoffrey Gearheart

Committee in charge:

Gerald L. Kooyman, Chair
Jay Barlow
Neal W. Driscoll
Peter H. Dutton
Jonathan B. Shurin
Janet Sprintall

2014

The Dissertation of Geoffrey Gearheart is approved, and it is acceptable in quality and form for publication on microfilm:

_____

_____

_____

_____

_____

_____

Chair

University of California, San Diego

2014

I dedicate my thesis to
Hester, my mother and patron of the Arts & Sciences;
to Liz, Ella Soleil, Maia and Liza: daily sunshine; and
to Jerry, Alfred Russel, and Jacques-Yves: true explorers.
And nothing could have happened without the fateful participation of Mother Nature,
steadfast provider of wondrous subject materials

“Mais qu’importe l’éternité de la damnation à qui a trouvé dans une seconde l’infini de la jouissance?”

Baudelaire – Le Spleen de Paris

Table of Contents

List of Figures

List of Tables

ACKNOWLEDGEMENTS

When I was a little boy, Hester and Phil, my parents, planted in me the seed of Nature. I grew up in a watermill in the French countryside and, starting in the late 70's, we'd migrate to Indonesia on a yearly basis. My father took me snorkeling in the Java Sea and I discovered the magic of coral reefs. Stories about my ancestors, who were geneticists, botanists and chemists during the early and mid-twentieth century, strengthened my resolve to pursue a career in science. Happily I did not follow the advice of certain "third parties": at my French high school, the "orientation specialist" asked me about my career choices. I wanted to become an ecologist. She looked puzzled, then said she doubted there was any future in studying the "école" ("school" in French)! Back in the intellectual safety of my home I could count on the support and enthusiasm of my family, as well as on a weekly episode of the Commandant Cousteau. Recently, at a low point in my studies, I ran into a "funding crisis": I couldn't go to Indonesia to finish my fieldwork. Hester bailed me out, no questions asked… Without my loyal patron of the "Arts and Sciences" I would not be writing these lines.

Jerry Kooyman is an important person in this story. He too believed in me, providing all the space and flexibility I needed. Saying that he is an inspiration is an understatement. Upon landing at the tiny Island of Piai, after having spent 10 harrowing hours on a Papuan dugout canoe squeezed in between leaky 55-gallon drums of gasoline (and a chain-smoking boat driver), I asked him: "what do you think of this place, Jerry"? "What do you mean?" came his reply, "Fantastic!!"… and off he went with his camera to shoot birds. Later, being able to go to Antarctica with him and share thoughts on the land and the animals he so cherishes was a real privilege. I have always admired his modesty and open-mindedness. When you are really that good, you just let your science (and your surfing, and your flying) talk for you.

Prior to coming to Scripps, I was working for Mark V. Erdmann in Indonesia. Mark is not a “tame” biologist: his relentless passion for nature, an unmatched knowledge of Papua’s coral reefs and his willingness to take considerable risk (to health and career) to protect what he loves, make him one of the finest marine conservationists in the world. He inspired me greatly and helped me get started in Papua. Later, he provided the funding needed for my enrollment in the PhD program.

I am indebted to Janet Sprintall, a great lady who epitomizes how, in my eyes, a scientist should be: without prejudices and without borders, rigorous and honest. Thank you so much for your coaching and your friendship, Janet!

I’d like to thank Jay Barlow, Jonathan Shurin and Peter Dutton, for giving me lots of their time and for sharing their expertise. I hope some of it rubbed off on me.

Arnould Lefébure, free-diver extraordinaire, showed me you don’t need complicated contraptions to discover the underwater world: a major contribution.

Paul Barber (UCLA) and Satoshi Mitarai (OIST), thank you so much for entrusting me with your precious Lagrangian drifters!

Josh Reeves, Becky Burrola, Gayle Arruta, Gilbert Bretado, Adam Petersen and Denise Darling (SIO graduate office) have helped me navigate bureaucratic meanders since my arrival in 2008. Thanks a lot for your generosity! Neal Driscoll (GRD) has provided funding in 2011.

I am very grateful to the generous donors of the Stout foundation and to Cheryl Peach and Hubert Staudigel, from the NSF-GK12 program.

Ron Burton and Doug Bartlett (MBRD) helped me obtain department funding for my fieldwork.

Judy Bird, my special editor-in-chief, has greatly contributed to the improvement of my manuscripts! Thank you, Ibu burung!

My many friends and colleagues have been involved to varying degrees in this

academic (ad)venture. In decreasing order of involvement I want to mention: Dian Putrasahan (terima kasih banyak buat masakanmu yg enak sekali, dan buat bantuanmu!), Martin Gassmann, Deasy Lontoh, Kim Goetz, Birgitte McDonald, Mike Tift and Alexandra Wright (Ponganis Lab), Juan Ugalde, Valerie Sahakian (my roommates) and Jorge & Paula Montesinos Saravia (¡qué ricos sus asados domingueros!).

On the other side of the Pacific, Ricardo Tapilatu and all my friends from UNIPA have provided essential administrative, logistical and existential help. None of this could have happened without you.

Finally, I could not have pulled this off without the constant, day-to-day support of my partner Liz Johnstone. She knows how grateful I am, but I wanted to put it on paper too. This last paragraph should be in giant fonts, but it wouldn't pass OGS censorship.

MATERIAL PUBLISHED/SUBMITTED FOR PUBLICATION IN THE DISSERTATION

Chapter 2, in full, was published as:

Gearheart, G. Maturbongs, A., Dutton, P.H., Sprintall, J., Kooyman, G.L., Tapilatu, R.F. and Johnstone, E. (2011). Tracking leatherback (*Dermochelys coriacea*) hatchlings at sea using radio and acoustic tags. *Marine Turtle Newsletter* 130, 2-6.

The dissertation author was the primary investigator and author of this paper.

Chapter 4, in full, was published as:

Gearheart, G., Kooyman, G.L., Goetz, K.T. and McDonald, B.I. (2014). Migration front of post-moult emperor penguins. *Polar Biology* 1-5.

The dissertation author was the primary investigator and author of this paper.

Chapter 5, in full, has been submitted for publication as:

Gearheart, G., Kooyman, G.L., Goetz, K.T. and McDonald, B.I. (2014). Autumn distribution of seabirds, seals and whales in the Ross Sea, Antarctica: the “St. Tropez” effect. Submitted to: *PlosONE*

The dissertation author was the primary investigator and author of this paper.

CURRICULUM VITAE

Education

1999	Bachelor of Science Marine Biology Universidad Nacional Autónoma, Costa Rica
1999	Bachelor of Science Tropical Forestry and Nature Management Larenstein International Agricultural College, The Netherlands
2002	Master of Science Tropical Biology Universidad de Puerto Rico-Río Piedras, PR, USA
2014	Doctor of Philosophy Oceanography Scripps Institution Of Oceanography University of California, San Diego, CA, USA

Publications

Gearheart, G., Kooyman, G.L., Goetz, K.T. and McDonald, B.I. (2014). Migration front of emperor penguins. *Polar Biology* 1-5.

Gearheart, G., Maturbongs, A., Dutton, P.H., Sprintall, J., Kooyman, G.L., Tapilatu, R.F. and Johnstone, E. (2011). Tracking leatherback (*Dermochelys coriacea*) hatchlings at sea using radio and acoustic tags. *Marine Turtle Newsletter* 130, 2-6.

Adnyana, W. Soede, L.P., Gearheart, G., and Halim, M. (2008). Status of green turtle (*Chelonia mydas*) nesting and foraging populations of Berau, East Kalimantan, Indonesia. *Indian Ocean Turtle Newsletter*. 7:2-11.

ABSTRACT OF THE DISSERTATION

Marine megafauna in environmental extremes:
distribution and oceanic dispersal of polar and tropical tetrapods
by
Geoffrey Gearheart
Doctor of Philosophy in Oceanography
University of California San Diego, 2014
Gerald L. Kooyman, Chair

Early autumn visual surveys carried out in the Ross Sea in February-March 2013 reveal Emperor penguins congregate and feed in migratory "hubs" located in stable pack ice of the eastern Ross Sea, close to the Antarctic Slope Front. From there, based on their annual cycle, they travel to the marginal ice zone, or the eastern and western Ross Sea colonies. We hypothesize that Adélie penguins migrate with the expanding pack ice from breeding colonies in the western Ross Sea to lower latitudes with sufficient light to forage. This movement appears synchronous, as evidenced by the gradual increase in the relative abundance of this species along our survey transect, and the large concentration of birds in the eastern Ross Sea, beyond the shelf break. The Antarctic Slope Front is a hotspot for Weddell and crabeater seals, the former remaining in pack ice on the continental shelf, the latter being more numerous beyond the shelf break, possibly due to higher concentrations of krill.

Acoustic tracking and Lagrangian drifters enabled us to build a model for the first month of dispersal of leatherback hatchlings from Papua, Indonesia. This "critical period" corresponds to the duration of the yolk reserves, the limit beyond which turtles need to be

in productive waters to survive. We show that hatchlings' movements strongly influence their trajectories, especially in flows not opposed to their swim direction. Offshore the Bird's Head Peninsula, the seasonally reversing New Guinea Coastal Current (NGCC) entrains hatchlings born in summer into the oligotrophic North Equatorial Counter Current (NECC). This process starts within the first hours of dispersal. In October-December, when predominant winds shift, causing the reversal of the NGCC, hatchlings deviate from prevailing currents, reaching after 30 days waters similarly unproductive as the NECC's. Winter dispersal is mediated by the southeastward NGCC. River outflow and upwelling are responsible for the productive areas traversed by hatchlings; the turbid waters potentially shielding turtles from predators. We suggest that local oceanography prevailing when turtles disperse mediates survival, with winter hatchlings having the best chances of overcoming the critical dispersal period.

1

General Introduction

1.1 MARINE MEGAFAUNA IN ENVIRONMENTAL EXTREMES

The study of the distribution of animals in the ocean poses some fundamental challenges. The connectedness of water masses has a "diffusing" effect on habitat boundaries. Where on land the distribution of animals (excluding birds) is spatially determined by sharp edges, such as roads, riverbanks or the rim of a forest, movements of marine fauna aren't as restricted. Boundaries do exist though. Two of the most significant, water temperature and currents (Wares et al., 2001), play a key role in the distribution of marine megafauna.

Despite two millennia of scientific endeavors marked with milestones such as Aristotle's description of tides, the Challenger expedition, the invention of SCUBA and remotely operated instruments, we have only scratched the surface of our ocean knowledge. Many facets of the life history of the largest marine tetrapods remain unstudied, despite their apparent conspicuity. For my thesis, I will focus on how the physical environment in two very different parts of our planet -Antarctica and New Guinea- mediates the movements and spatial distribution of these large animals.

1.1.1 Leatherback sea turtle hatchling dispersal

The question of where sea turtle hatchlings go after entering the water for the first time during the "lost year(s)" has puzzled sea turtle biologists for decades (Carr, 1984; Witherington, 2002). Some advances have been made with loggerheads (*Caretta caretta)* (Witherington, 2002), but nothing is known of the fate of leatherback hatchlings (*Dermochelys coriacea*) (Fig. 1.1). The first part of my thesis used a combination of Lagrangian surface drifters and behavioral data collected using a specially adapted tracking method, to model the oceanic migration of leatherback hatchlings departing their natal beaches of West Papua (Indonesia). I limited my study to the first 30 days of dispersal, the "critical dispersal period", as that is the approximate extent of the

leatherback hatchling's yolk reserves (Jones et al., 2007). Beyond that timeframe hatchlings need to be in productive waters to feed and survive. The influence of currents at different spatial scales as well as the turtles' swimming behavior are included in the model. By integrating chlorophyll-a data, a proxy for primary productivity, the model would enable the assessment of the oceanic conditions the turtles will face during and at the end of the critical period.

1.1.2 Distribution of Antarctic megafauna

An oceanographic cruise aboard the *R/V N.B. Palmer* provided a unique opportunity to carry out observations of megafauna in the Ross Sea. The timeframe of the cruise, early austral autumn, corresponds to a period of rapid flux in light levels and biological productivity. Only one other study has taken place in the Ross Sea in late autumn when most of the 24 hr day is experiencing total darkness (Van Dam & Kooyman, 2003). During this period the cold intensifies, the sun sets for days to months, sea ice forms, and penguins, seals and whales move to the north. A hitherto unseen mass-migration of Adélie penguins as well as of emperor penguins is described, and the abundance and distribution of other megafauna species (seals, volant sea birds and whales) is put in the context of the rapid expansion of sea ice.

1.2 STUDY AREAS

1.2.1 The Bird's Head Peninsula

The first study area is the Bird's Head Peninsula, West Papua, Indonesia. This is the location of the two main West Pacific leatherback sea turtle rookeries: Jamursba Medi and Wermon (Fig. 1.2). Tracking experiments and Lagrangian drifter deployments were carried out at both sites, during the months of July-August 2010-2012 and November 2012-February 2013 (deployments only).

1.2.2 The Ross Sea

The second study area is the Ross Sea of Antarctica, considered the anthropogenically least-affected stretch of ocean remaining on Earth (Ballard et al., 2012) (Fig. 1.3). We conducted continuous daytime visual surveys of marine megafauna along the entire route of the *R/V N.B. Palmer*, in February-March 2013.

1.3 RESEARCH QUESTIONS

1.3.1 Leatherback sea turtle hatchling dispersal

"Where do Papuan leatherback hatchlings end up after 30 days of travel and what can we say about the factors influencing dispersal and the characteristics of the marine environments they traverse?"

1.3.2 Distribution of Antarctic megafauna

"How does sea-ice in early autumn control the migratory behavior and distribution of Antarctic megafauna?"

1.4 OUTLINE OF DISSERTATION

The second chapter of my thesis describes a method to efficiently track leatherback hatchlings at sea. In the following chapter I expand the scope of my study to include sea surface currents (measured with Lagrangian drifters) in order to build a series of models showing the seasonal dispersal pathways taken by leatherback hatchlings. The fourth chapter consists in a description of a hitherto unseen phenomenon: a migration front of emperor penguins traveling from the eastern to the western Ross Sea. The final chapter focuses on the abundance of seals, sea birds and whales throughout the Ross Sea, and how it relates to environmental variables.

1.5 REFERENCES

Ballard, G., Jongsomjit, D., Veloz, S.D., & Ainley, D.G. 2012. Coexistence of mesopredators in an intact polar ocean ecosystem: the basis for defining a Ross Sea marine protected area. *Biological Conservation,* 156, 72-82.

Carr, A. 1984. Mystery of the missing year - chasing sea turtles to their secret sanctuary. *Sciences-New York,* 24(4), 44-49.

Jones, T.T., Reina, R.D., Darveau, C.A., & Lutz, P.L. 2007. Ontogeny of energetics in leatherback (Dermochelys coriacea) and olive ridley (Lepidochelys olivacea) sea turtle batchlings. *Comparative Biochemistry and Physiology a-Molecular & Integrative Physiology,* 147(2), 313-322.

Wares, J.P., Gaines, S., & Cunningham, C.W. 2001. A comparative study of asymmetric migration events across a marine biogeographic boundary. *Evolution,* 55(2), 295-306.

Witherington, B.E. 2002. Ecology of neonate loggerhead turtles inhabiting lines of downwelling near a Gulf Stream front. *Marine Biology (Berlin),* 140(4), 843-853.

Figure 1.1: Adult leatherback sea turtle off the Kei Islands, Indonesia. Photo courtesy of Jason Idley, Scubazoo.

Figure 1.2: Leatherback nesting sites of the Bird's Head Peninsula, West Papua, Indonesia

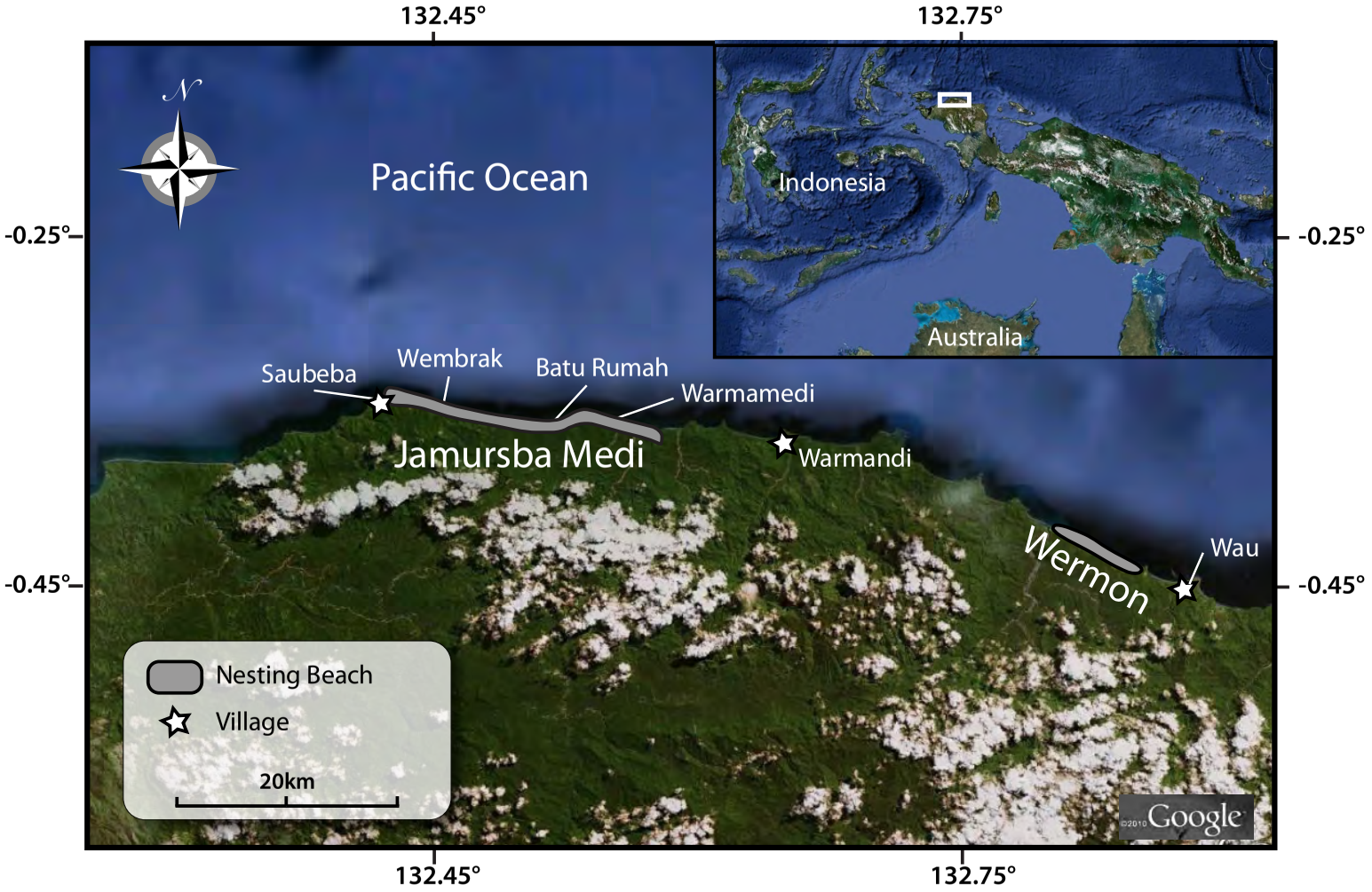
132.45°
132.75°
-0.25°
-0.45°
N
Pacific Ocean
Indonesia
Australia
Saubeba
Wembrak
Batu Rumah
Warmamedi
Jamursba Medi
Warmandi
Wermon
Wau
Nesting Beach
Village
20km
©2010 Google

Figure 1.3: Ross Sea, Antarctica. Megafauna surveys were carried out along the ship's track, indicated in black. Abbreviations: BoW=Bay of Whales, CC=Cape Colbeck

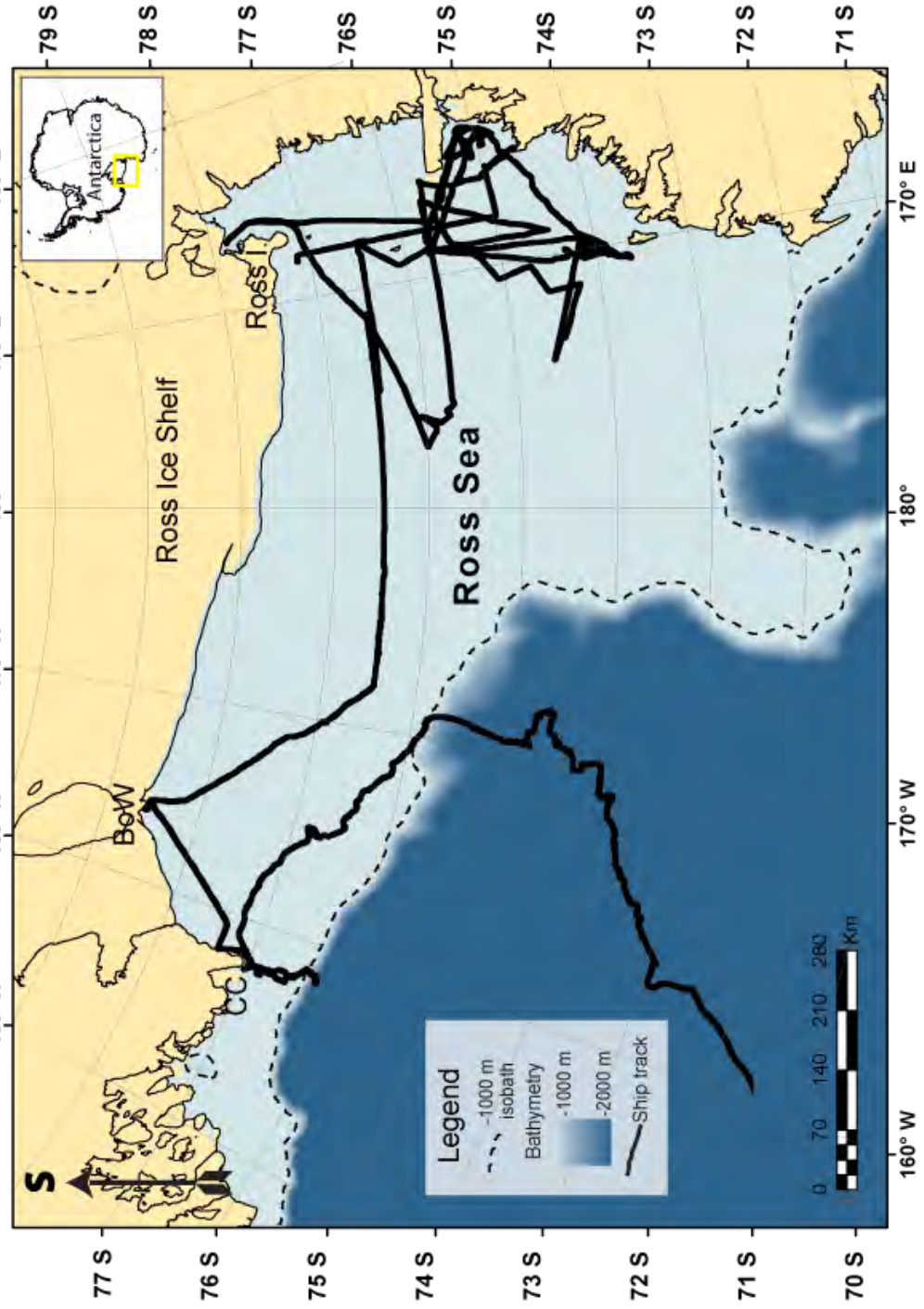
Ross Ice Shelf
Ross I.
Ross Sea
BoW
CC
Antarctica
Legend
-1000 m isobath
Bathymetry
-1000 m
-2000 m
Ship track
0 70 140 210 280 Km
S
79 S
78 S
77 S
76S
75 S
74S
73 S
72 S
71 S
70 S
160° E
170° E
180°
170° W
160° W
150° W

2

Tracking Leatherback (*Dermochelys coriacea*) Hatchlings at Sea Using Radio and Acoustic Tags

Tracking Leatherback (*Dermochelys coriacea*) Hatchlings at Sea Using Radio and Acoustic Tags

Geoffrey Gearheart[1], Adi Maturbongs[2], Peter H. Dutton[3], Janet Sprintall[1], Gerald L. Kooyman[1], Ricardo F. Tapilatu[2] & Elizabeth Johnstone[1]

[1]Scripps Institution Of Oceanography, 9500 Gilman Dr., La Jolla CA 92093, USA (E-mail: ggearhea@ucsd.edu); [2]Marine Laboratory, State University of Papua (UNIPA) Manokwari, 98314 Papua Barat, Indonesia; [3]NOAA-National Marine Fisheries Service, Marine Turtle Research Program, Southwest Fisheries Science Center, 8604 La Jolla Shores Dr. La Jolla, CA 92037, USA

For leatherback turtles relatively little is known about the "lost year(s)" – the time elapsed between a hatchling's first contact with the ocean and the moment it is sighted again as a juvenile in neritic foraging grounds (Carr 1987) – and the factors that might drive the oceanic dispersal during this phase. Although floating particle models have been used to predict dispersal pathways of sea turtle hatchlings (Blumenthal *et al.* 2009), on the near-shore scale, where remotely sensed current data are unavailable, the trajectories taken by hatchlings are more difficult to predict. Frenzied swimming and strong coastal currents may distort the predictions of these "passive drifter" models. This justifies the need to study the actual movements of neonates as well as the near-shore processes that influence them. Tracking hatchlings can be challenging. Due to the animals' small size, the technological options are limited: satellite-based transmitters are (still) too large and heavy so tracking efforts need to be carried out entirely *in-situ* with lighter tags. Neonate sea turtles have been tracked successfully with miniaturized radio transmitters that were either fitted directly onto the hatchlings' carapace (leatherbacks: Liew & Chan 1995) or tethered to a float or "bobber" (green turtles: Okuyama *et al.* 2009). These efforts were limited to tracking a small number of turtles and typically used radio signals as a secondary cue, i.e. as backup in case the tracker(s) would lose sight of the turtle. Thus, the need to keep within visual range of the hatchlings makes it almost impossible to track more than one individual at a time. Interestingly, the use of active acoustic telemetry has been largely dismissed, despite the availability of very small tags (<5 g weight out of water) and the advantage of uninterrupted transmissions (unlike VHF signals that stop when a hatchling is diving). As part of a multi-year effort to study the oceanic dispersal of West-Pacific leatherback hatchlings departing the beaches of Papua's Bird's Head Peninsula (Indonesia, Fig. 1), a pilot study was carried out in July-August 2010 to determine the best tracking methods to use. We tested both acoustic and VHF (radio) tags in the field using stationary buoys and live hatchlings in order to evaluate tag performance and the practicality of each method.

Experiment 1: Overall performance of sonic vs. VHF transmitters. For this experiment, we hung one Sonotronics (www.sonotronics.com) acoustic tag (IBT 96-2-E, w = 4.9 g out of water, transmitting at 68 KHz) from a mooring buoy at a depth z = 0.8 m. We attached an ATS (www.atstrack.com) VHF tag (R1655, w = 1.1 g out of water, 149.102 MHz) to the upper (dry) part of the buoy, so that the antenna was at ~20-25 cm above sea surface, the same

Meters from moored buoy		Buoy location	Tag type†	Transmitter frequency	Z (m from sea surface)	Directionality (arc length in degrees)	Max signal strength (1-5 scale)
100	Exp 1	Surface	VHF	149.102 MHz	0.2	50	5
			IBT	68 KHz	-0.8	8	5
	Exp 2	Surface	VHF	149.280 MHz	0.2	50	5*
		Surface	IBT	72 KHz	-1.0	6	5*
		Submerged	IBT	78 KHz	-3.0	7	5
		Submerged	EMT	75 KHz	-3.0	6	5
200	Exp 1	Surface	VHF	149.102 MHz	0.2	70	5
			IBT	68 KHz	-0.8	10	5
	Exp 2	Surface	VHF	149.280 MHz	0.2	65	5
		Surface	IBT	72 KHz	-1.0	10	5
		Submerged	IBT	78 KHz	-3.0	10	5
		Submerged	EMT	75 KHz	-3.0	10	5
500	Exp 1	Surface	VHF	149.102 MHz	0.2	70	3
			IBT	68 KHz	-0.8	10	4
	Exp 2	Surface	VHF	149.280 MHz	0.2	70	4
		Surface	IBT	72 KHz	-1.0	10	4
		Submerged	IBT	78 KHz	-3.0	10	4
		Submerged	EMT	75 KHz	-3.0	10	5
800	Exp 1	Surface	VHF	149.102 MHz	0.2	65	3**
			IBT	68 KHz	-0.8	10	4**
	Exp 2	Surface	VHF	149.280 MHz	0.2	75	2
		Surface	IBT	72 KHz	-1.0	12	2
		Submerged	IBT	78 KHz	-3.0	10	2
		Submerged	EMT	75 KHz	-3.0	10	4
1200	Exp 1	Surface	VHF	149.102 MHz	0.2	Irreg.	2
			IBT	68 KHz	-0.8	10	2
	Exp 2	Surface	VHF	149.280 MHz	0.2	Irreg.	1
		Surface	IBT	72 KHz	-1.0	10	1
		Submerged	IBT	78 KHz	-3.0	10	1
		Submerged	EMT	75 KHz	-3.0	10	3
1500	Exp 1	Surface	VHF	149.102 MHz	0.2	Irreg.	1
			IBT	68 KHz	-0.8	10	1
	Exp 2	Surface	VHF	149.280 MHz	0.2	Irreg.	1
		Surface	IBT	72 KHz	-1.0	10	1
		Submerged	IBT	78 KHz	-3.0	10	1
		Submerged	EMT	75 KHz	-3.0	10	2

Table 1. Results of transmitter range, directionality and optimum depth tests (Experiments 1 and 2). †: IBT = Sonotronics IBT96 acoustic tag, VHF = ATS R1655 radio tag, EMT = Sonotronics EMT01-3 acoustic tag. * In Experiment 2, receivers were set at maximum gain from d = 100-1500m. ** In experiment 1, maximum gain was used for both the acoustic and VHF receivers at d ≥ 800 m.

height as when affixed to a fishing bobber tethered to a hatchling (following the method of Okuyama *et al*. (2009)). We stopped the boat at distances of 100, 200, 500, 800, 1200 and 1500 m from the buoy to measure the maximum strength and directionality of the signals emitted by both transmitters. We used a 3-element VHF Yagi antenna and scanning receiver (ATS R410) to detect radio signals from the ATS tag, and a directional hydrophone (Sonotronics DH-4) with an ultrasonic receiver (Sonotronics USR-08) to detect "pings" from the sonic tag. We evaluated two parameters. The "maximum signal strength" received at each station and given on a qualitative scale of 1 to 5 (1 being weakest and 5 strongest) with the reference maximum strength (5) measured at 1 m from the transmitter. The second parameter we evaluated at each listening station was the "directionality", defined here as the arc length (in degrees) obtained

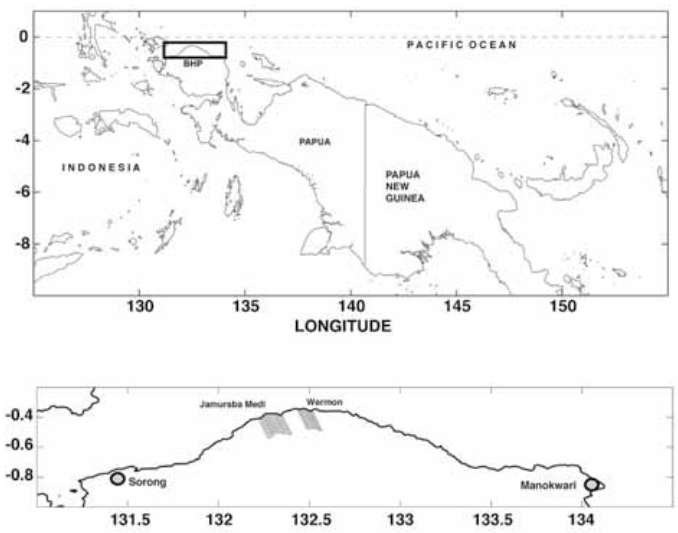

Figure 1. Leatherback nesting sites of Jamursba Medi and Wermon, on West-Papua's Bird's Head Peninsula (BHP).

by rotating the hydrophone or Yagi antenna while receiving signals of maximum strength. We measured the arc length using a digital compass (Garmin Oregon 450t) affixed to either the hydrophone pole or the handle of the Yagi antenna. We carried out this experiment during "calm (glassy)" sea state, following the World Meteorological Organization's Douglas sea scale (http://www.wmo.int/pages/prog/amp/mmop/faq.html).

Experiment 2: Optimum transmitting depth of sonic tag. The aim of the second experiment was to determine the optimal depth of the sonic tag when attached to the fishing bobber. It also provided an opportunity to repeat the radio tracking trial in order to see whether or not the results yielded during Experiment 1 were due to a malfunctioning VHF tag (Table 1). We used two buoys in an area where the water depth was 4 m, one floating at the surface and one consisting in a polystyrene disc floating in the water column at 2 m from the sea bottom. We tethered an IBT 96 tag (transmitting at 72 KHz) to the surface buoy so that it hung 1 m below the water surface (z=1m). We attached a new VHF tag (149.280 MHz) to the buoy as in Experiment 1. We hung an IBT 96 tag (78 KHz) 1m underneath the polystyrene disc (z=3m). We also attached a more powerful Sonotronics acoustic tag (Equipment Marking Transmitter EMT 01-3, transmitting at 75 KHz) to the disc at the same depth to assess the effect of higher transmission power on directionality and tracking range (signal strength). We used the same detection equipment and distances as in Experiment 1 and carried out the tracking during "calm (rippled)" sea conditions, with wavelets in the 0 to 0.1 m range.

Experiment 3: live trials with VHF tag. We tethered the VHF transmitter and bobber unit with a 2.5 m long strand of fishing line (0.13 mm, 2.7 kg strength) attached with a small hook to a pygal scute of a hatchling (Okuyama *et al.* 2009, see Fig. 2). A 1.9 cm plastic bobber (6.49 cm^3, weight out of water: 2.5 g) was tethered at the other end of the line. We glued a VHF tag onto the bobber so its antenna would rise 20 cm (its outstretched length) above the water line (Fig. 2). To contrast the dimensions of the tracking unit with the turtles, the reported average weights of Pacific leatherback hatchlings range from 40.5 g (East-Pacific: Jones *et al.* 2007) to 44.4 g (West-Pacific: Simkiss 1962). We painted the upper half of the bobber with fluorescent orange paint to facilitate spotting. We released a hatchling fitted with the bobber and VHF tag 250 m from shore during "smooth" sea state (wavelets in the 0.1-0.5m range) and tracked as follows: we recorded its initial position using a hand-held GPS unit (Garmin Oregon 450t) and then let it swim away for 10 min. The position of the hatchling was then tracked back using the Yagi antenna. After its new position was recorded we stopped the boat's engine and gave the hatchling a 20 min. head start before attempting to relocate it. Each subsequent lap was 10 min. longer than the previous one. We recorded 3 different laps, with the final one lasting 30 min. We repeated the experiment a second time with another hatchling and transmitter.

Experiment 4: live trials with acoustic tag. For this experiment, we fitted a hatchling with a 2.5 m strand of fishing line and one bobber (following the method employed in Experiment 3) to which we attached an IBT 96 tag (72 KHz) at z=0.8 m. We tethered another IBT 96 tag (78 KHz) to a second hatchling, using the same methods, but adding a bobber 2 m from the hook. We attached the tag to the second (distal) bobber, at 2.5 m from the hook and at z=0.8m (Fig. 3). We used two bobbers in order to facilitate spotting the hatchling, as previous experiments with the VHF tags showed a hatchling easily drags down one 6.49 cm^3 bobber during its frequent dives. The other advantage was that the alignment of the bobbers indicates the heading taken by the hatchling. We tracked both hatchlings simultaneously, in "smooth" sea conditions, and using the lap system of Experiment 3.

Superiority of acoustic tracking. The results given in Table 1 show that up to 200 m from the surface buoys (Experiments 1 & 2) the maximum signal strength of both the acoustic (sonic) and VHF tags was similar for up to 200 m from the surface buoys (Experiments 1 & 2). However, we found that the directionality

Figure 2. Bobber and VHF tag attached to a leatherback hatchling.

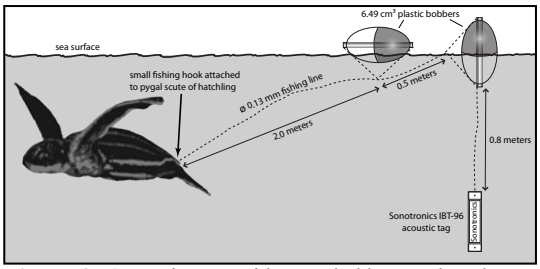

Figure 3. Acoustic tag with two bobbers tethered to a leatherback hatchling.

of the VHF transmitter was 50˚, versus 8˚ for the sonic tag. At subsequent distances we found that the directionality of VHF was never less than 65˚ arc length whereas we picked up the signal of the sonic tags within an arc length of 10-12˚ at all listening stations. At the 1200 m and 1500 m listening stations the directionality of the VHF tag was inconsistent: repeated sweeps with the Yagi antenna would each yield different arc length readings (Fig. 4). Both the IBT and VHF tags had similar signal strength decay throughout the testing range (Fig. 5). By enhancing the gain of the receivers, signals were still audible up to a distance of 1,500 m. There was no apparent difference in directionality and signal strength between IBT tags placed at z=0.8 m (Experiment 1), z=1 m and z=3m (Experiment 2). However, the more powerful EMT transmitter (which weighs 223 g and can by no means be used to track hatchlings) outperformed the smaller IBTs in signal strength, but had the same directionality (Experiment 2). The two live trials with VHF tags both failed within the first hour. The first two tracking laps (10 and 20 min) where successful with hatchlings traveling a total distance of 395 and 420 m. At the end of the third lap (30 min interval) we were unable to relocate the turtles. We interrupted the simultaneous tracking of two hatchlings using Sonotronics IBT tags after 60 min., since we were able to seamlessly relocate the hatchlings at the end of the first 3 laps using on average 3 listening stations.

First tracks of leatherback hatchlings. To validate the acoustic method, 20 hatchlings were tracked in July-August 2010. The main results of this preliminary study (to be published in the near future), were: (1) none of the tracked turtles were predated, (2) the presence of a near-shore tidal current deflecting hatchlings towards the West, (3) all turtles swam North to Northeast, (4) the effect of hydrodynamic drag of the tracking unit on the turtles' swimming behavior was *less* important than a) the effect of this West-flowing surface current, b) the level of fitness of the hatchlings and c) the state of the tide.

Conclusions and future directions. Tracking of VHF radio signals proved difficult even in calm sea conditions. The directionality was insufficient to easily find the correct bearing of the signal's source. A good level of directionality (small arc length) is especially important as the hatchlings' small size make them hard to spot at distances of over 40 m, even when dragging an orange bobber. At the distances of 1200 and

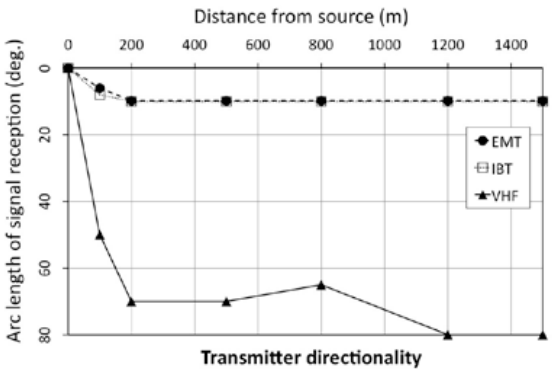

Figure 4. Transmitter directionality (Experiments 1&2). The NaN value represents the inconsistent arc length readings at d=1200 and 1500m.

1500 m, the irregular directionality is likely caused by the signal's range limit. The limitations of VHF tags were further illustrated during the two live trials, which we carried out in slightly rougher sea conditions. Failure to locate the hatchlings was likely the result of the compounded effect of poor directionality, intermittent diving and wave height possibly shielding VHF signals (waves occasionally taller than antenna). The outcomes of Experiments 1-3 show the inadequacy of using VHF signals as primary cue when tracking hatchlings. Conversely, the directionality of the sonic tags remained more than sufficient to move the boat to a closer listening station and consistently obtain a stronger and more spatially accurate signal. During the live trial (simultaneous tracking of 2 hatchlings) we only needed an average of 3 listening stops to move the boat close enough to sight the hatchling and record its exact position. The small arc length of the signal's reception area therefore reduces the chance of the tracker moving out of range of the signal, an important feature when tracking small organisms at sea, and even more so when taller waves make it difficult to spot the hatchling and/

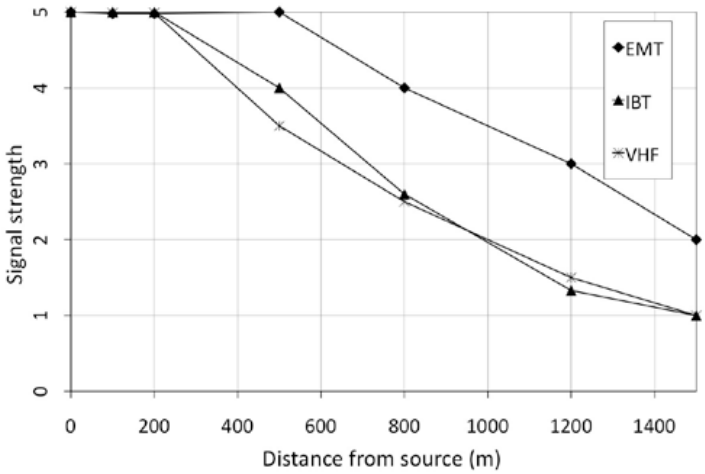

Figure 5. Transmitting range of acoustic and VHF tags (Experiments 1&2).

or the bobber. An additional advantage of acoustic telemetry is that the ultrasonic receiver is tuned to the specific frequency of the tag. The hydrophone picks up a limited amount of background noise, enabling to track without turning off the boat's engine. The more powerful EMT only surpasses the miniature IBTs in transmitting range, further supporting the suitability of the IBTs. The results of the four experiments enabled us to determine the type of tag and the basic setup to track Papuan leatherback hatchlings. Future improvements include reducing drag by using one larger bobber instead of two and fitting a small LED inside the bobber, allowing to track at least two hatchlings simultaneously at night. The first series of live trials using acoustic tags suggests that in the specific case of the Bird's Head Peninsula (Fig.1), predation at sea is limited. The presence of a surface current deflecting hatchlings towards the West shows the importance of resolving the oceanography on the near-shore scale in order to determine how and where hatchlings get entrained in larger scale features such as the New Guinea Coastal Current (NGCC), which reverses its direction seasonally (Ueki et al. 2003). The NGCC might therefore act as a "conveyor belt" distributing hatchlings either into the North or the South Pacific. Future work will focus on connecting the different spatial and temporal scales through a dispersal model that merges in-situ tracking data, Lagrangian drifters and remote-sensing data. This will provide a useful tool to validate existing "passive drift" models for hatchlings such as the one developed by Hamann *et al.* (2011).

Acknowledgments. We thank Dr. Mark V. Erdmann for his unwavering support of GG over the years. Thanks to Pak Ishak, Pak David, all UNIPA and WWF staff and students at Jamursba Medi for their day-to-day assistance during field work, as well as to Barakhiel Heri and Deasy Lontoh for providing hatchlings from Warmamedi. This work was carried out under permit through UNIPA with funding from Conservation International and Scripps Institution Of Oceanography.

BLUMENTHAL, J.M., F.A. ABREU-GROBOIS, T.J. AUSTIN, A.C. BRODERICK, M.W. BRUFORD, M.S. COYNE, G. EBANKS-PETRIE, A. FORMIA, P.A. MEYLAN, A.B. MEYLAN & B.J. GODLEY. 2009. Turtle groups or turtle soup: dispersal patterns of hawksbill turtles in the Caribbean. Molecular Ecology 18: 4841-4853.

CARR, A. 1987. New perspectives on the pelagic stage of sea turtle development. Conservation Biology 1:103-121

HAMANN, M., A. GRECH, E. WOLANSKI & J. LAMBRECHTS. 2011. Modelling the fate of marine turtle hatchlings. Ecological Modelling 222: 1515–1521.

JONES, T.T., D.R. REINA, C.A. DARVEAU & P.L. LUTZ. 2007. Comparative Biochemistry and Physiology, Part A 147: 313–322.

LIEW, H.C. & E.H CHAN. 1995. Radio-tracking leatherback hatchlings during their swimming frenzy. In: J.L. Richardson & T.H. Richardson (Comps). Proceedings of the 12th Annual Symposium on Sea Turtle Biology & Conservation. NOAA Technical Memorandum NMFS-SEFSC-361, pp. 67-68.

OKUYAMA, J., O. ABE, H. NISHIZAWA, M. KOBAYASHI, K. YOSEDA & N. ARAI. 2009. Ontogeny of the dispersal migration of green turtle (*Chelonia mydas*) hatchlings. Journal of Experimental Marine Biology and Ecology 379:43-50.

SIMKISS, K., 1962. The source of calcium for the ossification of the embryos of the giant leathery turtle. Comparative Biochemistry & Physiology 7: 71–79.

UEKI, I., Y. KASHINO & Y. KURODA.2003. Observation of current variations off the New Guinea coast including the 1997-1998 El Niño period and their relationship with Sverdrup transport. Journal of Geophysical Research-Oceans 108(C7), 3243, doi:10.1029/2002JC001611.

This work (Chapter 2), in full, is presented as published in the *Marine Turtle Newsletter* (130, 2-6) with the following co-authors: Adi Maturbongs, Peter H. Dutton, Janet Sprintall, Gerald L. Kooyman, Ricardo F. Tapilatu, and Elizabeth Johnstone. The dissertation author was the primary investigator and author of this paper.

3

Leatherback (*Dermochelys coriacea*) hatchlings during the critical dispersal period: how local oceanography and swimming behavior can mediate survival

3.1 ABSTRACT

Acoustic tracking and Lagrangian drifter data are used to build a model for the first month of dispersal of leatherback hatchlings from West Papua, Indonesia. This "critical dispersal period" is the approximate duration of the yolk reserves, beyond which leatherbacks need to be in productive waters to feed and survive. Our model, the first to include observed swim behavior and near-shore currents, shows that hatchlings' directed movements strongly influence their trajectories. This finding contradicts the "passive drift" paradigm for sea turtle hatchling dispersal. Near-shore oceanography, often overlooked or inaccurately rendered by numerical models, plays a key role in early dispersal. The seasonally reversing New Guinea Coastal Current (NGCC) entrains hatchlings born in boreal summer into oligotrophic waters of the North Equatorial Counter Current (NECC). This process starts within the first hours of dispersal. During the monsoon transition (October-December), when the NGCC gradually reverses, hatchlings are able to deviate significantly from prevailing but weak near-shore currents. At the end of the critical dispersal period they reach waters similarly oligotrophic to the NECC. Winter dispersal is determined by the strong southeastward NGCC. Hatchlings reach chlorophyll-a rich waters within 2 weeks, and end in the Bismarck Sea. Outflow from New Guinea's rivers and seasonal upwelling result in highly productive areas traversed by hatchlings; the turbid waters potentially shielding them from predatory fish. Local oceanographic conditions prevailing at the time of dispersal thus play a crucial role in the probability of survival, with hatchlings born in winter having better chances of completing the initial stage of their oceanic migration. This result has implications for conservation of this critically endangered population. In a more general sense, future sea turtle hatchling dispersal studies could be improved if, as a preliminary step, they addressed the critical dispersal period.

3.2 INTRODUCTION

Leatherback sea turtles are listed as vulnerable globally and critically endangered in the Pacific (IUCN, 2013). The eastern Pacific population in Mexico and Central America has collapsed (Sarti Martinez et al., 2007; Spotila et al., 2000) and the West Pacific leatherback is depleted and declining, with the last remaining sizeable population nesting in West Papua's Bird's Head Peninsula, Indonesia (Tapilatu et al., 2013).

Despite their geographic proximity, the two Bird's Head rookeries of Jamursba Medi and Wermon (Fig. 3.1) have distinct "peak seasons" of higher nesting activity. At Wermon, turtles nest year round with a main peak in January during the northwest monsoon (boreal winter), and a secondary peak in June during the southeast trades season (boreal summer). At Jamursba Medi the nesting season occurs in summer, in May-September, and peaks in July (Hitipeuw et al., 2007; Tapilatu et al., 2013). Physical processes likely play an important role in these seasonal nesting trends, as the distinct coastal orientation of both nesting sites exposes them to the opposing prevailing winds and their associated oceanographic conditions. This is translated by a cycle of beach erosion (unfavorable to nesting) and accretion (favorable), which alternates between Jamursba Medi and Wermon (Hitipeuw et al. 2007) and the effect is stronger at the former than at the latter. In addition, the adult nesting population that uses the beaches of Jamursba Medi appears to be demographically independent from the population that primarily nests at Wermon: satellite telemetry showed that the Jamursba Medi summer nesting females migrate to foraging areas dispersed across the northern Pacific, while the Wermon winter nesters migrate mainly to the southwest Pacific (Benson et al., 2007; Benson et al., 2011). These divergent post-nesting migratory pathways are all the more remarkable given the close geographic proximity of the two nesting sites (approximately 40 km).

Very little is known of leatherback hatchlings and post-hatchlings, as they are

essentially cryptic at sea. Only one study has addressed juvenile dispersal of West Pacific leatherbacks (Gaspar et al., 2012), so the question of the "lost years", defined as the fate of hatchlings after they have departed their natal beaches (Carr, 1952), remains unanswered.

When hatchlings enter the water for the first time they rely completely on the energy contained in their yolk sacks which fuels their initial "frenzied" swimming (Carr, 1962; Wyneken & Salmon, 1992). After 24 hours, turtles enter a state of post-frenzy with slower, and in the case of leatherbacks, sustained swimming (Wyneken & Salmon, 1992). Hatchlings' energetic expenditure during the first weeks varies greatly among sea turtle species. In leatherbacks, the yolk provides enough energy to sustain swimming for 3 weeks. This is complemented by feeding, which starts approximately 8 days after emergence, so the yolk reserves are extended to 4-6 weeks (Jones et al., 2007). Setting the "critical dispersal period" at 30 days, beyond which leatherbacks rely completely on external sources of food, the compelling question is whether or not hatchlings are capable of reaching productive areas of the ocean within this timeframe (Jones et al., 2007; Putman et al., 2010). Information on this critical dispersal period is paramount to understanding the natural history and conservation needs of leatherbacks.

Coastal currents strongly influence the distribution of emergent leatherback hatchlings in the eastern Pacific (Shillinger et al., 2012). A prominent oceanic feature along the coast of New Guinea is the New Guinea Coastal Current (NGCC) (Kuroda, 2000; Wyrtki, 1961), which is driven by seasonal wind forcing. Southeast trade winds during the summer cause the NGCC to flow equatorward, while the northwest monsoon drives the poleward flow of NGCC during winter (Kashino et al., 2007; Lukas et al., 1996; Ueki et al., 2003). The dramatic seasonal reversal of this large-scale boundary current likely affects the dispersal of hatchlings from the Bird's Head Peninsula (Gearheart et al., 2011). Hatchlings produced during the winter at Wermon could

initially be transported in the opposite direction by the prevailing currents to those born in summer at Jamursba Medi. Yet, the details of how the near-shore circulation (within ~10-20 km of the coastline) connects with these large-scale currents remains poorly understood, hampered by the low *in situ* data coverage in this remote region and the inability of satellite data to resolve the near-shore and the shorter-time scales.

Numerical models that treat hatchlings as "passive drifters" following ocean currents have been used to predict their dispersal pathways and end destinations (Blumenthal et al., 2009; Hamann et al., 2011; Okuyama et al., 2011; Polovina et al., 2004; Reich et al., 2007; Revelles et al., 2007). Scott et al. (2012) were the first to include hatchling behavior into a dispersal model and showed that a limited amount of directed swimming can have a strong impact on their trajectories, even in strong flows such as the Gulf Stream. Shillinger et al. (2012), although not factoring in hatchling swimming behavior into their model (no data were available at that time for Pacific leatherbacks), suggest that east Pacific leatherback hatchlings departing nesting sites that are closely located to each other may have very different dispersal pathways and end destinations. Divergence in their trajectories may start in the near-shore zone, but models that rely mostly on remote sensing data do not resolve this scale. The dispersal model of West Pacific leatherback hatchlings and juveniles built by Gaspar et al. (2012), uses as a baseline NEMO, a numerical ocean model (www.nemo-ocean.eu/). In their study, different pulses of virtual hatchlings are released randomly from a 0.25° X 0.25° quadrant centered 40 km perpendicularly offshore from the nesting beaches. The assumption is that near-shore (<40 km) currents do not cause turtles to be deflected sideways (i.e., East or West from the Bird's Head nesting beaches), as this could distort predictions, especially in a region known for its complex and highly variable oceanography (Gordon et al., 2010). Additionally, in the same model, turtles are considered passive drifters during their first year at sea. However, in the Gulf Stream, hatchling swimming behavior

was shown to greatly affect dispersal trajectories (Scott et al., 2012), and so the same assumption could be made for hatchlings entrained in a more variable oceanographic setting such as the one encountered off New Guinea. Thus, the inclusion of site-specific behavioral parameters would improve the predictive power of future dispersal models.

In this paper we construct dispersal models for hatchling leatherback turtles from Bird's Head nesting beaches. Our first step was to carry out tracking experiments of hatchlings while simultaneously measuring the currents in which they are entrained. The resulting information on the direction and speed of their dispersal in calm waters and in currents with different characteristics is used to parameterize our models. As we employed a novel tracking technique (Gearheart et al., 2011), we also assessed the impact of the tracking hardware on the dispersal parameters. Our second step was to map the near-to-far shore circulation off the two nesting beaches in West Papua, using Lagrangian surface drifters.

In the last part of this paper we present a drifter track-based model for the initial 30 days of dispersal of leatherback hatchlings, parameterized with site-specific behavioral data and overlaid with chlorophyll-a imagery. We use this model to examine seasonal dispersal scenarios and their significance in the context of the critical dispersal period.

3.3 METHODS

3.3.1 Tracking hatchlings using active acoustic telemetry

3.3.1.1 Swim behavior experiments

Technological constraints preclude the use of satellite transmitters, which are still too bulky to be fitted on hatchlings (Gearheart et al., 2011; Thums et al., 2013). Arrays of submerged hydrophones have been used to track small aquatic organisms equipped with sonic tags, such as juvenile salmonids (Clements et al., 2005) and, more recently, a "cloud" of sea turtle hatchlings (Thums et al., 2013). As the detection range

of these stationary arrays is limited (typically, less than 1000 m), they are only suitable for small- scale studies. Therefore, to date the only technique capable of effectively tracking hatchlings beyond the first few hours of dispersal is active acoustics, where a "listening" vessel follows a small number of turtles equipped with miniature pingers (for a full description, see: Gearheart et al., 2011). The goal of our first series of tests was to gather information on the performance of this tracking method and the physical/ biological factors influencing hatchling dispersal. To this effect, we carried out tracking experiments in July-August of 2010 and 2011, off the central beach of the Jamursba Medi rookery (Fig. 3.1). We tracked turtles that were collected by local conservation staff from the surface of nests that hatched naturally, plus turtles found at the bottom of nests, which had failed to crawl out ("stragglers"). The approximate time since collection was noted for each hatchling and they were tracked as soon as possible thereafter. Some of the hatchlings, born on a beach located far from the central camp, were brought to us one day after collection. We tracked those individuals during the next round of experiments (<36 hrs after collection). At the beginning of each tracking day, we randomly selected a hatchling, attached an acoustic pinger, and let it crawl down the beach and reach the water. We helped the animal get past the waves by holding the line and tracking unit slack. We then followed the hatchling with our inflatable boat, remaining at all times 3-5 m behind the turtle, so as to not influence its swimming behavior (Okuyama et al., 2009; Salmon & Lohmann, 1989). Whenever visual contact was lost we used a directional hydrophone to locate the acoustic tag tethered to the animal. GPS position of the vessel was recorded automatically every five minutes using a Garmin Oregon 450t GPS unit (Garmin Ltd., Olathe, KS, USA). As the main objective of these first experiments was to measure the influence of the tracking unit on the turtle's behavior in different currents, we tried to track each animal for as long as possible. At the end of each track, we detached the tracking unit from the turtle before releasing it. We then followed the untethered

animal for as long as possible to compare natural behavior and behavior when dragging the unit. As we relied completely on visual cues for this final part of the experiment, our success depended mostly on sea state. Swimming direction (heading) was recorded using a digital compass every 5 minutes with the tracking unit attached, and every minute when the turtle was swimming freely. Due to the variable precision of these heading estimates, the recorded values were categorized *a posteriori* into 45-degree bins, on a 360-degree scale, where 0º=N, 90º=E, 180º=S, -90º=W (Fig. 3.2). Whenever we could track more than one animal a day, we would return to shore and repeat the entire protocol.

3.3.1.2 Model parameters calculated from tracks and simultaneous current measurements

In July-August 2012 our tracking experiments at Jamursba Medi were aimed at measuring the change in dispersal direction and speed of turtles subjected to different current regimes (i.e., in still water and in currents with different speeds and directions). Our methodology was as follows: prior to tracking the first turtle we deployed a Microstar Lagrangian surface drifter (Pacific Gyre Inc. Oceanside, CA, USA), which was programmed to record its GPS position every 10 minutes, and transmit this data in near real-time via the Iridium network. A corner-radar-reflector-type drogue, located 1.5 m below the surface, allowed the Microstars to adequately follow the portion of the water column where hatchlings are located most of the time during dispersal (Salmon et al., 2004; Wyneken & Salmon, 1992). With a half-life of 7 days on full-transmission mode, Microstars are useful for repetitive sampling of flows with short time and/or small spatial scales and are widely used in oceanographic research (Ohlmann, 2011).

Following the release of the drifter, we would track turtles using the same methodology as described above but the duration of each experiment was reduced to 15 minutes. This enabled us to sample a wide range of current scenarios while still obtaining

high-resolution data (the GPS recorded position every minute, yielding 15 coordinate pairs per track). Because of the shorter experiments, we would typically bring a group of ten turtles of known age, collected from the same nest. They were allowed to crawl down the beach before being recovered and transported in a dark container pending their use in offshore experiments. At the end of each 15-minute track, we detached the tracking unit from the turtle and let it go. We then returned to the drifter's position and repeated the procedure with another hatchling. The goal of the experiments was to obtain a combination of drifter tracks with simultaneous turtle dispersal trajectories, allowing us to calculate the velocity vector characteristics (direction and speed) of both the currents and the hatchlings while they deviated from the drifter's path. These parameters could then be integrated into the algorithm of the drifter track-based model.

Leatherback hatchling's *swimming speed* during the swimming frenzy ranges from 0.25 $m.s^{-1}$ (measured in a laboratory setting by Davenport, 1987) to 0.3 $m.s^{-1}$ (in the ocean, but with no simultaneous current measurements; Wyneken, 1997). We calculated the *swimming speed* of our hatchlings from tracks that were in currents flowing less than 0.03 $m.s^{-1}$ ("weak currents"). This value is adapted from B. Witherington's work on loggerheads, where weak currents are defined as flowing at less than 12% of a hatchling's swimming speed (Witherington, 1991).

3.3.1.3 Permanent drifter deployments

In order to map the near-shore to large-scale circulation off the Bird's Head Peninsula and obtain a baseline for our model, we deployed five Microstar drifters at Jamursba Medi in July-August 2012 (corresponding to the summer nesting season), and five from Wermon in November 2012-February 2013, during the winter nesting season. These drifters, which were separate to the ones used in the turtle tracking experiments described above, allowed us to sample the near-shore to large-scale circulation during

the opposing nesting seasons. The Microstars were released approximately 1000 m off-shore and their sampling rate was set to 10 minutes in the near-shore zone, then gradually increased to 24 hours towards the end of their tracks in order to maximize battery life. The interval between each drifter deployment at Jamursba Medi was approximately 7 days. Social unrest in the Wermon area caused us to cancel part of the winter field season of 2012-2013, so that drifter deployments were less regular than at Jamursba Medi (Table 3.1).

3.3.2 Data analysis

3.3.2.1 Swimming behavior experiments without Lagrangian drifter deployments: impact of currents, age and tracking unit-induced drag

The hatchling *dispersal speed*, *dv* (a compound value of *swimming speed* and the unknown current speed, expressed in $m.s^{-1}$), was analyzed in a Generalized Additive Modeling framework (GAM) (Hastie & Tibshirani, 1990). GAMs are linear models in which the predictors depend linearly on unknown smooth functions or some predictor variables, and interest focuses on inference about these smoothers. We used the MGCV package 1.7-27, developed by Wood (2001) for the R software environment (R Development Core Team, 2010).

Field observations of sudden changes in drift direction of the boat combined with the analysis of the individual tracks, i.e., a turtle's trajectory that did not follow its swimming direction, suggested the presence of a westward current flowing approximately 1 km offshore Jamursba Medi (Fig. 3.2). In the absence of local tidal data for 2010 and 2011 (the oceanographic station at Manokwari started measuring tides in mid-2011), we included in our GAM a tide-related continuous variable, *hrs*, hours elapsed since the most recent full or new moon, to assess the effect of near-shore tidal currents on the dependent variable *dv*. It was further smoothed using a spline-fit algorithm with variable degrees

of freedom. The smoothing function was represented using penalized regression splines, estimated by penalized iterative least squares. The time elapsed since collection of the hatchlings was given as *age* and consisted of three categories: (1) turtles tracked less than 24 hrs after collection, (2) turtles tracked 24 to 36 hrs after collection, and (3) stragglers. We included the categorical variable *tet* (presence/absence of the tracking unit) to measure the effect of the hydrodynamic drag of the bobber and tag on dispersal speed. The full linear predictor was as follows:

$$\log(E[dv]) = f(hrs, n) + d(tet) + d(age) + (d[age] * d[tet]) \quad (1)$$

Where:

E= expected value of the dependent variable *dv*

d= parameter value for each categorical variable *tet* and *age*

f= a spline fit to the continuous variable *hrs*, with *n* degrees of freedom

($d[age]$•$d[tet]$)= an interaction term between categorical variables *age* and *tet*

Step-wise backfitting regression models were built by adding and subtracting explanatory variables to minimize the Akaike Information Criterion (AIC) (Burnham et al., 2011). AIC provides a parsimonious balance between model predictive power and complexity, the preferred model being the one with the minimum AIC value. The AIC is: $AIC=2k - 2\ln(L)$, where k is the number of parameters in the model and L is the maximized value of the likelihood function for the estimated model. We used Δ_i, the change in AIC between competing models, to select the most parsimonious GAM (Burnham & Anderson, 2002). When two models were within two AIC units from each other ($\Delta_i \leq 2$), the simplest (i.e. the one with the smallest number of parameters) was chosen as the best model and reported alongside the competing model(s) (Richards, 2008).

Results are reported as means ± standard error, unless stated otherwise.

3.3.2.2 Drifter, turtle trajectories and model algorithm

Lagrangian drifter data was processed in ArcGIS 9.3 (ESRI, 2011). We removed outliers and spikes from the raw data and used the cosine-haversine formula (Ruppel et al., 2013) to compute distance and bearing between coordinate pairs. The baseline for our turtle dispersal model consisted of "a mean current trajectory", calculated from different sets of drifter trajectories. We provide a detailed description of the procedure for this calculation in the results section of this paper. Ocean surface current analysis—real time (OSCAR) 5-day gridded velocity vector fields (monthly means at 1/3° resolution), derived from satellite altimeter, scatterometer and SST (Bonjean & Lagerloef, 2002), were plotted with the drifter track-based models. This provided a three-dimensional (i.e., including time) representation of the surface circulation during the modeled periods. MODIS-A Chlorophyll data (monthly means at 0.1° resolution for corresponding modeled periods) were downloaded from NASA's Earth Observations (NEO) portal (http://neo.sci.gsfc.nasa.gov/) and used as proxy for primary productivity (Ware & Thomson, 2005).

3.4 RESULTS

3.4.1 Factors influencing near-shore dispersal of leatherback hatchlings

3.4.1.1 Overall trends

A total of 26 leatherback hatchlings were tracked in July-August 2010-2011, totaling 149 hours at sea. Of these, 8 were stragglers, 9 were of age<24 hrs and 9 of age 24-36 hrs. Track length ranged between 239 and 7,311 m (mean=3,358 m, median=2,834 m). Twelve turtles were tracked both while *tethered* and *untethered* to the tracking unit. The *untethered* sections of these tracks, which could last more than one hour and 1,000 m in length, appeared to always be within the observed current (Fig. 3.2, red lines).

The 14 remaining tracks were of *tethered* turtles only. None of the hatchlings suffered predation, although on two occasions we had to fend off attacks by a white-bellied sea eagle (*Haliaeetus leucogaster*) on hatchlings that were swimming through the surf zone. The swim directions were consistently perpendicular to the coastline, ranging from NW to ENE. The mean swim direction was -45° to 0° (northwest to north) (Fig. 3.2).

3.4.1.2 Factors affecting dispersal speed

Of the set of candidate models for dispersal speed, *dv*, M1 had the lowest AIC score (Table 3.2). It included the proxy for tidal flow, *f(hrs)*, and the interaction term between the age of the hatchlings and the presence/absence of the tracking unit (*d*[*age*]•*d*[*tet*]). Model M2, which included both parameters *age* and *tet* separately, had a Δ_i=2.84. Therefore, M1 is the best model for *dispersal speed* that can be inferred from the dataset. The smooth function *f(hrs)* is given in Figure 3.3 (right panel). Dispersal speed fluctuated in the 14-day window between both moon phases, with peaks at around 75 hrs and 200 hrs after the last full or new moon. This suggests a tidal influence on turtle dispersal speed. The divergence between the dispersal trajectories and the swim directions of the turtles, given in Figure 3.2, shows that turtles are deflected towards the west, at a distance starting approximately 1000 m from shore. Comparisons of categorical variables *age* and *tet* in the baseline GAM model, log (*dv*) ~ *f*(*hrs*) + (*age*=<24 * *untethered*), show there was no significant difference in dispersal speed of turtles of age 24-36 hrs and age<24 hrs (two sample t-test with α=0.05; t (8.93)=-0.18, p=0.84) and between stragglers and turtles of age <24hrs (t (8.93)=0.10, p=0.92). The effect of the tracking unit, *tet*, on the dispersal speed was highly significant however (t (8.93)=-11.97, p=<$2e^{-16}$). The mean dispersal speed for a turtle of age<24 hrs, when *untethered*, was 0.51 $m.s^{-1}$ (±0.02) while a turtle of the same age that was *tethered* to the tracking unit had a mean dispersal speed of 0.29 $m.s^{-1}$ (± 0.01), a 43 % decrease (Fig.

3.3). The interaction between the tracking unit and the age of hatchlings was significant only for the straggler category (t (8.93)=2.1, p=0.003), while turtles tracked 24-36 hrs after collection were not significantly more affected by the tracking unit than turtles that were less than 24 hours old (t (8.93)=-0.99, p=0.32) (Fig. 3.3).

3.4.2 Large-scale regional currents

3.4.2.1 Jamursba Medi summer drifter trajectories

The five drifters released during the summer at Jamursba Medi followed a near-shore trajectory consistent with the turtle trajectories that also suggest a westward current flowing along the Bird's Head Peninsula (Fig. 3.4). The mean current speed calculated from the five drifter trajectories, within a 15 km-wide band stretching from 132.5ºE (Jamursba Medi) to 132.2ºE, was 0.294 $m.s^{-1}$ (± 0.004). Variation in current speed was strongest during the month of July. Within the same 15 km-band, the mean speed of drifters 68 and 70 increased from 0.198 (± 0.005) to 0.346 $m.s^{-1}$ (± 0.015), over a period of 7 days. The mean speed of the remaining summer drifters ranged from 0.301 (drifter 71) to 0.387 $m.s^{-1}$ (drifter 69). There appears a gradual strengthening of the west-flowing current over the summer months. Drifter 68 (deployed in July) followed the coastline for some 20 km then took a meandering, northerly path until approximately 0º where it veered west. Subsequent drifters all followed a similar western trajectory until 131.5ºE, where they deflected northwest, avoiding the Dampier Strait (Fig. 3.4). The last drifter deployed (69) took a somewhat different route: it remained within a distance of approximately 25 km from the coast, traveling at speeds of up to 0.76 $m.s^{-1}$ until reaching an area with slower currents (range=0-0.5 $m.s^{-1}$) at 131.8ºE. At less than 1 km from the coast it was deflected, possibly by an eddy, towards the northeast, then took a meandering path until approximately 0º where it followed a track similar to the previously deployed drifters. Drifters 68 and 69 stopped transmitting in the Ayau area

(Table 3.1), while drifter 72 veered due north until it was deflected to the northeast within the lower limb of the Halmahera Eddy. It stopped transmitting shortly afterwards (Fig. 3.5). Between 132ºE and the lower limb of the Halmahera Eddy (~2ºN), the mean current speed was 0.523 $m.s^{-1}$ (± 0.009). Drifters 70 and 71 had the longest tracks (2,712 km and 2,265, respectively; Table 3.1). They took a clockwise path around the Halmahera Eddy, where the mean current speed increased to 0.779 $m.s^{-1}$ (±0.045). The drifters exited the Halmahera Eddy at around 131º E, and became entrained in a series of smaller eddies or inertial currents (131º E-133º E) where the mean current speed was 0.402 $m.s^{-1}$ (±0.033). At 133º E, the drifters followed a meandering path along the North Equatorial Counter Current (NECC; Fig. 3.5), at a mean speed of 0.726 $m.s^{-1}$ (±0.061).

3.4.2.2 Wermon winter drifter trajectories

The drifters released off Wermon during the winter months of November 2012-February 2013 followed a poleward (i.e., southeastward) trajectory, remaining within 100 km of the Bird's Head Peninsula (132º E -134º E). The mean speed of drifters 73 and 74, released in November 2012, was 0.162 $m.s^{-1}$ (±0.022) north of the Bird's Head Peninsula (Fig. 3.6), and 3 months later, the mean current speed had almost doubled to 0.311 $m.s^{-1}$ (±0.071). Drifters 74 and 76, intercepted by fishermen, did not pass Manokwari (134º E), while drifters 73, 75 and 77 continued their way along the NGCC (Fig. 3.7). From 137º E to 144.5º E, they drifted within 100 to 200 km off the coast of New Guinea (Fig. 3.7). At 144.5º E, drifter 73 bifurcated towards the northeast, and went north of New Ireland on February 15th, 2013 (150.5º E). The mean speed of drifter 73, from 134º E to 152º E, was 0.542 $m.s^{-1}$ (±0.004). The other two drifters, which were deployed 4 days from each other in February 2013 (Table 3.1), followed the NGCC from 134º E to 147.5º E, at a mean speed of 0.844 $m.s^{-1}$ (±0.002), while remaining within 100 km off the coastline. Their trajectories diverged at the entrance of the Bismarck Sea

(147.5º E): while drifter 77 traveled counter-clockwise at 0.33 $m.s^{-1}$ (±0.041), drifter 75 turned clockwise, following the New Ireland-New Britain arc at a mean speed of 0.377 $m.s^{-1}$ (±0.028).

3.4.2.3 Mean drifter tracks

Mean drifter tracks, representing the baselines for our dispersal models, where computed as follows: for Jamursba Medi one mean track was calculated from the 5 drifters deployed during the summer, while for Wermon we determined two mean tracks to account for (1) the winter monsoon "transition period" with weak currents off the Bird's Head Peninsula (November-December; drifters 73 and 74) and (2) the fully developed NGCC, in February-March (drifters 75-77). As these sets represented different time-series of geographical coordinates (i.e. drifters had the same spatial starting point but were deployed on different dates), we plotted individual tracks over arc length, using the equation:

$$\sum_{i=1}^{n} \sqrt{(x_i - x_{i-1})^2 + (y_i - y_{i-1})^2} \quad (2)$$

where: x = longitude; y = latitude.

This provided us with a common reference point, starting at arc length=0, to calculate the mean current tracks representative of the summer, transition and winter seasons. These length-referenced tracks were subsequently re-parameterized by interpolation (i.e., we reassigned values of latitude, longitude and time interval for each track), then smoothed with a moving average smoother to eliminate random variations such as abrupt direction changes. Finally, the mean tracks were reduced in length to include only the first 30 days of drift, corresponding to the time frame of the critical dispersal period for leatherback hatchlings.

3.4.3 Turtle tracking and simultaneous current measurements

3.4.3.1 Overall results

For the simultaneous current and hatchling trajectory experiments, we tracked a total of 79 turtles, all within 36 hours after collection, while simultaneously measuring the currents in which they were entrained. Seventeen hatchlings were tracked in near-shore, "weak" currents, where their swimming speed ranged from 0.12 to 0.24 $m.s^{-1}$, with mean of 0.15 $m.s^{-1}$ (± 0.01), and their swimming direction was -45° to 0°. Corrected for the effect of drag of the tracking unit (a 43 % decrease in dispersal speed when tethered to the bobber and tag) the mean swimming speed was 0.29 $m.s^{-1}$ (± 0.02).

3.4.3.2 Model parameters: current scenarios and calculation of turtle dispersal vectors

Each 15-minute hatchling track was paired to its corresponding section of the drifter track. We assigned four drifter data points (40 minutes of drift) to each 15-min turtle track (Fig. 3.8). For each of these "track pairs" we calculated the mean speed and direction of the current, then categorized all the track pairs into "current scenarios", consisting of a specific current speed class (Vc) and current direction class (Bc). This classification allowed us to determine the turtle vector characteristics for different current scenarios (Table 3.3). As we did not track turtles in currents with bearing south to southwest (Bc 5) we combined the data of Bc 4 and Bc 6 for that category. Similarly, because of the lack of tracks in currents flowing east to south we pooled the data from Bc 3 and Bc 4 into one direction category (Bc 3-Bc 4).

Turtle dispersal speed

Current speeds of the mean drifter tracks ranged from 0.001 $m.s^{-1}$ to 1.81 $m.s^{-1}$, while our tracking experiments with simultaneous drifter deployments were made in

currents flowing at a maximum of 0.43 $m.s^{-1}$. Therefore, the turtle vector parameters for the dispersal model (based on the mean drifter tracks) had to be extrapolated from the near-shore data. In order to achieve this, we first determined the relationship between the turtle dispersal speed v_t and current speed v_c, by plotting $\bar{v}_t$, (the mean v_t, taken from each 15-minute turtle track) and $\bar{v}_c$ (the mean v_c, calculated for each corresponding 40-minute drifter trajectory; Fig. 3.8). The equation of the least squares fit,

$$\bar{v}_t = a \cdot \bar{v}_c + b \quad (3)$$

gives $\bar{v}_t$ for current speeds outside the range measured during the tracking experiments (Fig. 3.9).

Turtle dispersal direction

The second vector characteristic, the mean dispersal direction, $\bar{\Phi}_t$, was calculated similarly: we plotted Φ_t against v_t of all the turtle tracks in each current direction category Bc. This relationship shows the change in dispersal direction with increasing dispersal speed, for current direction classes Bc 1 to Bc 8 (Fig. 3.10). To extrapolate $\bar{\Phi}_t$ for current speeds beyond those measured in the near-shore experiments, we plugged in the values of $\bar{v}_t$ obtained through eq. (3) into the least squares equation of the Φ_t / v_t relationship:

$$\Phi_t = a \cdot v_t + b \quad (4)$$

The turtle dispersal vector parameters were then calculated for 64 current scenarios and are given in Table 3.3.

The difference between the number of values used in the turtle dispersal speed and dispersal direction calculations (Figs. 3.9 & 3.10) is due to the fact that for dispersal speed, we used *means* calculated from the 4 drifter positions and 15 turtle positions representing each track pair (i.e., yielding one value of speed per turtle and one value of current speed for that specific section of the drifter track; Fig. 3.8), while for the direction calculations we plotted the turtle data only. This data was categorized in the different

current scenarios the turtles were tracked in, so that in this case we had 15 values of speed and direction for each tracked turtle.

3.4.4 Drifter track-based model

3.4.4.1 Model algorithm

Turtle dispersal is simulated by concurrently releasing, in silico, a cloud of virtual hatchlings at the initial location of the mean drifter (current) track, at time t_0. At each subsequent time step, the virtual hatchlings take a random step based on the mean and standard deviation of both turtle speed and turtle direction given by the current flow condition. Turtle speed and direction statistics at each time step are based on the mean current track. For instance, if at t_1, the current in which the turtle is entrained has characteristics Bc 6/Vc 2 (Table 3.3), then the turtle's dispersal speed, V_t, is computed as follows:

$V_t(t_1)$ = mean turtle speed at Bc 6/Vc 2 + random number generator [0-1] * standard deviation of turtle speed at Bc 6/Vc 2

The turtle's dispersal direction, Φ_t, at t_1 is similarly computed. This procedure is repeated 500 times at each time step, yielding an uncertainty range in the turtle trajectories. The virtual turtles use the characteristics of the mean current at each time step to compute their corresponding trajectories. This allows the 500 virtual hatchling tracks to become spatially independent from the mean drifter track.

3.4.4.2 Model assumptions

We have made the following model assumptions:

1. In weak currents ($\bar{v}_c$ <0.03 m.s^{-1}), during the first 24 hours of dispersal, the dispersal vectors parameters were (1) the *corrected* mean *swimming* speed and (2) the mean

dispersal direction (-45° to 0°).

2. As all near-shore measurements were made with hatchlings less than 36 hours old, our data is biased towards speeds representative of faster and more sustained "frenzied" swimming. Therefore, we consider the uncorrected dispersal speeds calculated during our experiments (i.e. with turtles in frenzy but submitted to the hydrodynamic drag force of the tracking unit) as a best approximation of the slower mean dispersal speed expected of turtles in post-frenzy state (i.e. slower/intermittent swimming). For the first 24 hours of dispersal our model applies a correction factor of 1.76 to the values given in Table 3.3. Determined during our first series of experiments without drifters, this correction factor (a 76 % increase in dispersal speed when a turtle is untethered) cancels out the effect of drag of the tracking unit on dispersal speed values. For the next 29 days, we used the (uncorrected) turtle dispersal vectors presented in Table 3.3, as a best approximation of their post-frenzy behavior.

3. We parameterized diel swimming activity following Wyneken & Salmon (1992): non-stop swimming during the first 24 hours, then 65% of the time during the remaining 29 days (post-frenzy/intermittent swimming).

4. We kept hatchlings underneath a layer of moist sand prior to tracking, which restrained their energetic expenditure. The moment of contact with the ocean was therefore considered the start of the swim frenzy.

5. We did not carry out tracking experiments at Wermon, but given the similar orientation of the nesting beach as well as its geographic proximity to Jamursba Medi we used the same turtle dispersal vector parameters in our winter dispersal models (Table 3.3).

6. Hatchlings maintain the same swimming direction (-45° to 0°) throughout the critical dispersal period. This seems reasonable as changes in swimming direction, triggered mainly by changes in the magnetic intensity and inclination fields seem to occur on a scale of several months rather than days of dispersal (Lohmann et al., 2001; Scott et al.,

2012).

7. We assumed that the total current field covered by the dispersal model behaves similarly, at any point, to the current given by the mean drifter track. This much simpler oceanographic representation of the surface circulation off New Guinea has the advantage of being based entirely on direct GPS measurements many concurrent with turtle tracking in the nearshore environment.

3.4.4.3 Summer dispersal model

Virtual hatchlings departing Jamursba Medi in summer (Fig. 3.11) are able to deviate from the mean current's path while the direction of flow is within the -135º to 45º -range (Fig. 3.9, scenarios Bc 6-Bc 7 and Bc 8-Bc 1) and near-shore currents are relatively weak. As the current speed increases and the direction changes to a more northerly bearing (Fig. 3.9, scenario Bc 8-Bc 1) turtles drift along the NGCC, in close formation. The NGCC primarily determines the eastward path taken by hatchlings inside the Halmahera Eddy, as its high speed and a northeast to east direction of flow counteracts the hatchling's swimming (Fig. 3.9, scenarios Bc 2 and Bc 3-Bc 5). In those conditions, the model sets the turtle vectors equal to the current, so virtual hatchlings become entirely passive. At the end of the first 30 days of dispersal, the turtles have left the Halmahera Eddy and entered the NECC. The chlorophyll-a concentration coincident with this period is in the 0.01 to 0.02 $mg.m^{-3}$ - range. The OSCAR current vectors (mean of August 15th-September 15th, 2012) agree with the model and the mean drifter track (Fig. 3.11).

3.4.4.4 Monsoon transition period

Virtual hatchlings released in our model during the monsoon transition period (Fig. 3.12) disperse from Wermon in slow moving currents. In these weak flows, the

variability in dispersal direction and speed, given by the 95% confidence intervals in Figure 3.9, cause the cloud of virtual hatchlings to diffuse in the near-shore zone. Three weeks into their dispersal they get entrained by the poleward-flowing NGCC and deviate eastward. The distance traveled at the end of the 30-day period is approximately 350 km and chlorophyll-a concentration is similar to that encountered by hatchlings dispersing from Jamursba Medi in summer. The model is coherent with the offshore OSCAR current vectors (mean of November 15th-December 15th, 2012).

3.4.4.5 Winter

Dispersal from Wermon during the height of the northwest monsoon in February is essentially determined by the fully developed, poleward-flowing NGCC. Virtual hatchlings remain in a tight formation while traveling at speeds close to 1 m.s^{-1}. This current scenario (Bc 3-Bc 4) was the most common along the NGCC's mean trajectory and was opposed to the turtles' swimming direction. At current speeds > 0.2m.s^{-1} (Vc 2-Vc 8), hatchlings are incapable of deviating from the current's trajectory so the turtle dispersal vectors were equal to the current vectors (Fig. 3.9, Table 3.3). Twelve days after departing Wermon, hatchlings reached the Mamberamo watershed (Fig. 3.13), characterized by a spike in chlorophyll-a. Further along the coast, the trajectory of the hatchlings followed a "plume" of high chlorophyll-a waters, and reached the Bismarck Sea at the end of the 30-day drift. The Sepik river watershed (Fig. 3.13), characterized by chlorophyll-a values similar to the Mamberamo river, is reached approximately on the 25th day of dispersal. The model is coherent with the OSCAR current vectors (mean of February 15th-March 15th, 2013) further offshore (Fig. 3.13).

3.5 DISCUSSION

3.5.1 Tracking experiments

The tracking unit significantly affects hatchling dispersal behavior. The interaction effect between age after collection and presence/absence of the tracking unit suggests that turtles that were found at the bottom of nests ("stragglers") were more affected by the drag of the bobber and tag. Although there is no direct evidence that these turtles were less fit than turtles that emerged independently, stragglers are known to have a higher mortality rate (Hilterman & Goverse, 2003). This motivated our decision to use only turtles less than 36 hours old for our tracking experiments with drifters. The lunar signal detected in the dispersal speed data indicates that the observed westward deflection in the near-shore tracks is caused or amplified by tides. In the absence of simultaneous current measurements, we were not able to quantify this effect. Nonetheless, this result shows that current-mediated dispersal at Jamursba Medi starts less than 2 km from shore, emphasizing the need to consider the near-shore oceanographic processes when predicting hatchling dispersal. The only existing hatchling dispersal model for the region, by Gaspar et al. (2012), does not take into account this westward drift as the pulses of virtual, passive hatchlings are released 40 km due north of the Bird's Head nesting beaches. It must also be considered that this westward flow may also change seasonally. Once passed the breakers, turtles typically follow offshore trajectories (Lutz et al., 2002), with geomagnetic cues playing a major role in their orientation at sea (Lohmann & Lohmann, 1993; Lohmann & Lohmann, 1996). For the north facing nesting beaches of the Bird's Head Peninsula, the -45° to 0° bearing taken by our hatchlings is the most direct path away from the coast. This part of our study confirmed the efficiency of the tracking method and enabled us to quantify the influence of the tracking unit's hydrodynamic drag on hatchling dispersal. Our results suggest near-shore oceanography plays a key role in early dispersal. The subsequent tracking experiments with current

measurements confirm the remarkable swimming abilities of leatherback hatchlings, as even on short time-scales they are able deflect from the path of currents flowing faster than their own swimming speed. The angle and magnitude of this deflection, which varies with the current's direction and speed, is estimated here for the first time. This provides strong evidence that hatchlings should not be considered as purely passive drifters.

3.5.2 Boreal summer surface circulation

The trajectories of the five drifters deployed in July-August show that the near-shore currents flowed consistently alongshore and towards the west. The mean near-shore current speed of 0.29 $m.s^{-1}$ corresponds to the mean swimming speed of hatchlings during the swim-frenzy. Therefore, hatchlings that disperse during the boreal summer from Jamursba Medi face their first significant oceanic "conveyor belt" within a few hours after immersion. The distance from Jamursba Medi to Wermon being approximately 40 km, it is reasonable to assume that turtles born during the boreal summer at Wermon get entrained in the same westward flow. Our data shows variation in the current, with a gradual increase in speed and a more westward trajectory as the season progresses. On the larger scale, all drifters traveled north of the Island of Waigeo, circumventing the Dampier Strait (Fig. 3.4). This finding is in contrast to Gaspar et al. (2012), who predicted a significant number of Jamursba hatchlings disperse to the Indian Ocean via the Dampier Strait and through the Halmahera Sea. Our dataset is limited and gives no information about the variability of regional currents over seasonal time scales, variability which might be rendered by the NEMO model. However, the spatial resolution of NEMO (0.25° in longitude, corresponding to approximately 28 km at the equator) is not fine enough to characterize the flows near the coast and through the straits that are of the order of 1-10 km. A further analysis of the total 274 Surface Velocity Program

(Lumpkin & Pazos, 2007; Sybrandy et al., 1991) drifter tracks of 2000-2013 for our study region, shows that none entered the Dampier Strait while only one drifter entered and remained in the Halmahera Sea (Fig. 3.14). This suggests that in the surface layer, the Dampier and Halmahera Straits are very unlikely dispersal routes for Bird's Head leatherback hatchlings during any season.

3.5.3 Transition and winter surface circulation

Winter deployments at Wermon spanned 91 days while at Jamursba Medi all drifters were released within 38 days. This allowed us to sample currents for a longer period during the northwest monsoon season. The trajectories of drifters 73-77 show the gradual strengthening of NGCC off the north coast of the Bird's Head Peninsula, with speeds increasing from 0.16 $m.s^{-1}$ to 0.31 $m.s^{-1}$ between November and February (Fig. 3.6). As winter advances, the NGCC increases to a mean speed of 0.844 $m.s^{-1}$, a value close to the 1 $m.s^{-1}$ measured 50 km offshore at 142ºE by Kashino et al. (2007). These speeds are well above the swimming capabilities of leatherback hatchlings (0.29 $m.s^{-1}$, in frenzy). Moreover, the current direction is opposed to the swimming direction for most of the sampled period (Fig. 3.7), making it unlikely neonate leatherbacks have any influence on their dispersal while entrained in the NGCC during the boreal winter. Surface currents flow year-round from the southeast to the northwest through Vitiaz Strait, at speeds in excess of 0.5 $m.s^{-1}$ (Cresswell, 2000; Hristova & Kessler, 2012). This acts as a barrier that hatchlings from the Bird's Head Peninsula are unlikely to be able to break through to reach the South Pacific (Fig. 3.14). The end locations of drifters 75 and 77 are in gyres in the Bismarck Sea. Hatchlings caught in these gyres may exit through the narrow Saint Georges Channel, between New Ireland and New Britain (there are few data available, and only one SVP drifter that traveled this route went southward) or around the western tip of New Ireland.

The most likely period for exit of the Bismarck Sea is at the beginning of the boreal winter (Hristova & Kessler, 2012), possibly before the northwest monsoon has fully developed. This is illustrated by the trajectory of drifter 73 (Fig. 3.7). During the transition period of October-December predominant southeast trade winds are gradually replaced by the northwest monsoon. Our results suggest that hatchlings born during this period are likely to bypass the Bismarck Sea and enter the large-scale circulation (i.e., the South Equatorial Counter Current) within the same season (Fig. 3.7, drifter 73). Hatchlings born during mid-winter, in December-February, as shown by the trajectories of drifters 75 & 77 (Fig. 3.7) may get held up in the Bismarck Sea until the westward currents flowing off New Ireland have abated (Hristova & Kessler, 2012).

3.5.4 Modeling dispersal

The trajectories of virtual turtles released during the southeast trade winds season (summer), when the NGCC flows equatorward, is determined in its initial phase by swimming behavior. Near-shore currents flowing west to northwest act as conveyor belts from which hatchlings are able to deviate. Doing so, they instill a more northerly trajectory to their dispersal. Once entrained in the strong flows prevailing inside the Halmahera Eddy swimming behavior can no longer influence their trajectory. This is especially so when the current direction veers towards the east and so is opposed to the turtle's swimming direction, causing the modeled trajectories to approach the track of the mean current. Our simulation suggests hatchlings, despite their ability to deviate from passive drift, remain in a "close order formation". At the end of the 30-day period, once inside the NECC, hatchlings are in oligotrophic waters. Although we cannot say if conditions are unfavorable to the point of causing starvation, productivity in the West Pacific Warm Pool is known to be variable in space and time, and is linked to ENSO

cycles (Lehodey et al., 1997; Messie & Radenac, 2006). So, over longer time scales than considered here, starvation-induced mortality might be offset by periods of higher productivity that are more favorable to feeding. The fact that Jamursba Medi has a significant nesting population provides evidence that hatchlings entrained along this route are able to survive, as females later return to their natal breeding grounds (Dutton et al., 1999).

The transition and winter dispersal models (Figs. 3.12 & 3.13) show two very distinct pathways with potential implications for survival. While in relatively slow moving waters flowing in the general direction of swimming, the hatchlings' own swimming behavior can, to a great extent, influence their dispersal trajectories. The route taken by Wermon hatchlings during the transition period is an example of this phenomenon. Largely unaffected by the weak NGCC, they travel due north until, three weeks into their dispersal, they are deflected eastward by the strengthening NGCC. Their end-location, after 30 days of travel, is some 220 km northeast of the Bird's Head Peninsula, in oligotrophic waters (Fig. 3.12). Conversely, hatchlings born 3 months later, towards the end of winter, enter the NGCC within a few kilometers from shore (Figs. 3.12 & 3.13). Our model shows that the combination of high current speeds and bearing opposed to the hatchling's swimming direction causes them to drift passively along the NGCC. Precipitation off the north coast of New Guinea peaks during the winter monsoon (Marshall & Beehler, 2007), driving a discharge of sediments from the island's largest rivers comparable to that of the Amazon basin (Nittrouer & Brunskill, 1994). Combined with coastal upwelling during the northwest monsoon (Cresswell, 2000; Hasegawa et al., 2010), the waters off the north coast of New Guinea are highly productive. Phytoplankton concentrations peak within the surface freshwater plumes of the Mamberamo and Sepik Rivers (Higgins et al., 2006; Muchtar, 2004) creating potentially favorable feeding conditions for hatchlings. The first of these productive areas, the

Mamberamo rivershed, is reached within the second week of dispersal (Fig. 3.13), which corresponds to the period during which leatherbacks start feeding independently (Jones et al., 2007). This gives an interesting example of how geological processes (i.e., erosion and sediment discharge) can impact higher vertebrates. As hatchlings continue their drift along the coast and into the Bismarck Sea, they remain in highly productive waters. The Sepik River outflow (Fig. 3.13) during the northwest monsoon is characterized by a turbid layer of fresh water reaching 60 km from its mouth in all directions (Higgins et al., 2006). Although hatchlings might not pass through this plume, the modeled trajectory being more than 130 km away from the mouth of the Sepik, they likely traverse the turbid waters of the Mamberamo River, which is only 40 km away from their path. This passage through low-visibility waters might offer added protection against predatory fish (Gyuris, 1994). Our drifter trajectories show that beyond the 30-day period, the NGCC feeds directly into a pair of opposing circulating gyres in the Bismarck Sea (Figs. 3.7 & 3.13). Primary productivity levels in the Bismarck Sea are markedly higher than in the West Pacific Warm Pool (Le Borgne et al., 2002), and possibly linked to seasonal influx of nutrient-rich fresh water from as far north as the Mamberamo rivershed (Higgins et al., 2006). Hatchlings with exhausted yolk reserves would find a more favorable environment in the Bismarck Sea than hatchlings that dispersed during summer or during the transition period and ended up in unproductive seas.

The dispersal scenarios presented here suggest different outcomes in terms of the likelihood of finding sufficient food during and at the end of the critical dispersal period. The prevailing oceanography off the Birds' Head Peninsula may be of crucial importance for the early-life stages of leatherbacks and, therefore, plays a role in determining who returns later in life. On a seasonal timescale the outlook for survival could change drastically in function of when hatchlings disperse. We show the possible pathways to the large-scale circulation in a simple schematic (Fig. 3.15).

This finding sheds new light on the processes that affect the West Pacific leatherback metapopulation (Dutton et al., 2007). Surveys at Jamursba Medi and Wermon show a long-term decline in nesting at both beaches. Particularly impacted is Jamursba Medi, with a reduction of as much as 78% of the number of nests between 1984 and 2011; while Wermon (which hasn't been surveyed for as long) has seen a decline of over 62% between 2002 and 2011 (Tapilatu et al., 2013). Potential causes include widespread egg harvesting until the mid-1990's (Betz & Welch, 1992), industrial fisheries by-catch (Bailey et al., 2012) and a decrease in hatchling production due to predation and/or adverse physical conditions causing nests to fail (Tapilatu & Tiwari, 2007; Tiwari et al., 2011). If hatchlings born in winter have a higher rate of survival due to their dispersal into more productive waters, as suggested by our results, long-term conservation measures aimed at enhancing hatchling production at Wermon (Tiwari et al., 2011) would boost the number of returning adult turtles.

3.6 CONCLUSIONS

Our dispersal model predicts the trajectories of hatchlings from their first immersion until their inclusion into the large-scale circulation. The hatchlings' own swimming behavior, which is integrated for the first time in a dispersal model, is shown to be an important determinant in their trajectories, especially in currents that do not flow against the turtles' own swimming direction. Hatchlings therefore should not be considered as merely passive drifters. If their yolk energy reserve runs out after approximately 30 days, turtles are also swimming against the clock: the deviation they cause with respect to passive drift, and the consequent gain, or loss of time, determines when they reach areas favorable to feeding. More important, perhaps, is the timing of hatching, as off the Bird's Head Peninsula the seasonal oceanographic conditions may play a crucial role in the chances of surviving the critical first month at sea.

We suggest that investigating the critical dispersal period of sea turtles may improve subsequent predictions made over larger temporal and spatial scales. Beyond the realm of sea turtles, a multi-scale approach that includes key (critical) life-history stages and their corresponding interactions with the physical environment, would yield more realistic predictions of the movements of a given species.

Our study of the question of the "lost years" of West Papuan leatherbacks will hopefully motivate further research. Of particular interest is the behavioral response of Bird's Head hatchlings when crossing geomagnetic boundaries. Identifying these changes by, for instance, replicating *in situ* the experiments of Lohmann et al. (2001), which show post-hatchlings adjust their swimming direction when exposed to different magnetic fields, and quantifying diel swimming activity and speed in post-hatchlings, would help build more accurate dispersal models that combine near-shore drifter-based trajectories with large-scale numerical simulation systems. Finally, the potential effects of different global warming scenarios on hatchling dispersal and survivorship (e.g., through changes in the wind and current circulation off the Bird's Head Peninsula, impacts on primary productivity, etc.) also deserve to be investigated.

3.7 ACKNOWLEDGEMENTS

We acknowledge the help of: Hester Tjebbes (funding, assistance in the field), Karen Comstock (casatortuga.org, donated research vessel), Mark V. Erdmann (Conservation International Indonesia, funding), Ron Burton and Doug Bartlett (SIO, funding), Paul Barber (UCLA, technical help), Yukiko Murabayashi (OIST, Japan, technical help), Martin Gassman (SIO, technical help), Carsten Allefeld (Bernstein Center for Computational Neuroscience, technical help), Mati Kahru (SIO, data), Judith Bird (editing), Jonathan Shurin (UCSD, reviewing), Neal Driscoll (SIO, funding), Jay Barlow (NOAA, reviewing), Pierre Gaspar (CLS, France, data), Deasy Lontoh (Moss

Landing Marine Lab, assistance in the field), Pak Ishak and Pak David (boat drivers), Larry McKenna (generous donation of boat repair kit and fruit!). Thanks to my intrepid field assistant Adi Maturbongs (UNIPA), and to Ferdiel Ballamu, Silas Wiuw, Yusuf Aitem, and Capt. Hanafi (YPP, Sorong), for your friendship over the years, the insight and help. Hatchlings were collected by UNIPA field staff: Barakhiel Heri, Erik Sembor, Ricky, Yairus, Vidson, Hengky and Hadi Ferdinandus (WWF-Indonesia)… Many thanks to them! This study was carried out in strict accordance with the guidelines of the Institutional Animal Care and Use Committee (IACUC) under protocol S12144, to GK. All animals were released immediately upon completion of experiments. Fieldwork was carried out under Indonesian research permit from RISTEK no.: 11/TKPIPA/FRP/ SM/ XI/2010, issued to GG with support of UNIPA and the SIO-UNIPA collaborative science program (SURGA).

3.8 REFERENCES

Bailey, H., Benson, S.R., Shillinger, G.L., Bograd, S.J., Dutton, P.H., Eckert, S.A., Morreale, S.J., Paladino, F.V., Eguchi, T., & Foley, D.G. 2012. Identification of distinct movement patterns in Pacific leatherback turtle populations influenced by ocean conditions. *Ecological Applications,* 22(3), 735-747.

Benson, S.R., Dutton, P.H., Hitipeuw, C., Samber, B., Bakarbessy, J., & Parker, D. 2007. Post-nesting migrations of leatherback turtles (Dermochelys coriacea) from Jamursba-Medi, Bird's Head Peninsula, Indonesia. *Chelonian Conservation and Biology,* 6(1), 150-154.

Benson, S.R., Eguchi, T., Foley, D.G., Forney, K.A., Bailey, H., Hitipeuw, C., Samber, B.P., Tapilatu, R.F., Rei, V., & Ramohia, P. 2011. Large-scale movements and high-use areas of western Pacific leatherback turtles, Dermochelys coriacea. *Ecosphere,* 2(7), art84.

Betz, W., & Welch, M. 1992. Once thriving colony of leatherback sea turtles declining at

Irian Jaya, Indonesia. *Marine Turtle Newsletter,* 56, 8-9.

Blumenthal, J.M., Abreu-Grobois, F.A., Austin, T.J., Broderick, A.C., Bruford, M.W., Coyne, M.S., Ebanks-Petrie, G., Formia, A., Meylan, P.A., Meylan, A.B., & Godley, B.J. 2009. Turtle groups or turtle soup: dispersal patterns of hawksbill turtles in the Caribbean. *Molecular Ecology,* 18(23), 4841-4853.

Bonjean, F., & Lagerloef, G.S.E. 2002. Diagnostic model and analysis of the surface currents in the tropical Pacific Ocean. *Journal of Physical Oceanography,* 32(10), 2938-2954.

Burnham, & Anderson. 2002 Model selection and multimodel inference: a practical information-theoretic approach. *In* New York, New York, USA: Springer

Burnham, K.P., Anderson, D.R., & Huyvaert, K.P. 2011. AIC model selection and multimodel inference in behavioral ecology: some background, observations, and comparisons. *Behavioral Ecology and Sociobiology,* 65(1), 23-35.

Carr, A. 1952. *Handbook of turtles: turtles of the United States, Canada, and Baja California*. Ithaca, New York, USA: Comstock Publishing Association.

Carr, A. 1962. Orientation problems in high seas travel and terrestrial movements of marine turtles. *American Scientist,* 50(3), 359-&.

Clements, S., Jepsen, D., Karnowski, M., & Schreck, C.B. 2005. Optimization of an acoustic telemetry array for detecting transmitter-implanted fish. *North American Journal of Fisheries Management,* 25(2), 429-436.

Cresswell, G.R. 2000. Coastal currents of northern Papua New Guinea, and the Sepik River outflow. *Marine and Freshwater Research,* 51(6), 553-564.

Davenport, J. 1987. Locomotion in hatchling leatherback turtles (*Dermochelys coriacea*). *Journal of Zoology,* 212, 85-101.

Dutton, P.H., Bowen, B.W., Owens, D.W., Barragan, A., & Davis, S.K. 1999. Global phylogeography of the leatherback turtle (Dermochelys coriacea). *Journal of Zoology,* 248, 397-409.

Dutton, P.H., Hitipeuw, C., Zein, M., Benson, S.R., Petro, G., Pita, J., Rei, V., Ambio, L., & Bakarbessy, J. 2007. Status and genetic structure of nesting populations of leatherback turtles (Dermochelys coriacea) in the western Pacific. *Chelonian Conservation and Biology,* 6(1), 47-53.

ESRI. 2011. ArcGIS Desktop: Release 10. *In* Redlands, CA: Environmental Systems Research Institute.

Gaspar, P., Benson, S.R., Dutton, P.H., Réveillère, A., Jacob, G., Meetoo, C., Dehecq, A., & Fossette, S. 2012. Oceanic dispersal of juvenile leatherback turtles: going beyond passive drift modeling. *Marine Ecology Progress Series,* 457, 265.

Gearheart, G., Maturbongs, A., Dutton, P.H., Sprintall, J., Kooyman, G.L., Tapilatu, R.F., & Johnstone, E. 2011. Tracking Leatherback (Dermochelys coriacea) Hatchlings at Sea Using Radio and Acoustic Tags. *Marine Turtle Newsletter,* 130.

Gordon, A.L., Sprintall, J., Van Aken, H.M., Susanto, D., Wijffels, S., Molcard, R., Ffield, A., Pranowo, W., & Wirasantosa, S. 2010. The Indonesian throughflow during 2004-2006 as observed by the INSTANT program. *Dynamics of Atmospheres and Oceans,* 50(2), 115-128.

GRDC. 2014. GIS layers 405 & 687. GRDC in the Bundesanstalt fuer Gewaesserkunde, 56068 Koblenz, Germany http://grdc.bafg.de.

Gyuris, E. 1994. The rate of predation by fishes on hatchlings of the green turtle (*Chelonya mydas*). *Coral Reefs,* 13(3), 137-144.

Hamann, M., Grech, A., Wolanski, E., & Lambrechts, J. 2011. Modelling the fate of marine turtle hatchlings. *Ecological Modelling,* 222(8), 1515-1521.

Hasegawa, T., Ando, K., Mizuno, K., Lukas, R., Taguchi, B., & Sasaki, H. 2010. Coastal upwelling along the north coast of Papua New Guinea and El Niño events during 1981–2005. *Ocean Dynamics,* 60(5), 1255-1269.

Hastie, T.J., & Tibshirani, R.J. 1990. *Generalized Additive Models*. CRC Press.

Higgins, H., Mackey, D., & Clementson, L. 2006. Phytoplankton distribution in the Bismarck Sea north of Papua New Guinea: the effect of the Sepik River outflow.

Deep Sea Research Part I: Oceanographic Research Papers, 53(11), 1845-1863.

Hilterman, M., & Goverse, E. 2003. Aspects of nesting and nest success of the leatherback turtle (Dermochelys coriacea) in Suriname, 2002. *Guianas Forests and Environmental Conservation Project (CFECP). Technical report. Amsterdam, the Netherlands World Wildlife Fund Guianas/Biotopic Foundation*.

Hitipeuw, C., Dutton, P.H., Benson, S., Thebu, J., & Bakarbessy, J. 2007. Population status and internesting movement of leatherback turtles, Dermochelys coriacea, nesting on the northwest coast of Papua, Indonesia. *Chelonian Conservation and Biology,* 6(1), 28-36.

Hristova, H.G., & Kessler, W.S. 2012. Surface Circulation in the Solomon Sea Derived from Lagrangian Drifter Observations*. *Journal of Physical Oceanography,* 42(3), 448-458.

IUCN. 2013. The IUCN Red-list of Threatened Species: *Dermochelys coriacea*. *In*.

Jones, T.T., Reina, R.D., Darveau, C.A., & Lutz, P.L. 2007. Ontogeny of energetics in leatherback (Dermochelys coriacea) and olive ridley (Lepidochelys olivacea) sea turtle batchlings. *Comparative Biochemistry and Physiology a-Molecular & Integrative Physiology,* 147(2), 313-322.

Kashino, Y., Ueki, I., Kuroda, Y., & Purwandani, A. 2007. Ocean variability north of New Guinea derived from TRITON buoy data. *Journal of Oceanography,* 63(4), 545-559.

Kawabe, M., Kashino, Y., & Kuroda, Y. 2008. Variability and linkages of new guinea coastal undercurrent and lower equatorial intermediate current. *Journal of Physical Oceanography,* 38(8), 1780-1793.

Kuroda, Y. 2000. Variability of currents off the northern coast of New Guinea. *Journal of oceanography,* 56(1), 103-116.

Le Borgne, R., Feely, R.A., & Mackey, D.J. 2002. Carbon fluxes in the equatorial Pacific: a synthesis of the JGOFS programme. *Deep Sea Research Part II: Topical Studies in Oceanography,* 49(13), 2425-2442.

Lehodey, P., Bertignac, M., Hampton, J., Lewis, A., & Picaut, J. 1997. El Nino Southern Oscillation and tuna in the western Pacific. *Nature,* 389(6652), 715-718.

Lohmann, K.J., Cain, S.D., Dodge, S.A., & Lohmann, C.M.F. 2001. Regional magnetic fields as navigational markers for sea turtles. *Science,* 294(5541), 364-366.

Lohmann, K.J., & Lohmann, C.M.F. 1993. A light-independent magnetic compass in the leatherback sea-turtle. *Biological Bulletin,* 185(1), 149-151.

Lohmann, K.J., & Lohmann, C.M.F. 1996. Orientation and open-sea navigation in sea turtles. *Journal of Experimental Biology,* 199(1), 73-81.

Lukas, R., Yamagata, T., & McCreary, J.P. 1996. Pacific low-latitude western boundary currents and the Indonesian throughflow. *Journal of Geophysical Research-Oceans,* 101(C5), 12209-12216.

Lumpkin, R., & Pazos, M. 2007. Measuring surface currents with Surface Velocity Program drifters: the instrument, its data, and some recent results. *Lagrangian Analysis and Prediction of Coastal and Ocean Dynamics*, 39-67.

Lutz, P.L., Musick, J.A., & Wyneken, J. 2002. *The biology of sea turtles*. CRC press.

Marshall, A., & Beehler, B. 2007. The Ecology of Papua: Part II. *In* Periplus, Singapore.

Messie, M., & Radenac, M.H. 2006. Seasonal variability of the surface chlorophyll in the western tropical Pacific from SeaWiFS data. *Deep-Sea Research Part I-Oceanographic Research Papers,* 53(10), 1581-1600.

Muchtar, M. 2004. IndoTROPICS studies on the plume of the Mamberamo river into the Bismarck Sea, West Papua, Indonesia. *Continental shelf research,* 24(19), 2521-2533.

Nittrouer, C., & Brunskill, G. 1994. The gateway for terrestrial material entering the ocean. *EOS Transactions,* 75, 191-191.

Ohlmann, J.C. 2011. Drifter Observations of Small-Scale Flows in the Philippine

Archipelago. *Oceanography,* 24(1), 122-129.

Ohlmann, J.C., White, P.F., Sybrandy, A.L., & Niiler, P.P. 2005. A new kind of drifter to observe the coastal ocean. *Bulletin of the American Meteorological Society,* 86(9), 1219-1221.

Okuyama, J., Abe, O., Nishizawa, H., Kobayashi, M., Yoseda, K., & Arai, N. 2009. Ontogeny of the dispersal migration of green turtle (Chelonia mydas) hatchlings. *Journal of Experimental Marine Biology and Ecology,* 379(1-2), 43-50.

Okuyama, J., Kitagawa, T., Zenimoto, K., Kimura, S., Arai, N., Sasai, Y., & Sasaki, H. 2011. Trans-Pacific dispersal of loggerhead turtle hatchlings inferred from numerical simulation modeling. *Marine Biology,* 158(9), 2055-2063.

Polovina, J.J., Balazs, G.H., Howell, E.A., Parker, D.M., Seki, M.P., & Dutton, P.H. 2004. Forage and migration habitat of loggerhead (Caretta caretta) and olive ridley (Lepidochelys olivacea) sea turtles in the central North Pacific Ocean. *Fisheries Oceanography,* 13(1), 36-51.

Putman, N.F., Bane, J.M., & Lohmann, K.J. 2010. Sea turtle nesting distributions and oceanographic constraints on hatchling migration. *Proceedings of the Royal Society B-Biological Sciences,* 277(1700), 3631-3637.

R Development Core Team. 2010. R: A language and environment for statistical computing. *In* R Foundation for Statistical Computing, Vienna, Austria. .

Reich, K.J., Bjorndal, K.A., & Bolten, A.B. 2007. The 'lost years' of green turtles: using stable isotopes to study cryptic lifestages. *Biology Letters,* 3, 712-714.

Revelles, M., Isem-Fontanet, J., Cardona, L., Felix, M.S., Carreras, C., & Aguilar, A. 2007. Mesoscale eddies, surface circulation and the scale of habitat selection by immature loggerhead sea turtles. *Journal of Experimental Marine Biology and Ecology,* 347(1-2), 41-57.

Richards, S.A. 2008. Dealing with overdispersed count data in applied ecology. *Journal of Applied Ecology,* 45(1), 218-227.

Ruppel, M., Lund, M.T., Grythe, H., Rose, N.L., Weckström, J., & Korhola, A.

2013. Comparison of Spheroidal Carbonaceous Particle Data with Modelled Atmospheric Black Carbon Concentration and Deposition and Air Mass Sources in Northern Europe, 1850–2010. *Advances in Meteorology,* 2013.

Salmon, M., Jones, T.T., & Horch, K.W. 2004. Ontogeny of diving and feeding behavior in juvenile seaturtles: Leatherback Seaturtles (Dermochelys coriacea L) and Green Seaturtles (Chelonia mydas L) in the Florida current. *Journal of Herpetology,* 38(1), 36-43.

Salmon, M., & Lohmann, K.J. 1989. Orientation cues used by hatchling loggerhead sea turtles (*Caretta caretta*) during their offshore migration. *Ethology,* 83(3), 215-228.

Sarti Martinez, L., Barragan, A.R., Munoz, D.G., Garcia, N., Huerta, P., & Vargas, F. 2007. Conservation and biology of the leatherback turtle in the Mexican Pacific. *Chelonian Conservation and Biology,* 6(1), 70-78.

Scott, R., Marsh, R., & Hays, G.C. 2012. A little movement orientated to the geomagnetic field makes a big difference in strong flows. *Marine biology,* 159(3), 481-488.

Shillinger, G.L., Di Lorenzo, E., Luo, H., Bograd, S.J., Hazen, E.L., Bailey, H., & Spotila, J.R. 2012. On the dispersal of leatherback turtle hatchlings from Mesoamerican nesting beaches. *Proceedings of the Royal Society B: Biological Sciences,* 279(1737), 2391-2395.

Smith, W.H.F., & Sandwell, D.T. 1997. Global sea floor topography from satellite altimetry and ship depth soundings. *Science,* 277(5334), 1956-1962.

Spotila, J.R., Reina, R.D., Steyermark, A.C., Plotkin, P.T., & Paladino, F.V. 2000. Pacific leatherback turtles face extinction. *Nature,* 405(6786), 529-530.

Sybrandy, A.L., Niiler, P.P., & Ocean, T. 1991. *The WOCE/TOGA SVP Lagrangian drifter construction manual*. University of California, San Diego, Scripps Institution of Oceanography.

Tapilatu, R.F., Dutton, P.H., Tiwari, M., Wibbels, T., Ferdinandus, H.V., Iwanggin, W.G., & Nugroho, B.H. 2013. Long-term decline of the western Pacific leatherback, Dermochelys coriacea: a globally important sea turtle population. *Ecosphere,*

4(2), art25.

Tapilatu, R.F., & Tiwari, M. 2007. Leatherback turtle, Dermochelys coriacea, hatching success at Jamursba-Medi and wermon beaches in Papua, Indonesia. *Chelonian Conservation and Biology,* 6(1), 154-158.

Thums, M., Whiting, S.D., Reisser, J.W., Pendoley, K.L., Pattiaratchi, C.B., Harcourt, R.G., McMahon, C.R., & Meekan, M.G. 2013. Tracking sea turtle hatchlings—A pilot study using acoustic telemetry. *Journal of Experimental Marine Biology and Ecology,* 440, 156-163.

Tiwari, M., Dutton, D.L., & Garner, J.A. 2011. Nest relocation: a necessary management tool for Western Pacific leatherback nesting beaches. *Conservation of Pacific sea turtles.*, 87-96.

Ueki, I., Kashino, Y., & Kuroda, Y. 2003. Observation of current variations off the New Guinea coast including the 1997-1998 El Nino period and their relationship with Sverdrup transport. *Journal of Geophysical Research-Oceans,* 108(C7).

Ware, D.M., & Thomson, R.E. 2005. Bottom-up ecosystem trophic dynamics determine fish production in the Northeast Pacific. *science,* 308(5726), 1280-1284.

Witherington, B.E. 1991. Orientation of hatchling loggerhead turtles at sea off artificially lighted and dark beaches. *Journal of Experimental Marine Biology and Ecology,* 149(1), 1-11.

Wood, S.N. 2001. mgcv: GAMs and generalized ridge regression for R. *R news,* 1(2), 20-25.

Wyneken, J. 1997. Sea turtle locomotion: mechanisms, behavior, and energetics. *The biology of sea turtles,* 1, 165-198.

Wyneken, J., & Salmon, M. 1992. Frenzy and postfrenzy swimming activity in loggerhead green and leatherback hatchling sea turtles. *Copeia,* (2), 478-484.

Wyrtki, K. 1961. Physical oceanography of the southeast Asian waters.

Table 3.1: Deployment schedule of ten Microstar Lagrangian surface drifters deployed off the Bird's Head Peninsula in 2012-2013. Track length and drifter velocities are given.

Begin location		Drifter #	Deployment Begin	Deployment End	End location		Track length km	Track length days	Mean velocity $m.s^{-1}$	Mean velocity (±SE)
Jamursba Medi	(132.513; -0.339)	OIST-68	7/11/12	7/21/12	Ayau Archipelago*	(131.110; 0.334)	232	10	0.247	(0.003)
		OIST-69	8/14/12	9/5/12	Halmahera Sea	(130.238; 0.795)	494	22	0.284	(0.004)
		OIST-70	7/18/12	9/13/12	NGCC (north)	(141.359; 0.501)	2,712	57	0.556	(0.005)
		OIST-71	7/26/12	9/8/12	NGCC (north)	(138.834; 1.285)	2,265	44	0.583	(0.004)
		OIST-72	8/6/12	9/11/12	Halmahera Eddy	(130.275; 2.851)	775	36	0.264	(0.002)
Wermon	(132.867;-0.431)	OIST-73	11/22/12	3/7/13	New Ireland	(151.769; -1.793)	3,001	105	0.441	(0.004)
		OIST-74	11/29/12	12/27/12	Manokwari*	(134.035; -0.243)	383	28	0.14	(0.016)
		OIST-75	2/17/13	4/15/13	Bismarck Sea	(149.343; -4.711)	2,655	57	0.251	(0.015)
		OIST-76	2/21/13	2/26/13	Manokwari†	(134.188; -0.39)	52	5	0.245	(0.024)
		OIST-77	2/21/13	4/4/13	Bismarck Sea	(148.277; -3.424)	2,044	42	0.426	(0.025)

*Drifter picked up by local fishermen.
†Drifter initially deployed in Feb. 2013, picked up by fisherman, and recovered at his house in Manokwari. It was redeployed in June 2013 off Jamursba Medi, yielding an incomplete dataset, which was subsequently discarded.

Table 3.2: Evaluation of candidate models for dispersal speed (*dv*) based on Akaike Information Criterion (AIC). Models were sorted from best to worst. Estimated degrees of freedom of smoothing term (Edf), percentage of deviance explained and AIC differences (Δ_i) are also given.

Model	Linear predictor	Edf of smoother	Deviance explained (%)	AIC	Δ_i
M1	*dv~ s(hrs)+age•tet*	8.93	34.1	-1023.01	0
M2	*dv~ s(hrs)+age+tet*	8.93	33.6	-1020.17	2.84
M3	*dv~s(hrs)+tet*	8.91	32.8	-1014.1	8.91
M4	*dv~tet+age*	-	24.9	-933.27	89.74
M5	*dv~tet*	-	16.8	-849.37	173.64
M6	*dv~s(hrs)+age*	8.95	16.9	-830.14	192.87
M7	*dv~s(hrs)*	8.81	14.4	-809.07	213.94
M8	*dv~age*	-	6.77	-749.43	273.58

Table 3.3: Results of near-shore tracking experiments with simultaneous drifter deployments. 15-minute turtle tracks (n) were classified according to the current direction (Bc) and current speed class (Vc) they were in. Mean dispersal speed, $\bar{v}_t$ (with tracking unit on) and direction, $\overline{\Phi}_t$, are given. ±95% CI = lower and upper 95% confidence bounds. Model vector parameters $\bar{v}_t$ and $\overline{\Phi}_t$ are computed using the least squares equations given in Figs 9 and 10, respectively, for current direction classes Bc1 to Bc 8 and speed classes Vc 1 to Vc 8. The median of each speed class range is used to calculate $\vec{v}_t$ (Eq.3), which is then plugged into the least squares equation for the $\bar{v}_t$ versus $\vec{\Phi}_t$ relationship (Eq.4) to determine $\vec{\Phi}_t$. In our model, we used the mean *swimming speed* and swimming direction for currents <0.03 $m.s^{-1}$. We applied a correction factor of 1.76 to the dispersal speed vectors for t=0 to t=24 hours, in currents >0.03 $m.s^{-1}$, to account for faster swimming during the initial swimming frenzy (i.e. we canceled out the effect of drag of the tracking unit). Zeroes in the table occurred in currents flowing in opposite direction of hatchling's swimming direction, so that $\vec{v}_t \leq 0$. In these cases, the turtle dispersal vectors were set equal to the corresponding current vectors (passive drift).

Current speed ($m.s^{-1}$)		Current direction class	Bc 1 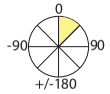		Bc 2 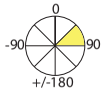		Bc 3-Bc 4 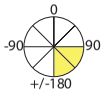		Bc 5 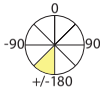		Bc 6 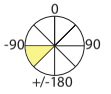		Bc 7 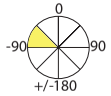		Bc 8 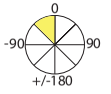	
			$\vec{v}_t$	$\vec{\Phi}_t$	$\vec{v}_t$	$\vec{\Phi}_t$	$\vec{v}_t$	$\vec{\Phi}_t$	$\vec{v}_t$	$\vec{\Phi}_t$	$\vec{v}_t$	$\vec{\Phi}_t$	$\vec{v}_t$	$\vec{\Phi}_t$	$\vec{v}_t$	$\vec{\Phi}_t$
class	Range (median)	n	5	2	11	10	11	3	11	11	43	8	43	37	5	3
Vc 1	.03-.2 (.115)	mean	0.21	-1.67	0.12	35.52	0.09	59.26	0.09	1.87	0.21	-54.88	0.21	-29.29	0.21	-1.31
		±95% CI	0.37 0.05	26.48 -59.1	0.2 0.05	46.98 24.05	0.3 0.02	93.81 24.7	0.3 0.02	18.54 -14.8	0.29 0.13	-37.88 -71.87	0.29 0.13	-20.48 -38.09	0.37 0.05	41.78 -44.41
Vc 2	.2-.3 (.25)	mean	0.27	-6.52	0.08	37.11	0	0	0	0	0.28	-56.64	0.28	-32.09	0.27	-12.5
		±95% CI	0.49 0.04	26.29 -66.87	0.19 0.01	47.16 27.06	--	--	--	--	0.29 0.18	-37.58 -75.68	0.29 0.18	-22.05 -42.12	0.49 0.04	35.89 -60.92
Vc 3	.30-.47 (.39)	mean	0.33	-11.38	0.04	38.71	0	0	0	0	0.37	-58.89	0.37	-35.69	0.33	-23.70
		±95% CI	0.62 0.04	26.10 -74.67	0.19 0.008	47.35 33.08	--	--	--	--	0.50 0.23	-37.20 -80.57	0.50 0.23	-24.07 -47.30	0.62 0.04	30 -77.42
Vc 4	.47-.6 (.535)	mean	0.39	-16.23	0*	0	0	0	0	0	0.45	-60.9	0.45	-38.89	0.39	-34.89
		±95% CI	0.75 0.03	25.91 -82.47	--	--	--	--	--	--	0.62 0.28	-36.86 -84.92	0.62 0.28	-25.86 -51.91	0.75 0.03	24.11 -93.93
Vc 5	.6-.72 (.66)	mean	0.44	-20.27	0	0	0	0	0	0	0.52	-62.65	0.52	-41.69	0.44	-44.22
		±95% CI	0.87 0.02	25.75 -88.97	--	--	--	--	--	--	0.72 0.33	-36.56 -88.73	0.72 0.33	-27.43 -55.94	0.87 0.02	19.2 -107.7
Vc 6	.72-.8 (.76)	mean	0.49	-24.32	0	0	0	0	0	0	0.58	-64.15	0.58	-44.09	0.49	-53.55
		±95% CI	0.97 0.01	25.59 -95.47	--	--	--	--	--	--	0.79 0.36	-36.30 -91.99	0.79 0.36	-28.78 -59.39	0.97 0.01	14.29 -121.4
Vc 7	.8-.87 (.835)	mean	0.52	-26.74	0	0	0	0	0	0	0.62	-65.16	0.62	-45.69	0.52	-59.15
		±95% CI	1.03 0.01	25.5 -99.37	--	--	--	--	--	--	0.86 0.39	-36.13 -94.17	0.86 0.39	-29.68 -61.7	1.03 0.01	11.35 -129.7
Vc 8	.87-1.5 (1.185)	mean	0.67	-38.87	0	0	0	0	0	0	0.83	-70.42	0.83	-54.1	0.67	-87.14
		±95% CI	1.35 0.001	25.02 -118.87	--	--	--	--	--	--	1.14 0.52	-35.24 -105.59	1.14 0.52	-34.39 -73.79	1.35 0.001	-3.38 -170.9

Figure 3.1: West Papua's Bird's Head Peninsula (top right) and leatherback nesting sites of Jamursba Medi and Wermon with individual beaches.

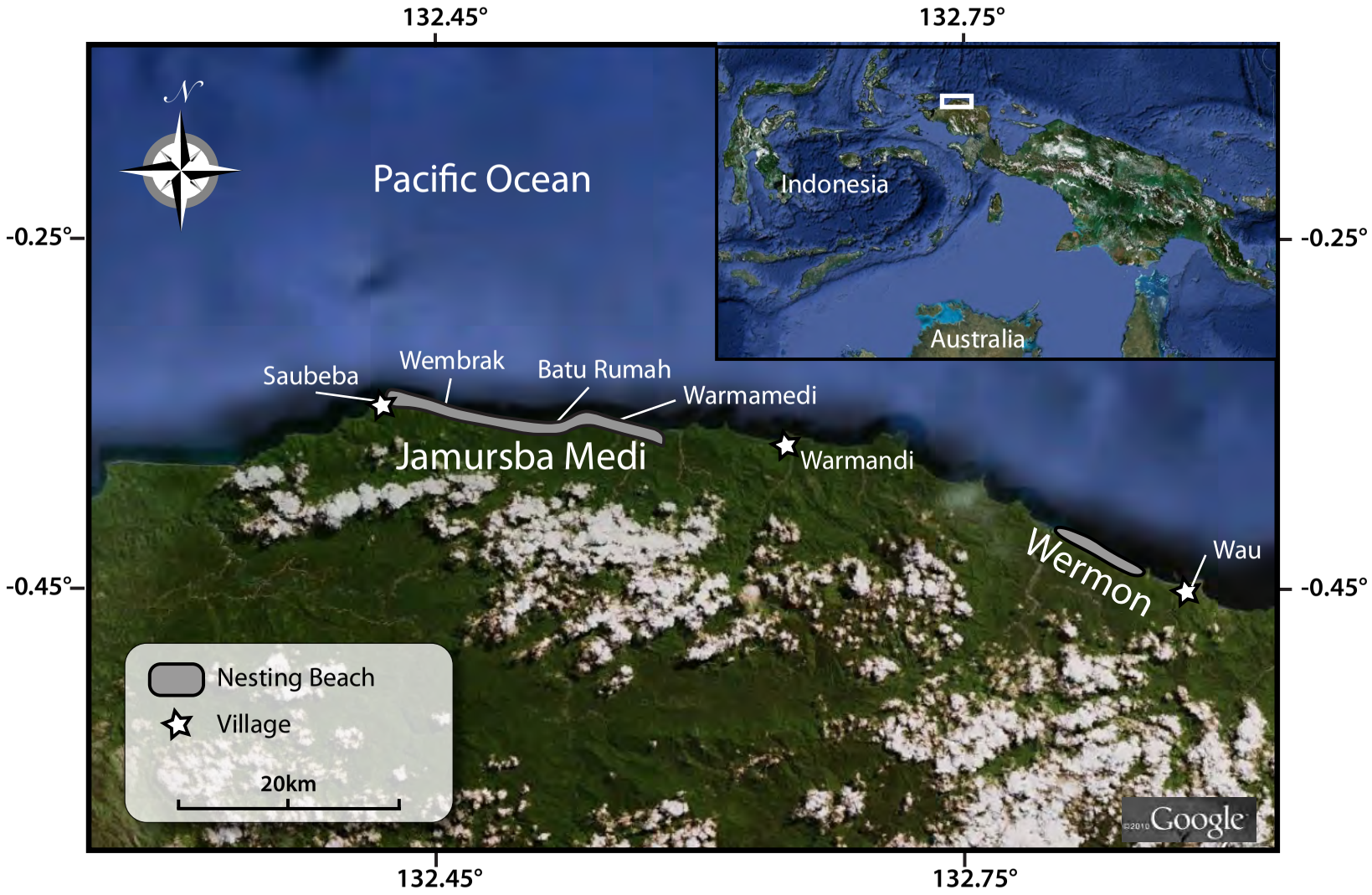
132.45°
132.75°
-0.25°
-0.45°
N
Pacific Ocean
Indonesia
Australia
Saubeba
Wembrak
Batu Rumah
Warmamedi
Jamursba Medi
Warmandi
Wermon
Wau
Nesting Beach
Village
20km
©2010 Google

Figure 3.2: Trajectories of 26 leatherback hatchlings tracked in July-August 2010-2011 at Jamursba Medi. Divergence between the mean direction of swimming for each track, given by the rosette, and the direction of the track suggests the existence of a westward surface current. Tracks that were affected by this current are indicated in red. Tracks where mean direction of the track and mean swimming direction were similar (tracks not affected by the current) are indicated in green. Full lines indicate portions of the tracks where turtles were dragging the tracking unit, while dashed lines indicate the portion of the tracks where turtles were swimming freely.

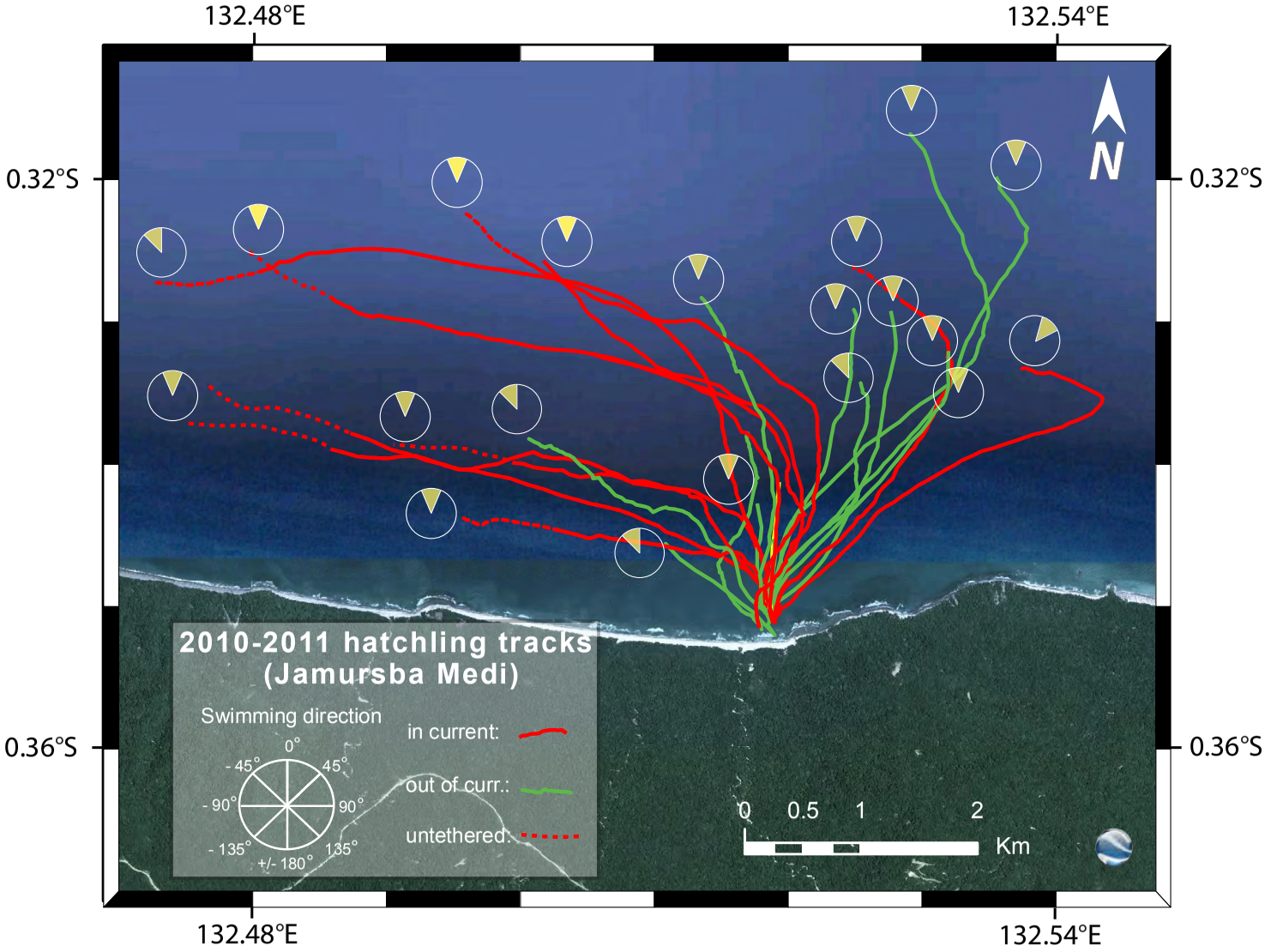
132.48°E
132.54°E
0.32°S
0.36°S
N
2010-2011 hatchling tracks
(Jamursba Medi)
Swimming direction
0°
- 45°
45°
- 90°
90°
- 135°
135°
+/- 180°
in current:
out of curr.:
untethered:
0 0.5 1 2
Km

Figure 3.3: Left panel shows boxplots (median, quartiles, data range and outliers) of the interaction term (*age*)•(*tet*) of model M1. Only the combinations that were significantly different ($p<0.05$) from the baseline model (*age*<24h• *untethered*) are given. Note the 76% increase in dispersal speed, *dv*, of turtles of *age*<24 hrs when they were untethered from the tracking unit. Right panel shows the estimated smooth term for *hrs*, hours past the full or new moon. Data locations are given by the black bars. Values of *f*(*hrs*) are given in the linear predictor scale (i.e. in log[*dv*]). Note the increase in *dv* at around 75 and 200 hrs, suggesting the influence of a tidal current on dispersal speed.

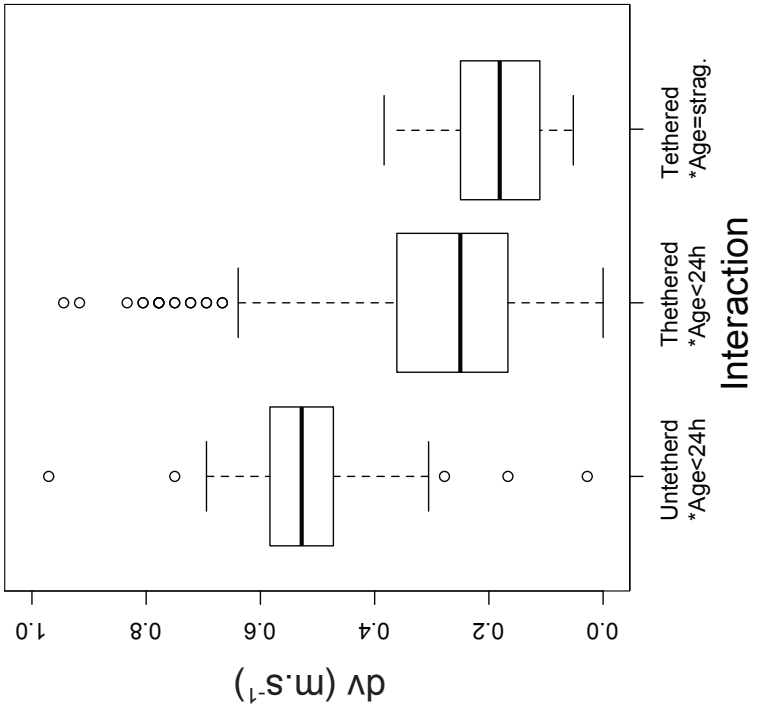
dv (m.s-1)
0.0
0.2
0.4
0.6
0.8
1.0
Untetherd *Age<24h
Thethered *Age<24h
Tethered *Age=strag.
Interaction

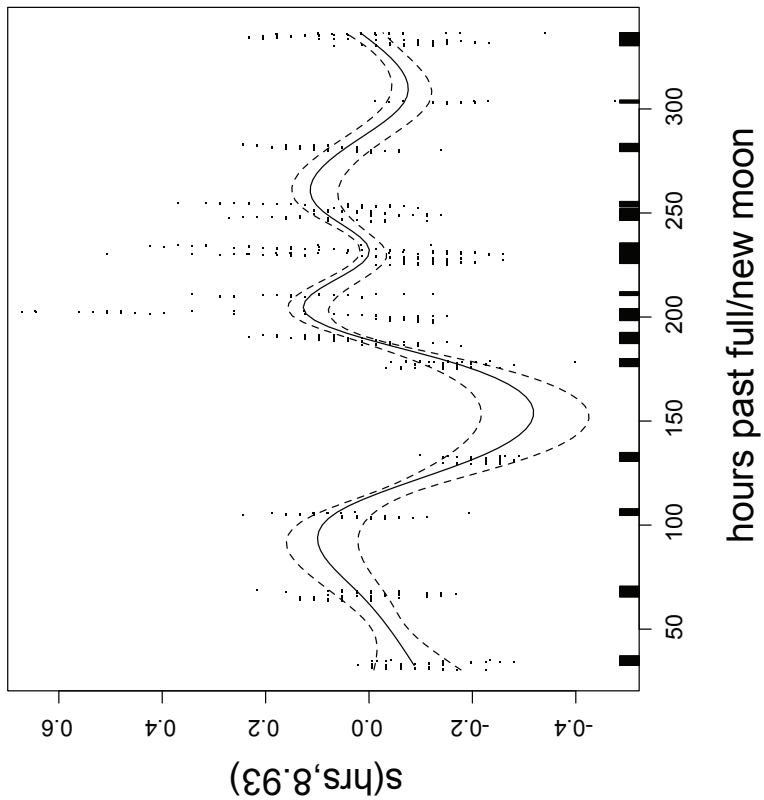
s(hrs,8.93)
-0.4
-0.2
0.0
0.2
0.4
0.6
50
100
150
200
250
300
hours past full/new moon

Figure 3.4: Meso-scale tracks of five Microstar Lagrangian surface drifters, deployed in July-August 2012 at Jamursba Medi. Current speed in the vicinity of the coast of the Bird's Head Peninsula (<15 km) did not exceed 0.5 $m.s^{-1}$. Drifters did not enter the Dampier Strait but took a NW route toward the shallow waters of Ayau, where drifter 68 was picked up, probably by a local fisherman.

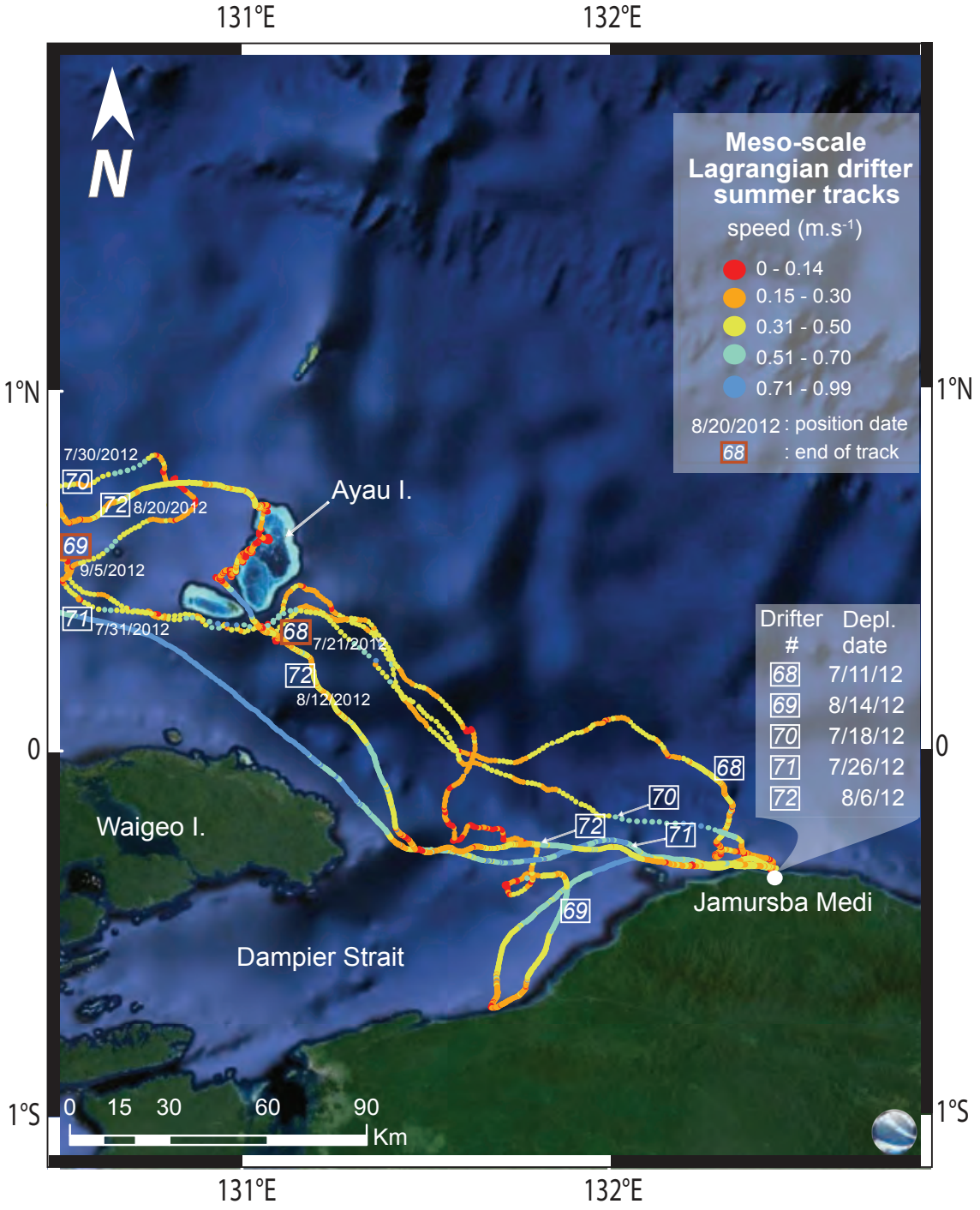
131°E
132°E
1°N
0
1°S
N
Meso-scale Lagrangian drifter summer tracks
speed (m.s-1)
0 - 0.14
0.15 - 0.30
0.31 - 0.50
0.51 - 0.70
0.71 - 0.99
8/20/2012 : position date
68 : end of track
Drifter # Depl. date
68 7/11/12
69 8/14/12
70 7/18/12
71 7/26/12
72 8/6/12
Ayau I.
Waigeo I.
Dampier Strait
Jamursba Medi
7/30/2012
8/20/2012
9/5/2012
7/31/2012
7/21/2012
8/12/2012
0 15 30 60 90
Km

Figure 3.5: Large-scale tracks of five Microstar Lagrangian drifters, deployed in July-August 2012 at Jamursba Medi (JM), on West Papua's Bird's Head Peninsula (BHP). The approximate trajectory of the summer equatorward flow of the New Guinea Coastal Current (NGCC) is given according to Kashino et al. (2007) and Kawabe et al. (2008). The Halmahera Eddy (HE) is fully developed during the southeast trade-winds season. The highest velocities were recorded within the HE by drifters 70 and 71.

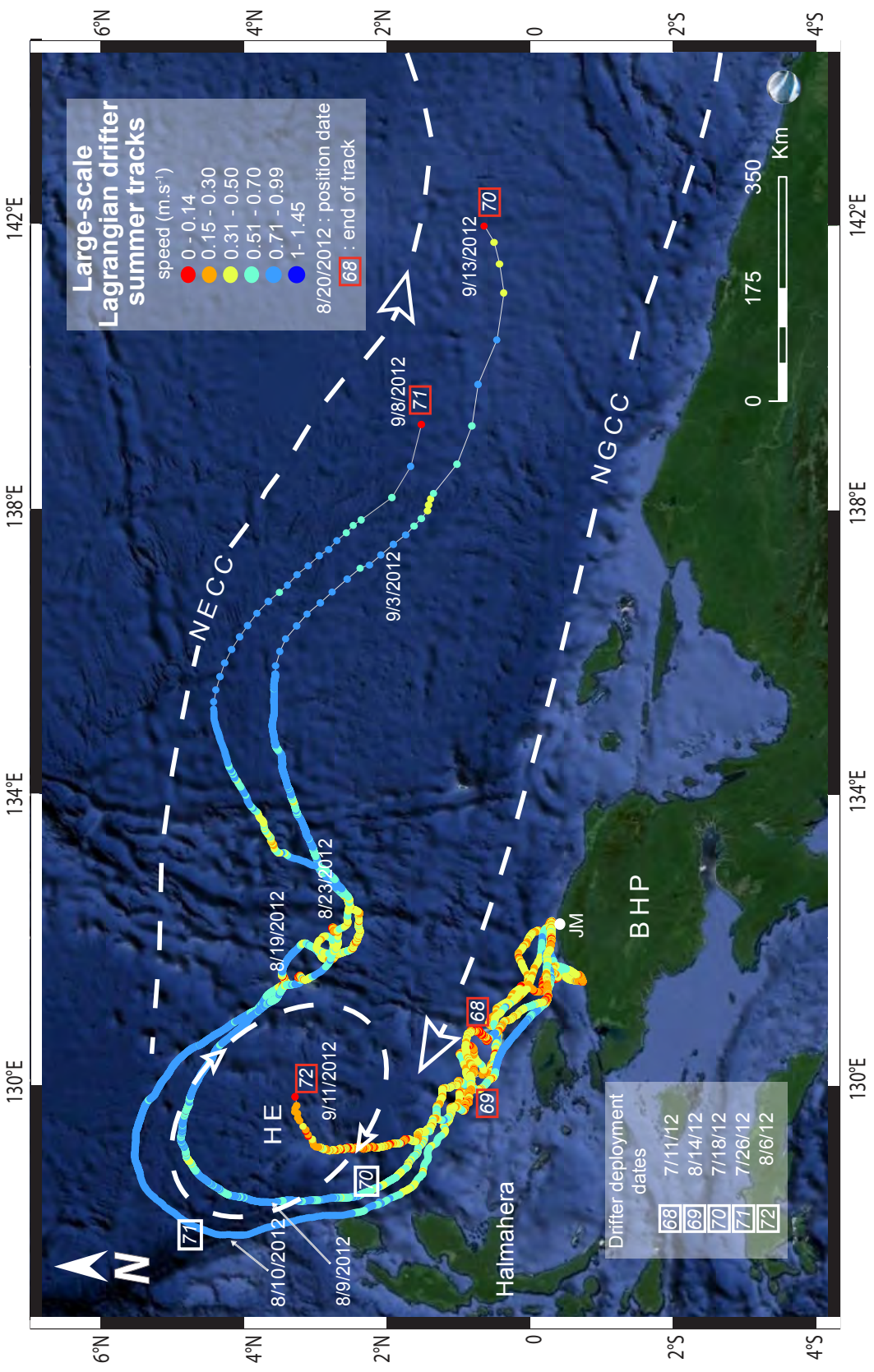
Large-scale
Lagrangian drifter
summer tracks
speed (m.s-1)
0 - 0.14
0.15 - 0.30
0.31 - 0.50
0.51 - 0.70
0.71 - 0.99
1 - 1.45
8/20/2012 : position date
68 : end of track
NECC
NGCC
HE
BHP
JM
Halmahera
N
0
175
350
Km
Drifter deployment dates
68 7/11/12
69 8/14/12
70 7/18/12
71 7/26/12
72 8/6/12
8/10/2012
8/9/2012
8/19/2012
8/23/2012
9/11/2012
9/3/2012
9/8/2012
9/13/2012
6°N
4°N
2°N
0
2°S
4°S
130°E
134°E
138°E
142°E

Figure 3.6: Near-shore and meso-scale tracks of the drifters deployed from Wermon (WM), in November 2012-February 2013. The gradual strengthening of the NGCC is noticeable from the trajectories of drifters 73 and 74 versus drifters 75-77, the former group lingered several weeks in the near-shore zone then, during the month of December, took a meandering eastward path, with drifter 74 traveling west before getting entrained in the NGCC (on 12/12/2012). The group deployed in February got caught in the NGCC at approximately 20 km from shore, traveling eastward at velocities > 0.6 $m.s^{-1}$.

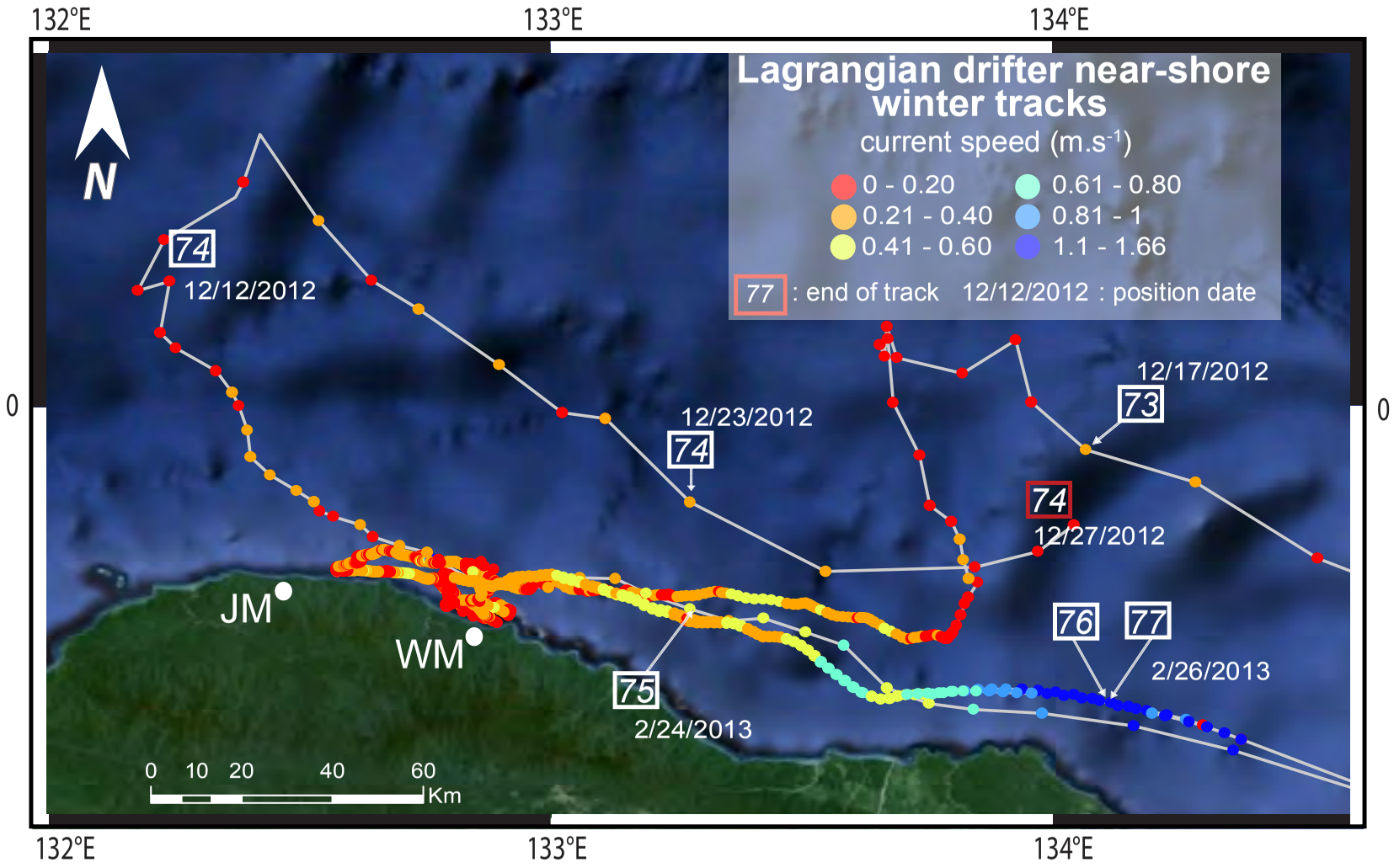
132°E
133°E
134°E
0
0
N
Lagrangian drifter near-shore winter tracks
current speed (m.s-1)
0 - 0.20
0.21 - 0.40
0.41 - 0.60
0.61 - 0.80
0.81 - 1
1.1 - 1.66
77 : end of track 12/12/2012 : position date
74
12/12/2012
12/23/2012
74
12/17/2012
73
74
12/27/2012
JM
WM
75
2/24/2013
76
77
2/26/2013
0 10 20 40 60
Km

Figure 3.7: Large-scale tracks of drifters deployed from Wermon, in November 2012-February 2013. Drifters 74 and 76 stopped transmitting off Manokwari when picked up by fishermen. An early deployment (drifter 73), during the transition phase of the NGCC, yielded a more northerly track that circumvented the Bismarck Sea. Current velocities sampled by this drifter were less than for drifters 75 and 77, illustrating the development of the NGCC during the course of the winter monsoon. Abbreviations: NB=New Britain, NI=New Ireland, MI=Manus Island, MKW=Manokwari.

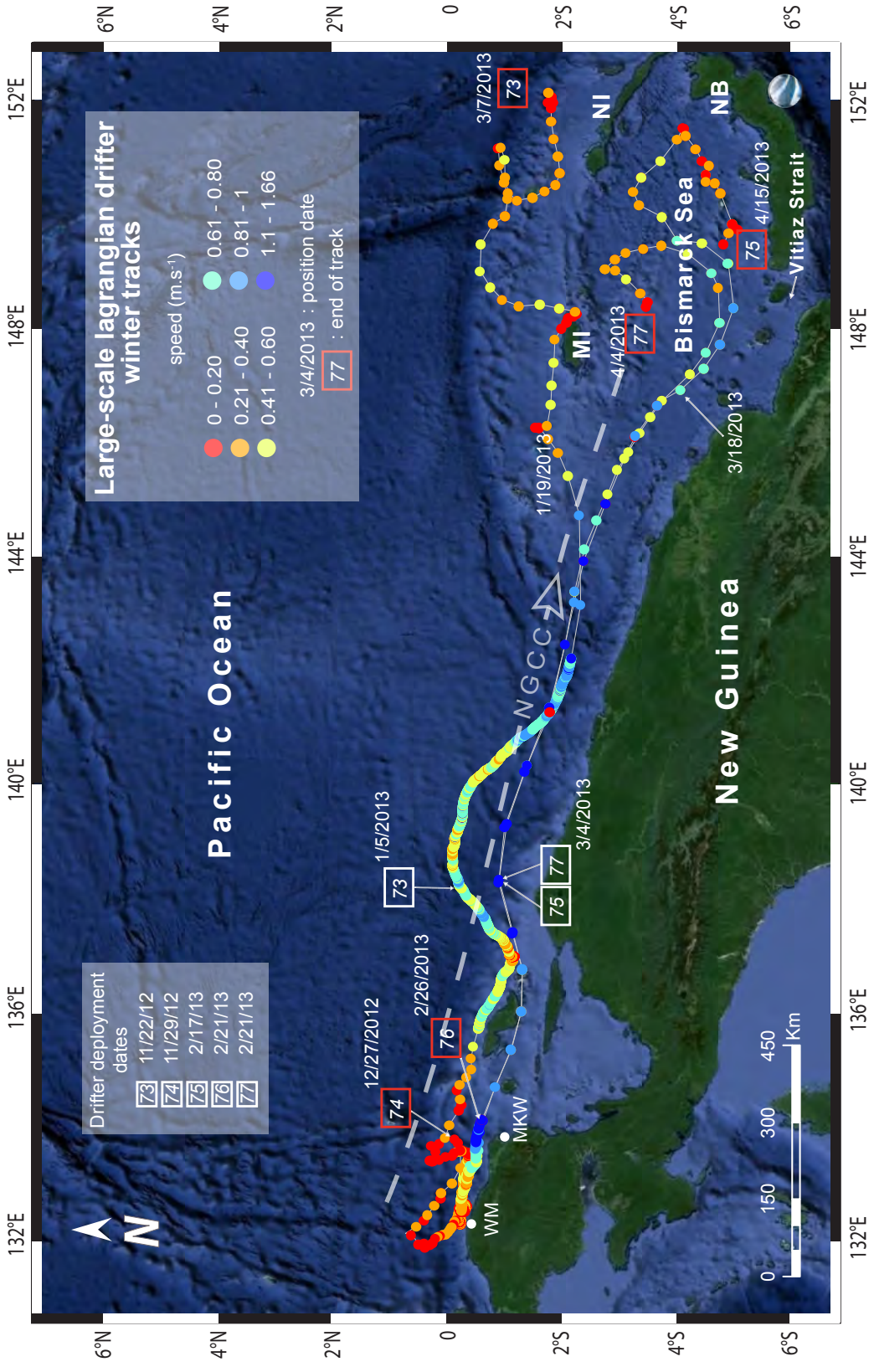
Large-scale lagrangian drifter winter tracks
speed (m.s-1)
0 - 0.20
0.21 - 0.40
0.41 - 0.60
0.61 - 0.80
0.81 - 1
1.1 - 1.66
3/4/2013 : position date
77 : end of track
Drifter deployment dates
73 11/22/12
74 11/29/12
75 2/17/13
76 2/21/13
77 2/21/13
Pacific Ocean
New Guinea
NGCC
MI
NI
NB
Bismarck Sea
Vitiaz Strait
WM
MKW
12/27/2012
1/5/2013
2/26/2013
3/4/2013
1/19/2013
3/7/2013
4/4/2013
3/18/2013
4/15/2013
0 150 300 450 Km
N
132°E
136°E
140°E
144°E
148°E
152°E
6°N
4°N
2°N
0
2°S
4°S
6°S

Figure 3.8: Hatchling tracking and simultaneous drifter deployments were carried out offshore Jamursba Medi in July-August 2012. The turtle tracks (circles) were 15 minutes long and position was recorded every minute. The Microstar drifter recorded position every 10 minutes (stars). White frames show the classification scheme of the data, yielding "track pairs" consisting of 15 turtle data points and 4 drifter data points. Current direction (Bc) and current speed (Vc), were determined for each track pair. Note that: (1) the drifters confirm the existence of a near-shore westward current flowing at approximately 0.3 $m.s^{-1}$, (2) hatchlings were able to deviate from this current's track within a very short time, (3) only a sample of the all the tracks is given here.

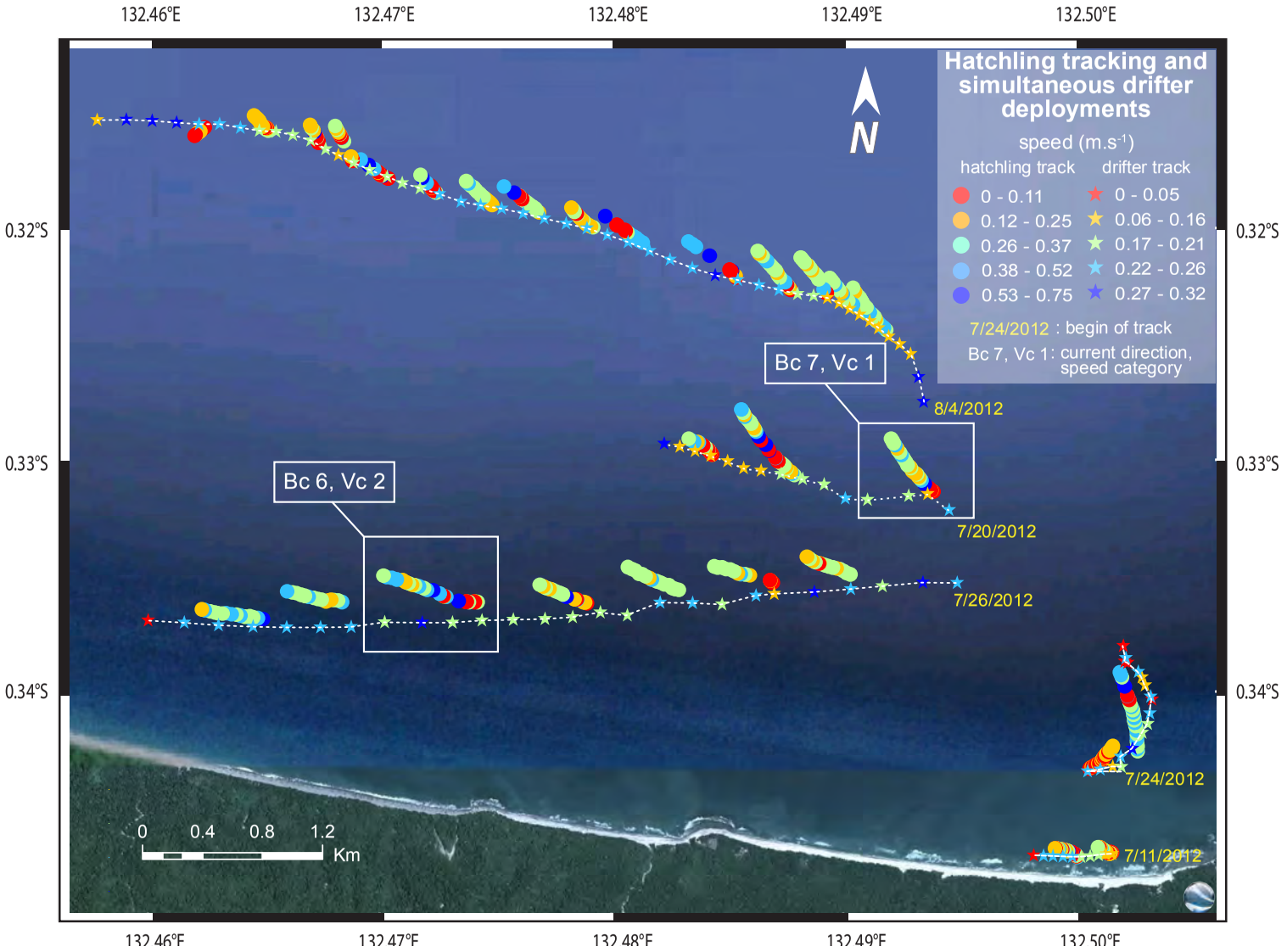
132.46°E
132.47°E
132.48°E
132.49°E
132.50°E
0.32°S
0.33°S
0.34°S
N
Hatchling tracking and simultaneous drifter deployments
speed (m.s-1)
hatchling track
drifter track
0 - 0.11
0.12 - 0.25
0.26 - 0.37
0.38 - 0.52
0.53 - 0.75
0 - 0.05
0.06 - 0.16
0.17 - 0.21
0.22 - 0.26
0.27 - 0.32
7/24/2012 : begin of track
Bc 7, Vc 1: current direction, speed category
Bc 7, Vc 1
Bc 6, Vc 2
8/4/2012
7/20/2012
7/26/2012
7/24/2012
7/11/2012
0 0.4 0.8 1.2
Km

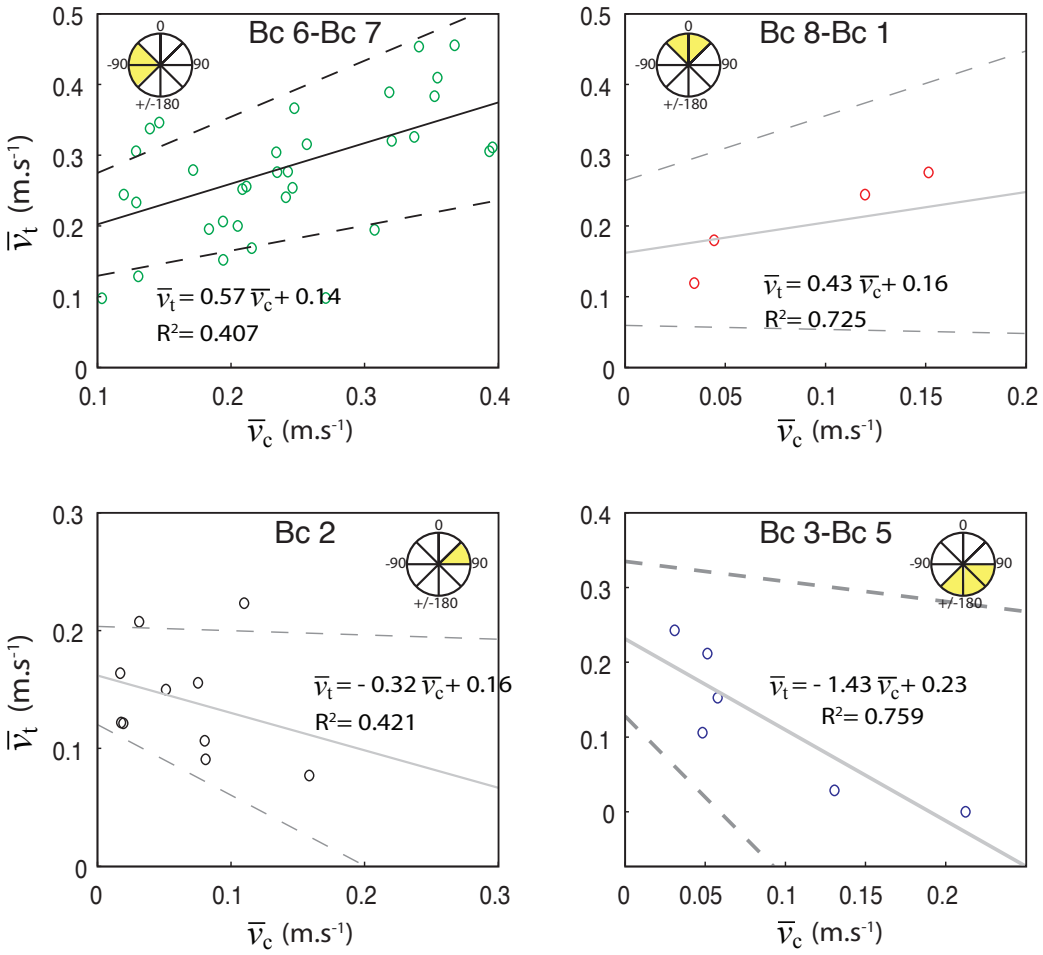

Figure 3.9: Relationship between the mean dispersal speed and mean current speed (m.s^{-1}), obtained during near-shore tracking experiments, for different current direction classes, Bc. The least squares and 95% confidence interval lines are given in grey (full and dashed, respectively). We used the least squares equations to calculate the dispersal speed vector (±95% CI) for current velocities beyond those measured during our experiments. Note the decrease in dispersal speed as current direction classes approaches values opposed to the mean NW-N (-45º to 0º) swimming direction (Bc 2 to Bc 5). In current flowing in the general direction of swimming (Bc 6 to Bc 1), the relationship is positive.

Figure 3.10: Relationship between hatchling dispersal speed, v_t, and dispersal direction Φ_t, obtained by plotting all the turtle track data (15 data points per turtle track) categorized into the different current scenario (Vc/Bc) they were in. The least squares and 95% confidence interval lines are given in grey (full and dashed, respectively). We see here that for current bearings that were not opposed to the NW-N (-45º to 0º) swimming direction (Bc 6-Bc 2) the turtles were able to keep a reasonably constant bearing, even as their dispersal speed increased (i.e., the current in which they were entrained had a higher speed), whereas for current directions Bc 3-Bc 5, the dispersal direction rapidly approached that of the current. Future work would enable to improve the dataset by increasing the sample size, especially in the Bc 8, Bc 3-Bc 4 and Bc 5 classes.

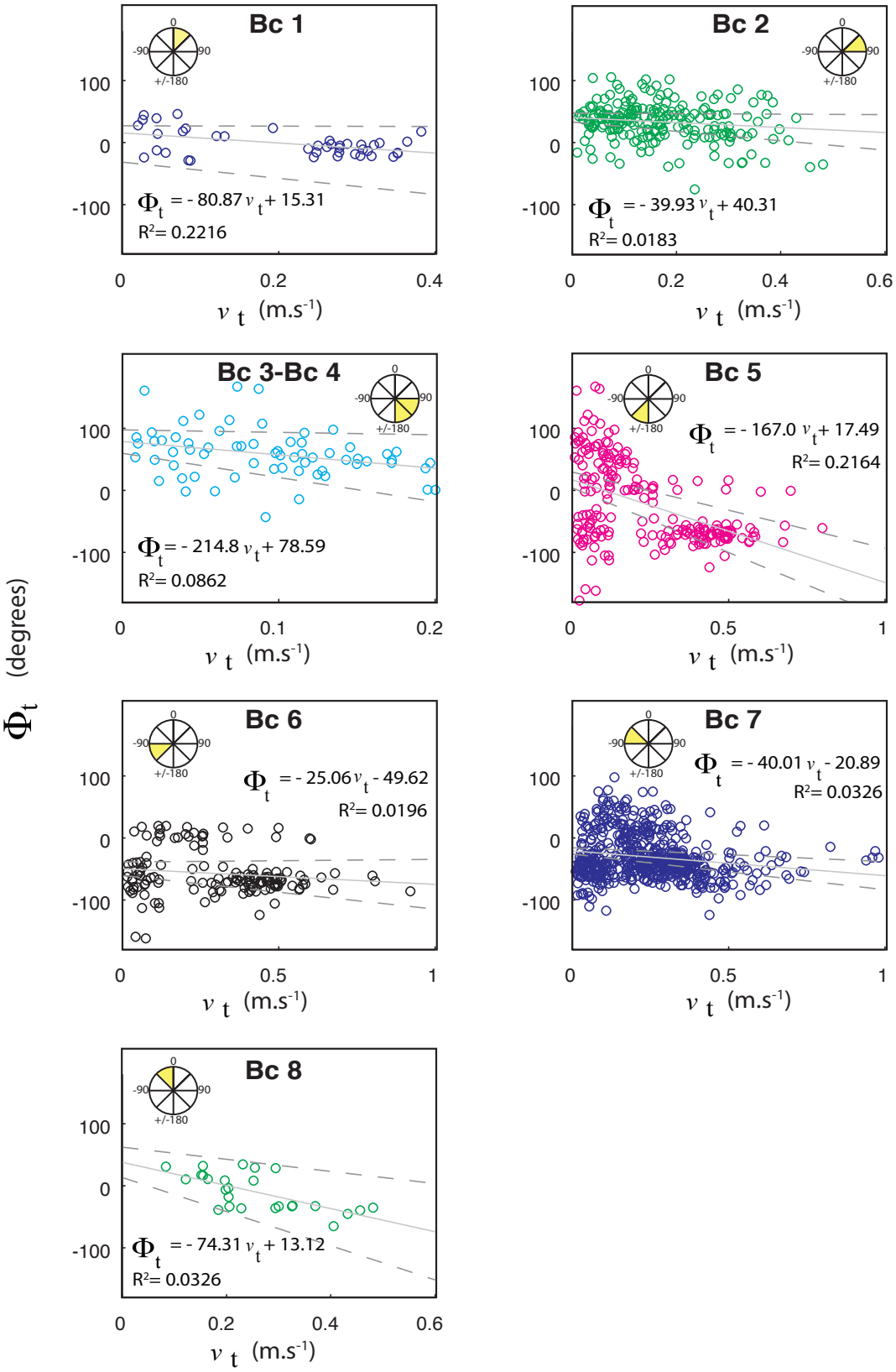
Bc 1
Φt = - 80.87 vt + 15.31
R²= 0.2216
Bc 2
Φt = - 39.93 vt + 40.31
R²= 0.0183
Bc 3-Bc 4
Φt = - 214.8 vt + 78.59
R²= 0.0862
Bc 5
Φt = - 167.0 vt + 17.49
R²= 0.2164
Bc 6
Φt = - 25.06 vt - 49.62
R²= 0.0196
Bc 7
Φt = - 40.01 vt - 20.89
R²= 0.0326
Bc 8
Φt = - 74.31 vt + 13.12
R²= 0.0326
Φt (degrees)
vt (m.s-1)
0
-90
90
+/-180

Figure 3.11: Summer dispersal model showing, in yellow, the tracks of 500 virtual hatchlings released simultaneously from Jamursba Medi on August 15th, 2012. The mean current track, calculated from drifters 68-72 is given in black. The turtles are able to deviate from the mean current's track at the initial stage of dispersal, then become entrained in the fast flows of the Halmahera Eddy. Exit is in chlorophyll-a poor waters at the western end of the NECC. The OSCAR near-surface currents, indicated by the black vectors, agree with our model. We used OSCAR data for the period August 15th-September 15th, 2012, which corresponds to the end point of the critical dispersal period. Note the absence of OSCAR data within 200 km of the coastline. Chlorophyll data is MODIS-A, monthly mean for September 2012, at 0.1° resolution (http://neo.sci.gsfc.nasa.gov/). White areas are data-deficient. Basemap: GEBCO (http://www.gebco.net/data_and_products/).

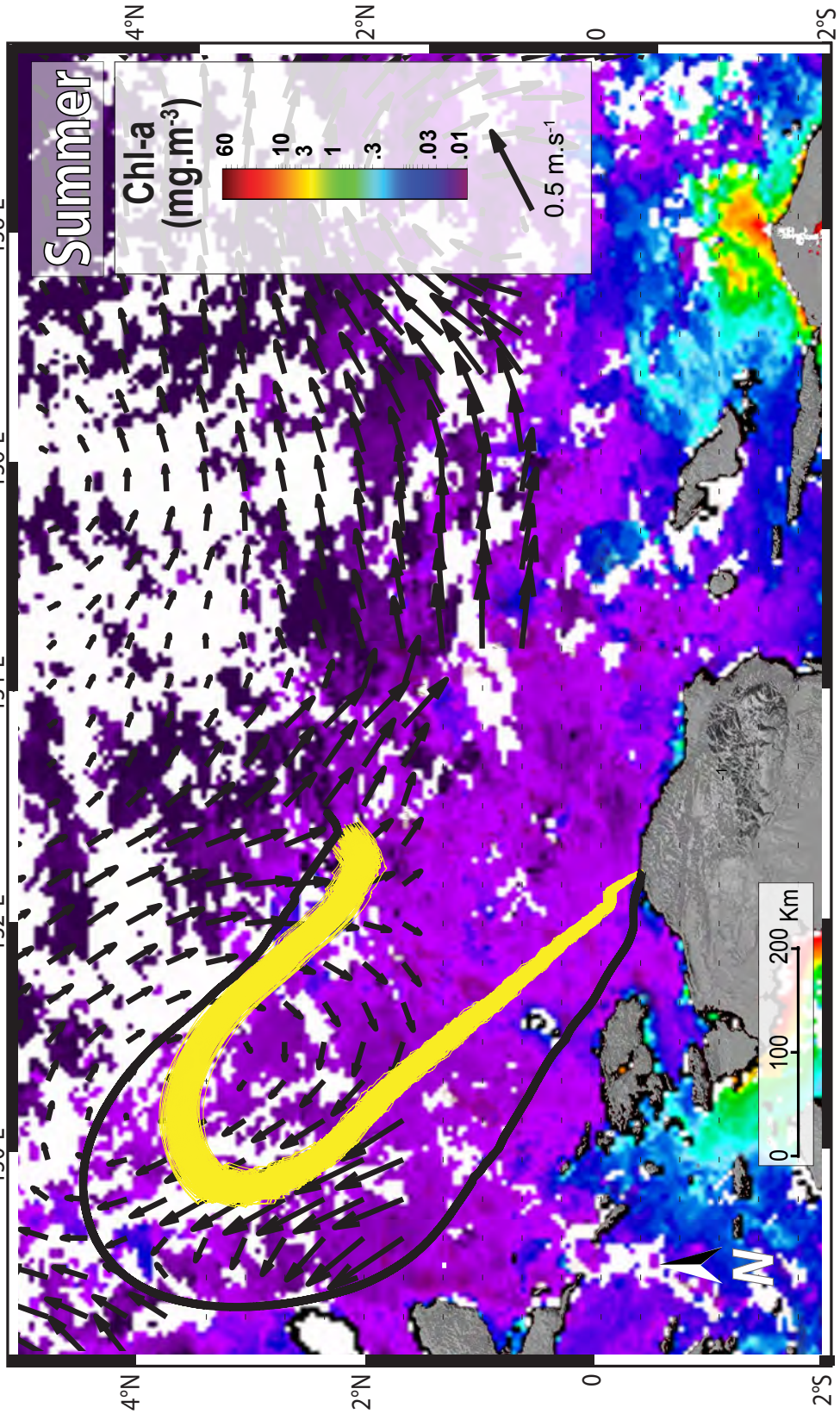
Summer
Chl-a
(mg.m-3)
60
10
3
1
.3
.03
.01
0.5 m.s-1
0
100
200 Km
N
130°E
132°E
134°E
136°E
138°E
4°N
2°N
0
2°S

Figure 3.12: Dispersal model for the winter monsoon transition period showing, in yellow, the tracks of 500 virtual hatchlings released simultaneously from Wermon, on November 22nd, 2012. The mean current track, calculated from drifters 73 and 74 is given in red. The turtles, under their own swimming are able to strongly deviate from the mean current's track until the third week, when the strengthening NGCC entrains them towards the east. Turtles are not able to reach the productive waters along the north coast of New Guinea, shown here at ~138°E, off the mouth of the Mamberamo river (GRDC, 2014). MODIS-A and OSCAR data are for the period November 15th to December 15th, 2012, which corresponds to the end point of the critical dispersal period. The offshore OSCAR current vector field is coherent with our model.

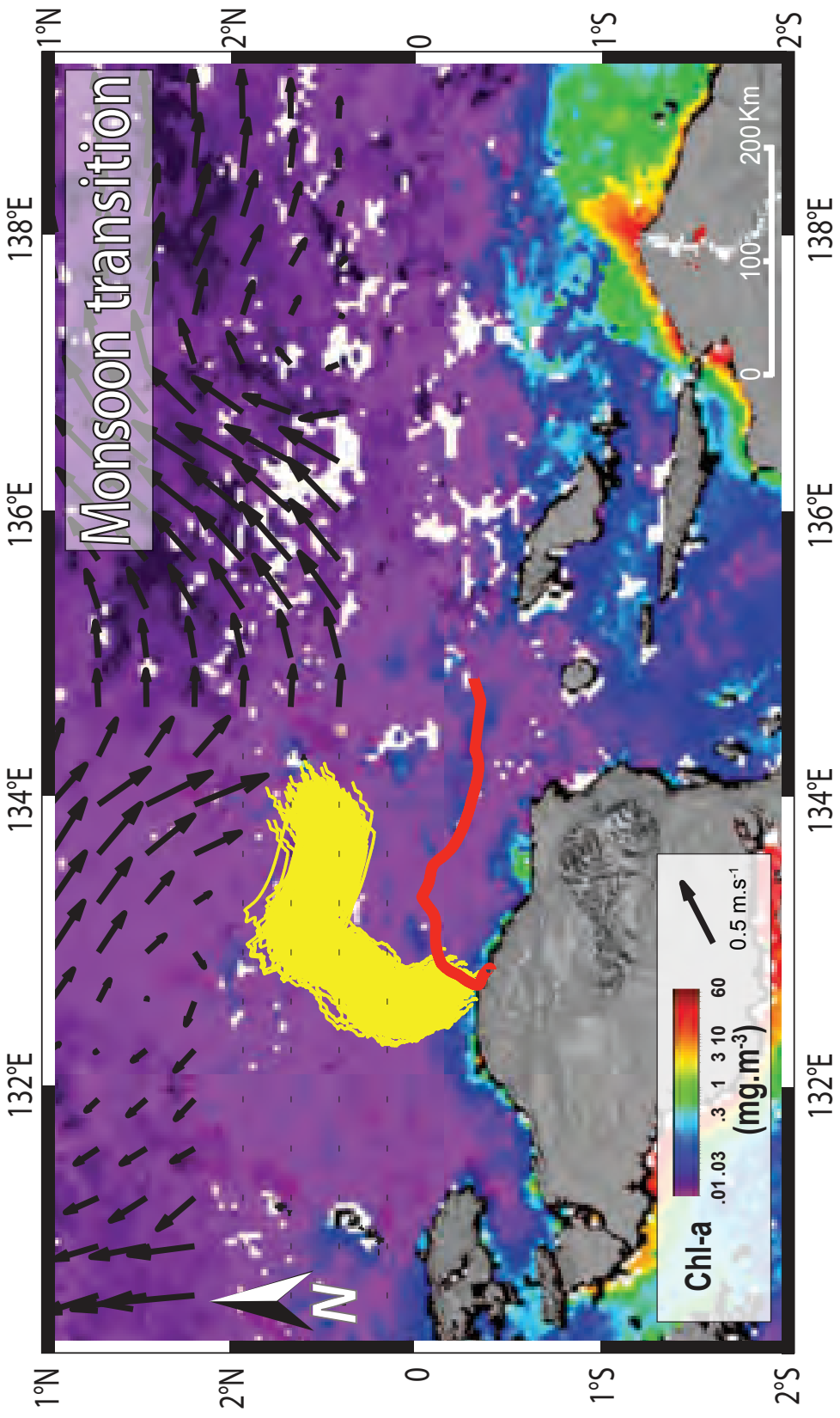
Monsoon transition
1°N
2°N
0
1°S
2°S
132°E
134°E
136°E
138°E
200 Km
100
0
N
Chl-a
.01 .03 .3 1 3 10 60
(mg.m-3)
0.5 m.s-1

Figure 3.13: Winter dispersal model. The tracks of 500 virtual hatchlings, released simultaneously from Wermon, on February 22nd, 2012, are given by the red lines. The mean current track, calculated from drifters 75-77, is given by the black line. Within a few kilometers from shore, the turtles become entrained into the fully developed NGCC. They are not able to deviate from its trajectory due to the combined effect of high current velocities (>0.8 $m.s^{-1}$) and bearing opposed to their swimming direction. The NGCC carries hatchlings into productive waters (indicated by the high chlorophyll-a concentration values) within the second week of dispersal (i.e., Mamberamo rivershed). This suggests that turtles born in winter may have better chances of finding food during and after the critical dispersal period. Major rivers, indicated in white (GRDC, 2014), drain sediments and nutrients from the central highlands, into the waters off the coast of New Guinea. Note the coherence between the offshore OSCAR current field and our model.

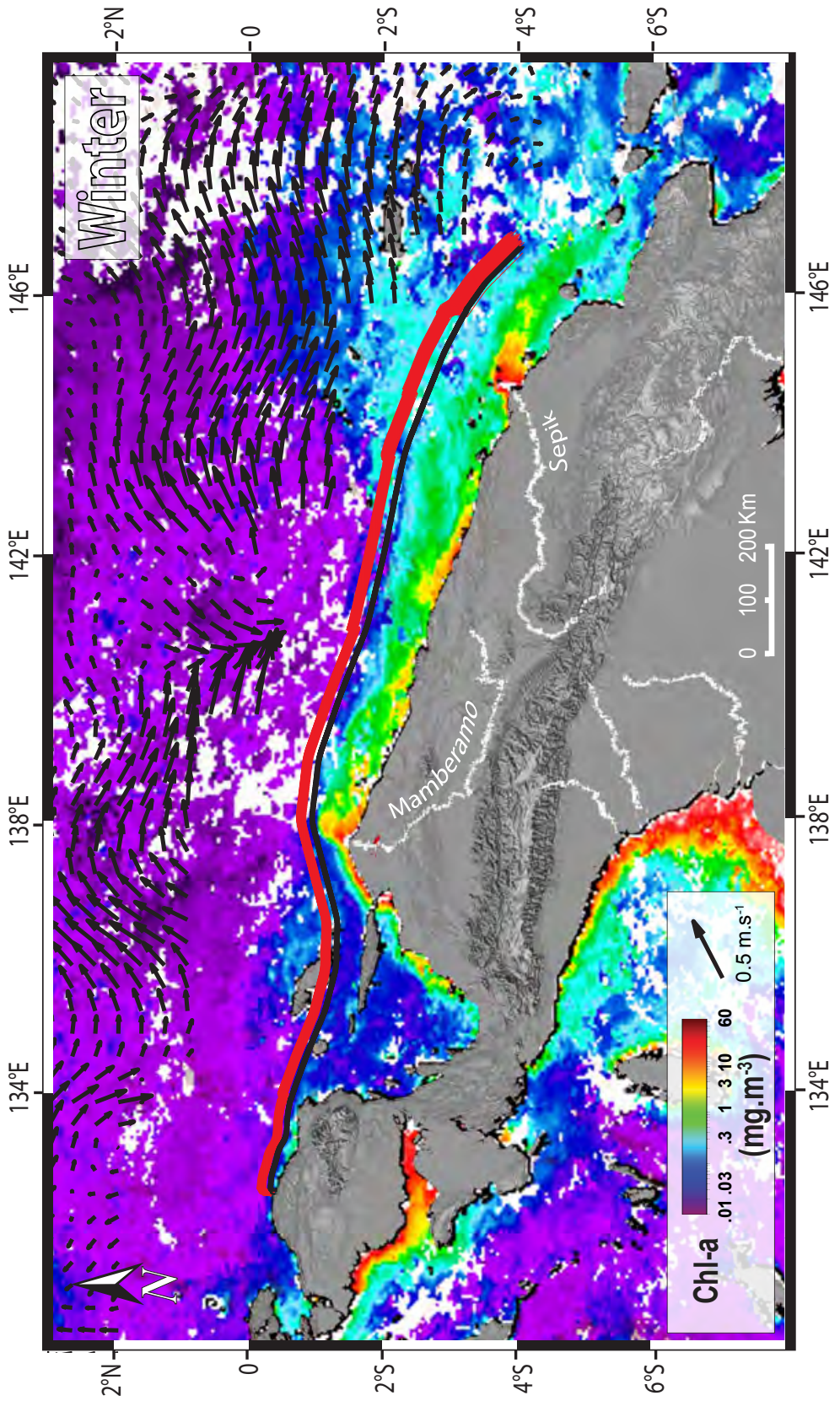
Winter
2°N
0
2°S
4°S
6°S
134°E
138°E
142°E
146°E
Mamberamo
Sepik
0 100 200 Km
Chl-a
.01 .03 .3 1 3 10 60
(mg.m-3)
0.5 m.s-1
N

Figure 3.14: Tracks of 274 Global Drifter Program (GDP) Surface Velocity Drifters, during the period January 2000 to June 2013 (all seasons are included), at a 6 hour sampling rate. Note: (1) the absence of tracks around the Birds'Head Peninsula, (2) no drifters traveled through the Dampier Strait (DS), (3) only one entered the Halmahera Sea (HS), (4) from a total of 35 drifters that crossed Vitiaz Strait (VS), none traveled southward. Mean velocity through VS was >0.5 $m.s^{-1}$ (Hristova & Kessler, 2012), suggesting that Vitiaz Strait is an unlikely conduit for hatchlings to reach the South Pacific. Bathymetry data: Smith & Sandwell (1997).

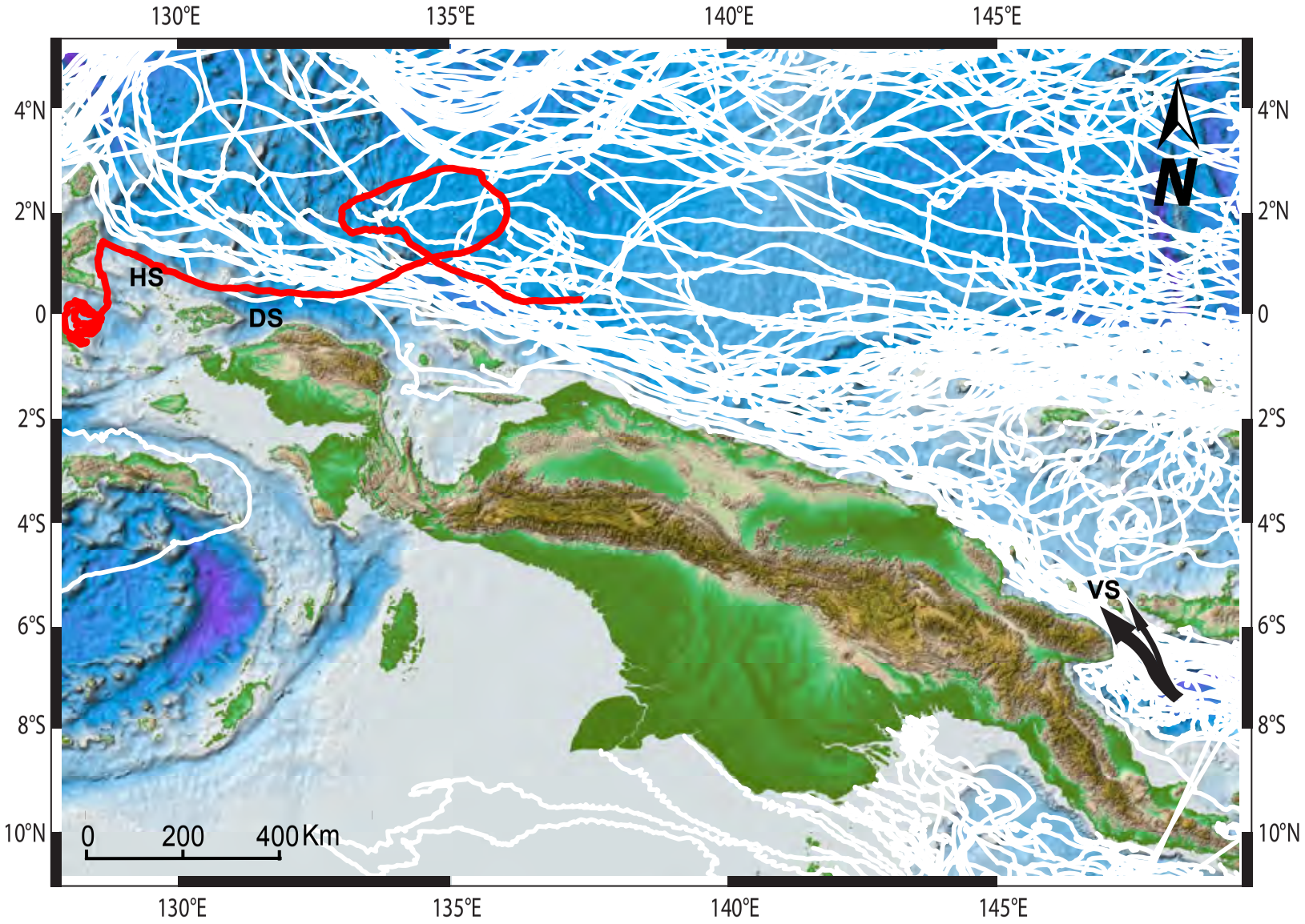
130°E
135°E
140°E
145°E
4°N
2°N
0
2°S
4°S
6°S
8°S
10°N
HS
DS
VS
N
0
200
400 Km

3.15: Summary schematic of potential dispersal pathways to the large-scale circulation. The colored arrows indicate dispersal from Bird's Head nesting beaches (departure from Jamursba Medi during the boreal summer and from Wermon during the monsoon transition and winter). The dashed arrow indicates exit from the Bismarck Sea of winter hatchlings after westward currents have abated, in early spring. The white stars indicate the location of turtles at the end of the critical dispersal period. NECC=north equatorial counter current; SEC=south equatorial current.

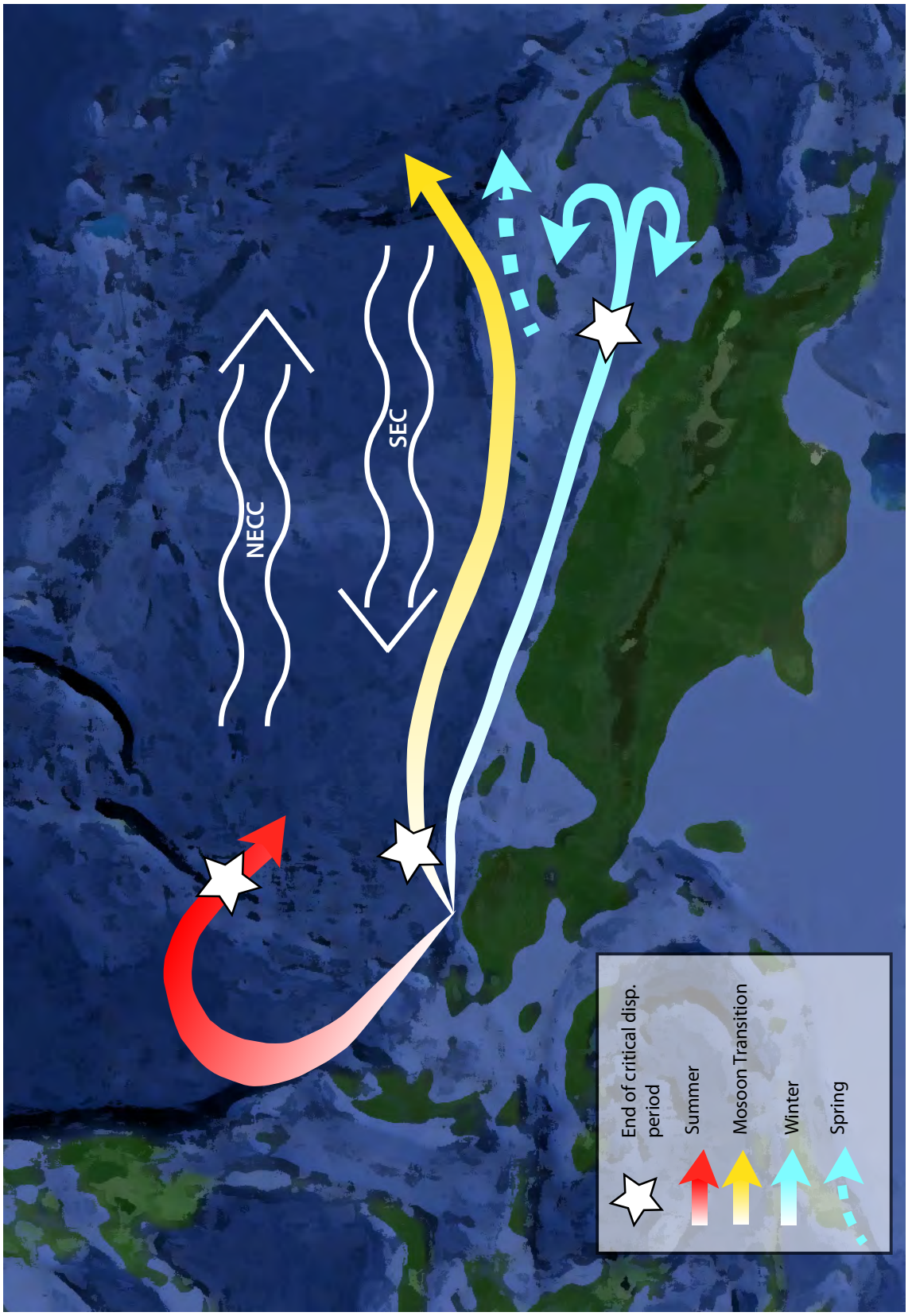
NECC
SEC
End of critical disp. period
Summer
Mosoon Transition
Winter
Spring

4

Migration front of post-moult emperor penguins

Polar Biol
DOI 10.1007/s00300-014-1449-2

SHORT NOTE

Migration front of post-moult emperor penguins

Geoffrey Gearheart · Gerald L. Kooyman · Kimberly T. Goetz · Birgitte I. McDonald

Received: 3 September 2013 / Revised: 2 January 2014 / Accepted: 4 January 2014

Abstract The moult is arguably the most critical period in the life of emperor penguins (*Aptenodytes forsteri*). Birds from western Ross Sea colonies travel yearly to and from the pack ice of the eastern Ross Sea to moult. Despite the suspected large numbers of penguins involved, this migration had never been directly observed. Here, we provide the first description of a migratory front of penguins travelling east to west between their moulting habitat and to the breeding colonies. Early autumn ship-bound visual surveys showed density of birds increased significantly as we approached the eastern Ross Sea and was not related to ice type, per cent ice cover or primary productivity. This supports the hypothesis of a dense "source" of post-moult birds in the eastern Ross Sea migrating in near-synchrony and gradually dispersing towards breeding colonies in the southwest and northwest Ross Sea. Emperor penguins travelled alone or in small groups of up to 8 individuals, concentrating around narrow leads or isolated water holes, and were occasionally seen far from open water, suggesting they move primarily by swimming, complemented by tobogganing. Their new coats indicated they had completed the moult. Aggregations of birds and guano stains suggested they were feeding while migrating.

G. Gearheart (✉) · G. L. Kooyman · B. I. McDonald
Center for Marine Biotechnology and Biomedicine, Scholander Hall, Scripps Institution of Oceanography, 9500 Gilman Drive No. 0204, La Jolla, CA 92093-0204, USA
e-mail: cortoeldemalta@yahoo.com.ar

K. T. Goetz
Department of Ecology and Evolutionary Biology, University of California, Long Marine Lab, 100 Shaffer Rd, Santa Cruz, CA 95060, USA

Keywords Post-moult migration · Moult · Emperor penguin · Penguin migration · Ross Sea · Sea ice · Antarctica

Introduction

Emperor penguins remain within the bounds of Antarctica's Seas and adjust well to the continent's extreme winter conditions (Wilson 1907; Prévost 1963). The yearly moult is perhaps the most dangerous and least understood period of their lifecycle. Lasting ~35 days, it takes place during the warmer months of January and February (Kooyman et al. 2000), when sea ice is receding around the continental coast (Cavalieri and Parkinson 2008). Due to their reduced thermal insulation and waterproofing, birds do not enter the water to forage; the ensuing fast can cause the loss of up to half of their pre-moult body mass (Groscolas 1978). The need to stay dry makes them dependent on floes that remain intact for at least one month, precluding most areas near breeding colonies in the western Ross Sea (WRS) as these become ice-free during summer. When finished moulting, the penguins, weakened from starvation, must resume feeding. Abundant prey in the immediate vicinity of the moult area is key to their survival (Kooyman et al. 2004).

The Ross Sea harbours seven emperor penguin colonies, six of which lie on its western shores (Fig. 1). Satellite telemetry showed that birds from four WRS colonies travel at least 1,200 km to moult in dense pack ice in the eastern Ross Sea (ERS; Kooyman et al. 2000). Kooyman et al. (2004) later confirmed post-moult penguins tagged in the ERS went back to WRS colonies (Fig. 1). This highlights the importance of the consistent heavy pack ice field of the ERS and Amundsen Sea as moulting habitat for emperor penguins.

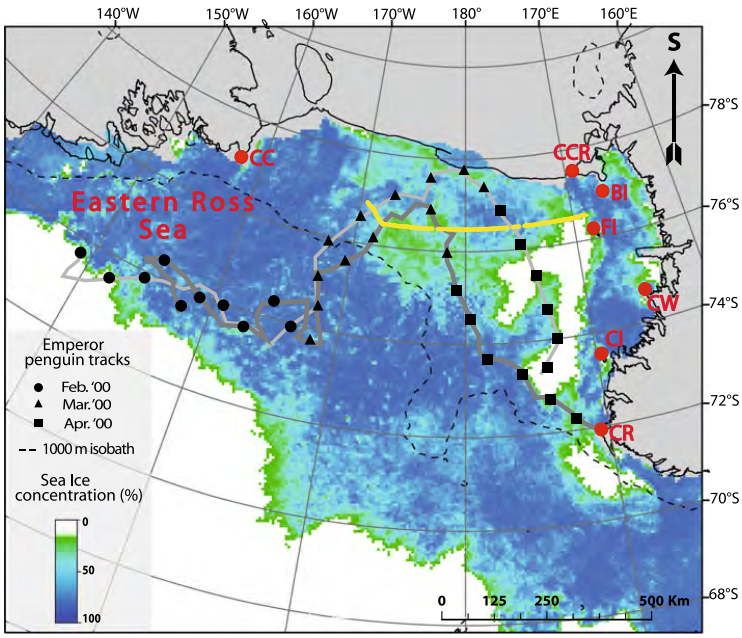

Fig. 1 Transect of the 2013 NBP cruise (*yellow*) and migratory routes (*grey*) of two penguins satellite-tracked in 2000 (data: Kooyman et al. 2004). Migratory routes coincide in space and time with the observed migration front. Sea ice concentration on March, 8th, 2013 (AMSR2, 6.25-km grid; Spreen et al. 2008) shows extensive pack ice coverage of the Ross Sea, including the transit section with only a few open areas in the WRS. Breeding colonies: *CR* Cape Roget, *CI* Coulman Isl., *CW* Cape Washington, *FI* Franklin Isl., *BI* Beaufort Isl., *CCR* Cape Crozier, *CC* Cape Colbeck. (Color figure online)

Arrival synchrony at breeding sites, a known trait in pygoscelid and emperor penguins (Prévost 1963; Lynch et al. 2012), implies concurrent departure and travel from the moulting areas (Battley 2006). This phenomenon has never been observed for emperor penguins in the ERS, despite the presence of large numbers of moulting birds (Kooyman et al. 2004), as it occurs at a time when most researchers have left Antarctica. Here, we report what we believe is the first sighting of a migration front of penguins travelling from ERS moulting floes back to their breeding colonies.

Materials and methods

Visual surveys were carried out aboard the icebreaker N.B Palmer during an early autumn cruise throughout the Ross Sea. This period corresponds to the end of the moulting season when birds in the ERS are travelling back to their colonies through reforming ice. The surveys consisted in uninterrupted daytime ("on-effort") counts of emperor penguins along a 450-km-long straight-line transect. This transect consisted in three on-effort sections following the 76.5°S parallel from 168°E to 171°W (Fig. 2), representing a longitudinal gradient from the breeding colonies to the ERS pack ice. The transect was characterized by a uniform seascape, precluding any edge effects on animal distribution (Buckland et al. 2001), and was within the known migration corridor of satellite-tracked penguins (Fig. 1). Transect width was 1000 m, beyond which penguins could not reliably be identified. An ipad 2 (Apple, Inc., Cupertino, CA, USA) with Bento (Filemaker, Inc., Santa Clara, CA, USA), a database application with an automatic georeferencing function, was used to record data. GPS data were fed into Bento by a BadElf Pro GPS unit (BadElf, West Hartford, CT, USA) with accuracy of 2.5 m. Each observation was referenced with a location and UTC time. Data on ice type and per cent ice cover (following the classification given by Smith 2007), sea state and weather were recorded when they changed. Information on behaviour (prior to the animals being flushed by the ship), life stage (juvenile/adult) and physiology (moulting/not moulting) was added whenever possible. Count data from on-effort sections were pooled a posteriori into 10-km bins to enable spatial comparisons and compute the mean density of penguins (sightings/kilometre along the transect, or the number of sightings in each bin divided by ten). Count data were analysed using stepwise generalized linear modelling (GLM) in R (R Development Core Team 2010), with "sightings/bin" as dependent variable and a quasi-Poisson model to account for overdispersion and excess zeroes. Location (latitude/longitude), ice type and percent ice cover, whose effect on the distribution of Antarctic birds is well documented (Ainley et al. 1984; Ballard et al. 2012), and chlorophyll-a (measured by underway fluorometry) were factored in the GLM as explanatory variables. QAIC

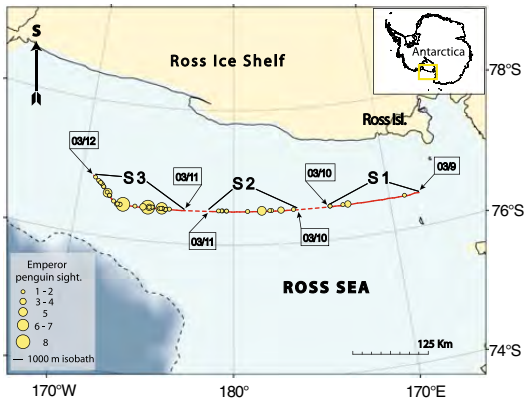

Fig. 2 West- to eastern Ross Sea transect along the 76.5°S parallel. "On" and "off-effort" (daytime and nighttime) portions given by the *solid* and *dashed red line*, respectively, with sects. 1–3 (S1–S3) totaling 450 km of on-effort surveys. Emperor penguin sightings (*yellow circles*) increase from west to east, suggesting birds are migrating back to breeding colonies. (Color figure online)

was used to select the best model (Richards 2008). Results are presented as mean ± standard error.

Results

From March 9 to 12, 2013, after completing the scientific agenda of other teams aboard the ship, the N.B Palmer transited from the WRS to ERS through a landscape of new ice (<25 cm thick) interspersed with small floes and 90–100 % ice cover. A total of 90 emperor penguins were observed, all of which had new coats, suggesting they had completed the moult. Chlorophyll-a concentration ranged from 0.04 to 1.44 mg m^3.

In Sect. 1 (164°W–173°W; Fig. 2), eight penguins (0.047 birds km^{-1}, ±0.024) were observed. Birds were standing upright or hauled out next to small leads or holes in the ice. They were either alone ($n = 2$) or clustered in 2 groups of 3 individuals. Most of this section was through new ice.

The density in Sect. 2 (March 10–11th) was 0.13 birds km^{-1} (±0.05), significantly higher than in Sect. 1 (Wilcoxon rank-sum test (WRSP), $P = 0.036$). From a total of 12 birds, one lone individual was seen standing with no open water in sight; the remaining birds were along narrow leads or next to isolated open water holes. Penguins were standing upright or hauled out on new ice or small floes in slightly larger groups of up to 5 individuals.

As the ship progressed along the 76.5°S line in Sect. 3 (March 11–12th), these aggregations became larger, with clusters of up to 8 birds (Fig. 3). The density of penguins along Sect. 3 was 0.38 birds km^{-1} (±0.1); three times that

Fig. 3 Group of 8 emperor penguins aggregated around a water hole at 76.5°S, 171.5°E

of Sect. 2 (WRSP, $P = 0.021$). All 70 penguins counted in this section were standing or hauled out next to leads and water holes. Large, dark-coloured guano stains were frequently observed, especially along leads.

The most parsimonious GLM model included only *longitude*, a proxy for distance to the ERS pack ice (Table 1).

Discussion

The environmental constraints of finding an area of stable pack ice with abundant food may force emperor penguins to travel yearly to the same region in the ERS. As 6 of the 7 breeding colonies of the Ross Sea are located on its western shores, the conditions are met for a synchronous flux of a large number of birds entering and leaving the ERS pack ice through a relatively narrow corridor. The return routes of two post-moult penguins satellite-tracked in 2000 were south of 75.5°S during the months of February and March (Kooyman et al. 2004), roughly the same latitudinal section and timeline as our cruise (Fig. 1).

One of the striking aspects of our surveys (confirmed by the most parsimonious GLM model, which included only the covariate *longitude*) was the gradual increase in the number of penguins as the ship approached the ERS: from a lone individual 40 km SE of Franklin Island, the location of a breeding colony, the sightings of small groups of birds became more frequent as the ship travelled eastward. As it was not possible to survey during the night, the gaps between 173.5°E–176.0°E and 178.6°W–176.6°W were not filled (Fig. 2). However, this trend of increasing density of penguins is likely to hold true for the entire transect, with the highest concentrations of birds close to the source (ERS pack ice, Fig. 1), and a gradual decrease towards the West as birds had yet to reach the most western areas, then

Table 1 The most parsimonious GLM model (in *bold*) for density of emperor penguins (number of birds.km^{-1} along the transect line), given as *count*, was obtained by stepwise selection. Δ QAIC shows the performance of other GLMs relative to the best model. Abbreviations: EV=explanatory variables; r.d=residual deviance, df=degrees of freedom, φ=dispersion parameter.

GLM (count ~ EV_1+ EV_2 + … + EV_n, family: quasi-Poisson)				
EV	r.d	df	*Δ* QAIC	ϕ
longitude	**123**	**44**	**0**	**3.13**
latitude, *longitude*, *ice type*	122.7	42	7.11	3.19
latitude	156	44	11.74	4.54

diverging to their respective colonies of the NW and SW Ross Sea (Fig. 1).

Swells open up the pack ice in the central Ross Sea even during winter, so the observed scarcity in leads may have been due to a period of calm weather (Langhorne et al. 1998). Not surprisingly, in a seascape covered by a uniform sheet of new ice, most sightings were of individuals standing or hauled out next to isolated holes or narrow leads. During such days of reduced access to open water, penguins may toboggan and swim from lead to lead.

In contrast to Adélie penguins (*Pygoscelis adeliae*), which also winter in Antarctica but don't breed until spring, emperors need to gain a maximum weight before the breeding fast (Le Maho 1977). Because of the thin ice, it was not possible to weigh birds or attach transmitters. Thus, from their aggregated position around leads and holes as well as from the presence of guano, we conclude they were feeding while travelling, possibly on *Pleuragramma antarcticum*, a common prey above the continental shelf (Kooyman et al. 2004). This behaviour was also apparent in the zigzagging trajectories of the birds tracked by Kooyman et al. (2004) and consistent with the body mass of over 30 kg of 20 individuals we weighed shortly after this survey at and around Cape Colbeck (Fig. 1). The gradual increase in the number of birds when approaching the ERS, as well the direction of travel of the post-moult birds tracked by Kooyman et al. (2004; Fig. 1), suggests the birds observed during the surveys were travelling from east to west.

GLM modeling showed that *ice type,* per cent *ice cover* and *chlorophyll-a* were non-significant predictors of penguin counts. The lack of variability in ice characteristics along the survey transect is the likely cause of this result. However, it does not rule out the possibility that birds may initially have migrated along a route through open water (low percent ice cover), favourable to travel and feeding, but due to sudden changes in weather they found themselves encased in new ice, biasing our observations and subsequent analysis. The absence of relationship between chlorophyll-a concentration and emperor penguin density in our best model is in line with Ballard et al. (2012), who found that among a suite of environmental covariates, chlorophyll concentration has the weakest predictive power for emperor penguin distribution. Again, the time frame and environmental conditions under which our survey was made make comparisons with other studies, carried out mostly during the austral summer, tentative.

This report sheds light on behavioural aspects of the post-moult migration of emperor penguins, a life stage that had hitherto never been directly observed. It includes: (1) the formation of a migratory front composed of small clusters of birds moving west, (2) the aggregation of penguins around ice holes maintained by bird activity, allowing them access to food and (3) the occasional sighting of birds far from open water suggesting they travel over-ice to distant leads.

Acknowledgments Research was funded by National Science Foundation grant NSF ANT-1043454 to G.Kooyman, (UCSD). We thank the crew of the Palmer and ASC personnel for logistical support. Brandon Bell and Gianluca Paglia helped collect field data; Joshua E. Meyer (MathWorks) provided Matlab code. Thanks to Jonathan Shurin (UCSD) for reviewing, Jay Barlow (NOAA) for reviewing and statistical insight and Elizabeth Johnstone (SIO) for help with GIS and figures.

References

Ainley DG, O'Connor EF, Boekelheide RJ (1984) The marine ecology of birds in the Ross Sea, Antarctica. Ornithol Monogr. doi:10.2307/40166773

Battley PF (2006) Consistent annual schedules in a migratory shorebird. Biol Lett 2:517–520. doi:10.1098/rsbl.2006.0535

Ballard G, Jongsomjit D, Veloz SD, Ainley DG (2012) Coexistence of mesopredators in an intact polar ocean ecosystem: the basis for defining a Ross Sea marine protected area. Biol Conserv 156:72–82

Buckland ST, Anderson DR, Burnham KP, Laake JL, Borchers DL, Thomas L (2001) Introduction to distance sampling. Oxford University Press, Oxford, p 432. doi:10.1002/0470011815.b2a16019

Cavalieri DJ, Parkinson CL (2008) Antarctic sea ice variability and trends, 1979–2006. J Geophys Res 113:C07004. doi:10.1029/2007JC004564

Groscolas R (1978) Study of moult fasting followed by an experimental forced fasting in emperor penguin *Aptenodytes-forsteri*—relationship between feather growth, body-weight loss, body-temperature and plasma fuel levels. Comp Biochem Physiol 61:287–295. doi:10.1016/0300-9629(78)90111-1

Kooyman GL, Hunke EC, Ackley SE, van Dam RP, Robertson G (2000) Moult of the emperor penguin: travel, location, and habitat selection. Mar Ecol Prog Ser 204:269–277. doi:10.3354/meps204269

Langhorne PJ, Squire VA, Fox C, Haskell TG (1998) Break-up of sea ice by ocean waves. Annals of Glaciology 27:438–442

Kooyman GL, Siniff DB, Stirling I, Bengtson JL (2004) Moult habitat, pre- and post-moult diet and post-moult travel of Ross Sea emperor penguins. Mar Ecol Prog Ser 267:281–290. doi:10.3354/meps267281

Le Maho Y (1977) Emperor penguin—strategy to live and breed in cold. Am Sci 65:680–693

Lynch HJ, Fagan WF, Naveen R, Trivelpiece SG, Trivelpiece WZ (2012) Differential advancement of breeding phenology in response to climate may alter staggered breeding among sympatric pygoscelid penguins. Mar Ecol Prog Ser 454:135–145. doi:10.3354/meps09252

Prévost J (1963) L'écologie du manchot empereur *Aptenodytes forsteri* (Gray). Bulletin de la Société Zoologique de France 87:295–301

R Development Core Team (2010) R: A language and environment for statistical computing. R Foundation for Statistical Computing, Vienna

Richards SA (2008) Dealing with overdispersed count data in applied ecology. J Appl Ecol 45:218–227. doi:10.1111/j.1365-2664.2007.01377.x

Smith OP (2007) Observer's guide to sea ice. National Oceanic and Atmospheric Administration NOAA Ocean Service. p 28

Spreen G, Kaleschke L, Heygster G (2008) Sea ice remote sensing using AMSR-E 89 GHz channels. J Geophys Res 113: C02S0. doi:10.1029/2005JC003384

Wilson EA (1907) National Antarctic expedition 1901–1904. Vol. 2. Zoology. British Museum, London, p 1–31

This work (Chapter 4), in full, is presented as published in *Polar Biology* (2014, 1-5) with the following co-authors: Gerald L. Kooyman, Kimberly T. Goetz, and Birgitte I. McDonald. The dissertation author was the primary investigator and author of this paper.

5

Autumn distribution of seabirds, seals and whales in the Ross Sea, Antarctica: the “St. Tropez” effect.

5.1 ABSTRACT

Early autumn visual surveys reveal hitherto undescribed distribution patterns and behavior of Antarctic megafauna, which are influenced by the rapidly expanding sea-ice. Emperor penguins congregate and feed in migratory “hubs” located in stable pack ice of the eastern Ross Sea, close to the Antarctic Slope Front. From there, based on their annual cycle, they travel to the marginal ice zone, or the eastern and western Ross Sea colonies. Generalized linear modeling (GLM) shows that movement to the latter is characterized by a “migratory front” composed of clusters of ≤ 8 birds traveling west and feeding en route. We hypothesize that Adélie penguins migrate with the expanding pack ice from breeding colonies in the western Ross Sea to lower latitudes with sufficient light to forage. This movement appears synchronous, as evidenced by the gradual increase in the relative abundance of this species along our transect, and the large concentration of birds in the eastern Ross Sea, beyond the shelf break. GLM results suggest this area, close to the Antarctic Slope Front, is a hotspot for Weddell and crabeater seals, the former remaining in pack ice on the continental shelf, the latter being more numerous beyond the shelf break, possibly due to higher concentrations of krill. Killer whales were most abundant above the shelf, their distribution tied to that of Weddell seals. We provide a new perspective on Antarctic megafauna distribution studies and stress the need to consider seasonal fluctuations in species abundance rather than base estimates solely on data collected in summer.

5.2 INTRODUCTION

As the southernmost navigable body of water, the Ross Sea intrudes deep into the Antarctic continent. At these high latitudes, the seasonal expansion and contraction of pack ice determines the spatial and temporal distribution of marine megafauna (penguins, volant sea birds, seals, and whales). Migratory movements of these animals have been documented for Adélie, *Pygocelis adeliae* (Davis *et al*. 2001), emperor penguins, *Aptenodytes forsteri* (Kooyman *et al*. 2000, Kooyman & Ponganis 2007, Kooyman *et al*. 2004), and Weddell seals, *Leptonychotes weddelli* (Burns *et al*. 1999).

Of the true Antarctic seal species, only adult Weddell seals overwinter in the Ross Sea, with a large concentration of animals residing on the fast ice of McMurdo Sound (Testa & Siniff 1987). At the end of the summer breeding season, juvenile and adult Weddell seals leave their near-shore colonies. While juveniles tend to remain close to the coast, potentially competing with emperor penguins for resources (Burns & Kooyman 2001), adults migrate in late summer, after the moult, to forage in areas of pack ice in the central Ross Sea (Ackley *et al*. 2003, Burns & Kooyman 2001, Hill 1987, Testa 1994). Pinnipeds that are not closely associated with fast ice have a more diffuse distribution, which complicates the study of their migratory behavior (Bengtson *et al*. 2011, Southwell *et al*. 2003, Southwell & Low 2009). As a consequence, little is known about the movement patterns of crabeater (*Lobodon carcinophaga*), leopard (*Hydrurga leptonyx*) and Ross seals (*Ommatophoca rossii*), although surveys and satellite tracking studies suggest they move seasonally to remain in areas of pack ice that offer the best combination of foraging and haul-out habitats (Nordøy & Blix 2009, Blix & Nordøy 2007, Bengtson *et al*. 2011). Even less is known of the movements of the two most common whales of the Ross Sea, the minke (*Balaenoptera bonaerensis*) and killer whale (*Orcinus orca*).

Six of the seven Ross Sea emperor penguin colonies occur around its western

boundaries (Cape Crozier, Beaufort Isl., Franklin Isl., Cape Washington, Coulman Isl., Cape Roget) while the seventh, Cape Colbeck, is located at the Eastern end of the Ross Ice Shelf (Kooyman 1993, Kooyman 2002). Satellite telemetry has shown that at the end of the chick-rearing season (mid-December), when sea-ice is receding at the colonies, emperor penguins travel over 1,200 km to the pack ice of the eastern Ross Sea (ERS) (Kooyman *et al*. 2000). There, stable ice floes provide support during the approximately 35 days of the moult, a period during which the birds cannot enter the water to forage. The energetic cost of the moulting fast results in a decrease in body mass of up to 50% which needs to be offset before the birds migrate back to the western Ross Sea (WRS) colonies. Prey in the vicinity of the moulting floes may limit survival of the weakened birds. Where the non-breeders go after the moult is unknown, although there is some evidence that they travel beyond the marginal ice zone (Kooyman *et al*. 2004, Goetz *et al*. *unpubl*. *data*). Later, during the winter incubation period (June-August), female emperor penguins leave their WRS colonies to forage in areas yet to be discovered.

Adélie penguin colonies occur along the western shores of the Ross Sea, which as a whole harbors up to 38% of the world's summer population of this species (Smith *et al*. 2007). After reproduction in November and fledging in January, most adults moult in the pack-ice in March (Davis & Miller 1992, Kerry *et al*. 1996). After the moult, Adélie penguins leave the Ross Sea, it is believed to follow the northern limit of the pack ice, where there is sufficient light to forage during the winter months (Wilson *et al*. 1993).

The abundance of prey species such as krill (crystal krill, *Euphausia crystallorophias*; Antarctic krill, *E*. *superba*) and fish (primarily Antarctic silverfish, *Pleuragramma antarcticum*) is driven by seasonal diatom and cryophilic algae blooms, which in turn are tightly coupled with ice cover (Smith *et al*. 2007). The delicate timing between ice conditions (coverage and structure) and the presence of prey must strongly influence the distribution of penguins and seals in the Ross Sea.

Past surveys have generally taken place during the Austral summer, when high primary productivity supports marine tetrapods distributed throughout the Ross Sea (Ainley 1985, Ainley *et al*. 1984). There have been no megafauna surveys during late-summer and early autumn, a period when most marine research in the Ross Sea has concluded; while one survey has occurred in late autumn (van Dam & Kooyman 2003).

Here we present the results of a visual sighting survey of seabirds and mammals in the Ross Sea during the months of February and March 2013. This trip provided an opportunity to carry out qualitative visual surveys of all these megafauna from the western to the eastern Ross Sea as we cruised from the vicinity of the Drygalski polynya to the deserted Cape Colbeck emperor penguin colony (Fig. 5.1). In addition, we recorded for the first time the transformation of the open water center of the Ross Sea to pack ice and the fauna associated with this rapid change.

5.3 METHODS

5.3.1 Visual surveys

The icebreaker *R/V Nathaniel B. Palmer* departed from McMurdo station, Antarctica, on Feb. 12th, 2013, and arrived at Punta Arenas, Chile, on April 5th. Four observers alternated in the ship's ice tower (approx. 24 m above the water line), to carry out uninterrupted daytime ("on-effort") surveys throughout the Ross Sea basin (Fig. 5.1). A single observer covered 180 degrees during a 3-hour shift. Sightings of volant sea birds, penguins, seals and whales were recorded with an estimate of group size, when applicable. Angle (deg.) from the front of the ship to the animal(s) was recorded using an angle board (to the nearest 15°) and distance (m) was measured using binoculars with reticles (when the horizon was visible) or a "best estimate" based on a known distance (ice-tower to bow of the ship). Animals were identified to species level whenever possible. High- powered binoculars (18x50 Canon with stabilizers) enabled

the identification of animals up to a distance of approximately 1000 m during clear days, a distance chosen as our transect width. The survey was interrupted ("off effort") when: (i) low visibility due to weather or low light prevented animal identification, (ii) we were transiting through open water, (iii) when the ship was stationary or traveling at slow speed (<4 kn) while conducting oceanographic experiments. In the latter case we still carried out "off-effort" watches, to record any megafauna sightings. An ipad 2 (Apple, Inc., Cupertino, CA, USA) with Bento (version 4; Filemaker, Inc., Santa Clara, CA, USA), a database application with an automatic geo-referencing function, were used to record data. A BadElf Pro GPS unit (BadElf, West Hartford, CT, USA) with accuracy of 2.5 m was interfaced with the Bento app to record GPS data. As a result, location and UTC time was recorded for each observation. Data on ice type and percent cover (following the classification scheme given by Smith [2007]), sea state and weather, were recorded whenever they changed. For seals, whales and penguins, we indicated whether sightings were in water or on ice. For volant sea birds, sightings were "in the air", unless indicated otherwise. When possible, we added information on behavior (prior to the animals being flushed by the ship), life stage (juvenile/adult) and physiological state (moulting/not moulting), as well as guano color, which is an indicator of diet in penguins (Kooyman *et al*. 2004). While transiting through pack ice with abundant wildlife, an additional observer helped the primary observer spot and record sightings.

5.3.2 Chlorophyll-a concentration

Underway fluorometry data, part of the Research Vessel Data Acquisition System (RVDAS), was collected with a "WETStar" flow-through fluorometer (Wet Labs, Philomath, Oregon, USA). Output was in mV and the following conversion, based on factory calibrations provided by Wet Labs, was used to obtain *chlorophyll-a* concentration (Chl-a):

$$\text{Chl-a } (mg.m^{-3}) = \text{scale factor} * [\text{output} - \text{clean water offset}]$$

Where: scale factor = 0.0054 μg/l/mV and clean water offset = 86 mV

5.3.3 Data analysis

The dataset was divided into 4 geographical sections: western Ross Sea (WRS), transit (TR), eastern Ross Sea (ERS) and east of shelf (ES; Fig. 5.1). The latter section, although not within the limits of the Ross Sea (defined here as the area delimited by the continental shelf), was included in our analysis as it represents an ecological transition zone. The upwelling of modified circumpolar deep water, occurring above the continental shelf break (indicated by the -1000 m isobath in all figures), enriches surface waters with a resulting change in krill and fish species composition (Jacobs & Comiso 1989, La Mesa *et al*. 2004, Smith *et al*. 2007). This, in turn, causes changes in the feeding behavior and distribution of marine birds and mammals (Ainley & Jacobs 1981, Ainley *et al*. 1984, Cherel & Kooyman 1998). Sightings data from on-effort sections were pooled *a posteriori* into 10-km transect bins (sightings per 10 km along the transect) to allow for spatial comparisons between sections and to compute the mean "animal density" (defined as sightings per kilometer along the transect and obtained by dividing the number of sightings in each bin by ten). The different killer whale ecotypes were identified following Pitman and Ensor (2003).

We analyzed the survey data using Generalized Linear Modeling (GLM) in R (R Development Core Team, 2010) with "animal density" as dependent variable and a quasi-Poisson error distribution model to account for over-dispersion and excess zeroes in the survey data. Location of the ship (latitude/longitude), ice type (i.e. the 13 "sea ice form" categories described by Smith [2007]) and ice cover (percentage of ice cover estimated by eye, using the ten ice concentration categories described by Smith [2007]) whose effect on the distribution of Antarctic birds is well documented (Ainley *et al*. 1984), and

chlorophyll-a (calculated from underway fluorometry measurements) were factored in the GLMs as explanatory variables using an "all-subset approach" to model selection (a justification for this method, suited for behavioral ecology studies, is given by Symonds & Moussalli [2011]). Sightings "in water" and "on ice" were lumped together for our seals, penguins and whales analyses. Pair-wise comparisons of mean density (sightings. km^{-1}) between sections were established, for each species, using Wilcoxon Rank Sum Tests (hereafter abbreviated as WRST) with continuity correction, in R. ArcGIS 10 (ESRI 2011) was used for spatial representation of the data. Results (which cover only the "on-effort" parts of our survey) are given as means +/- standard error.

5.3.4 Model selection

The full model is given as follows:

$$sp. \sim latitude + longitude + ice\ cover + ice\ type + chlorophyll\text{-}a$$

Where: "sp." is the species' density. We used the quasilikelihood Akaike Information Criterion, QAIC, to select the most parsimonious GLM model (Burnham & Anderson 2002). When two models were within two QAIC units from each other (Δ QAIC ≤ 2), the simplest (i.e. the one with the smallest number of parameters) was chosen as the best model and reported alongside the competing model(s) (Richards 2008).

5.4 RESULTS

5.4.1 Physical and biological setting

On-effort surveys in all sections were conducted outside polynyas. In the WRS section (February 13th-March 9th), the mean ice cover was 50-60% consisting primarily of pancake and new ice (Fig 5.1.A). New ice less than 25 cm thick with "medium" size floes (100-500 m across) covered 90-100% of the TR section (March 10th-13th; Fig 5.1.B). When approaching the Bay of Whales, at the end of the TR section (March 13th), we

encountered “medium” to “big” size floes (500 m-2000 m across) along with wider leads. At the eastern end of the Ross Ice Shelf polynya, en route to Cape Colbeck (ERS section, March 13th-March 18th), the seascape was a mix of new and brash ice (5 % cover) with small icebergs (15-60 m across; Fig. 5.1 B). Close to Cape Colbeck, which we reached on March 13th, we came across small to medium icebergs (61-122 m) scattered in a dense cover (90-100 %) of brash and new ice. We left Cape Colbeck on March 16th and took a northern route. During the first few hours, the new ice cover was sparse (5-10%) and mottled with “small” floes. This changed rapidly into a seascape of “giant” floes (>10km) with high relief and covered in sastrugi. As the ice became too thick to break through, the ship turned around to seek a northwestern route out of the pack (March 17th- 18th). On March 18th, the new ice (90-100% cover) gave way to a pack consisting of “medium” to “big” floes (80-90% cover), through which our progress was slow. We crossed the continental shelf break that same day and, on March 19th, veered northeast through the heavy pack to head to Punta Arenas, Chile. This marked the beginning of the ES section (Fig. 5.1 B). The seascape through the last part of our survey (March 19th-21st) was “big” to “vast” floes (2-10 km across) with almost 100% cover. We reached open water at 71°S on March 22nd.

Mean chlorophyll-a concentrations were 2.21 $mg.m^{-3}$ (±0.09) in the WRS (range=0.14-5.94 $mg.m^{-3}$, the highest values were measured during a phytoplankton bloom in the Drygalski polynya); 0.89 $mg.m^{-3}$ (±0.05) in the TR (range=0.04-1.44 $mg.m^{-3}$); 1.12 $mg.m^{-3}$ (±0.07) in the ERS (range=0.11-1.89 $mg.m^{-3}$) and 1.45 $mg.m^{-3}$ (±0.08) in the ES sections (range=0.39-1.93 $mg.m^{-3}$). Above the Antarctic Slope Front, the mean chlorophyll-a concentration was 1.54 $mg.m^{-3}$ (±0.08), almost twice the value of the TR section (Fig. 5.2).

5.4.2 Emperor penguins

We counted a total of 1315 emperor penguins in all four sections (0.41 birds.km^{-1} ± 0.08). Except for one individual in the WRS section that was still moulting, all birds had new coats. Emperor penguins were, with few exceptions, located close to leads or holes in the ice. Most birds were lying or standing at the edge of floes, or swimming.

We observed in the TR and ERS sections large patches of dark guano stains around the edges of leads and ice holes where emperor penguins were congregated, an indication of feeding. With 896 birds, representing almost 70% of all sightings, the ERS section had by far the highest density of emperor penguins: 1.7 birds.km^{-1} (± 0.39). This is significantly more than in the TR section (WRST; W=2330.5, P<0.001), where we counted 196 birds (0.33 birds.km^{-1} ± 0.17), the ES section (WRST; W=1592, P<0.001) with 133 emperor penguins (0.32 birds.km^{-1} ± 0.09) and the WRS section (WRST; W=7561, P<0.001), where we sighted only 90 birds (0.05 birds.km^{-1} ± 0.02; Table 5.1, Figs. 5.3.A & 5.4.A). In the ERS section emperor penguins were seen in large groups of up to 30 individuals around Cape Colbeck and up to 100 birds at the end of the section, close to the continental shelf break (Fig. 5.4 A). There was a clear reduction in density of emperor penguins once we passed that point and were transiting northeast (ES section, starting on March 19th). Group size in the WRS and TR sections was smaller, with clusters of no more than 8 birds, standing or hauled out at the edge of ice floes along leads. In the WRS section, the main areas where emperor penguins were sighted were between the Drygalski Ice Tongue and Cape Washington, and South of Coulman Island (Fig. 5.4 A).

Ice cover was a significant predictor of density of emperor penguins as it was included in the most parsimonious GLMs for all sections, with birds preferring areas with >80% cover. It is not clear whether this is due to the increased visibility of birds when hauled out on the ice or the effect of the animals selecting areas with high ice

concentration. The best GLM for the TR section only included *longitude* (Table 5.2). Predictor variables *latitude* and *icetype*, along with *ice-cover* and *chlorophyll a* were included in the most parsimonious GLMs for the ERS and ES sections, with density increasing from 1.6 birds.km^{-1} (± 0.45) to 2.57 birds.km^{-1} (± 0.76) as we approached the continental shelf break at 76.5º S and 74.5º S (Fig. 5.4 A). These locations were amongst the most productive in the eastern half of the Ross Sea (Fig. 5.2), which explains the positive relationship between the explanatory variable *chlorophyll-a* and emperor penguin density in the GLMs for the ERS and ES sections. The highest densities of emperor penguins were also associated with "giant" floes with >80% cover.

5.4.3 Adélie penguins

With 5332 individuals, Adélie penguins were four times more abundant than emperor penguins, the second most sighted species of our survey (Table 5.1). We counted 4448 birds in the ES section alone (10.8 birds.km^{-1} ± 2.13), representing almost 85% of the total number of Adélie penguins sighted during the cruise, significantly more than the ERS section, which had the second highest density with 0.53 birds.km^{-1} ± 0.29 (WRST; $W=1521.5$, $P<0.001$) (Fig. 5.3 A & 5.4 B). Many birds were still moulting, especially in the WRS section (84 moulting individuals). Due to the frequency of sightings and large group sizes in the ES section, we did not have enough time to reliably distinguish moulting from non-moulting birds. However, the general trend throughout the entire survey was that moulting birds tended to aggregate farther from the edges of floes, seeking shelter under pressure ridges when these were present, whereas non-moulting birds were sighted closer to leads and ice holes where they were often seen swimming and diving. The largest groups of Adélie penguins were encountered above and beyond the continental shelf break (ES section; Fig. 5.4 B), with numbers ranging from 85 to 200 individuals per group (our largest single-day tally, of 1653 Adélie penguins, occurred

on March 18th-19th). In this section, large patches of pink guano (indicative of a krill-dominated diet) were spotted at the edge of leads, along with numerous Adélie penguin tracks (discernible from emperor penguins by the smaller footprints) running from lead to lead or crossing over areas with little to no open water (ice cover of 90-100%). These tracks frequently extended beyond our sight. The most parsimonious GLM for the ES section included all variables but *chlorophyll-a* (Table 5.2). As this section consisted overwhelmingly of "giant" floes with >80% ice coverage of thick, multi-year pack, it is not surprising to find a relationship between density of Adélie penguins and ice-related parameters. The more notable effect was the sharp latitudinal effect on density as we traveled from South to North. In the first two ES "on-effort" transects (Fig. 5.4 B) the density was 16.21 birds.km^{-1} (± 2.89), whereas in the third and last transect, at the northern limit of the pack ice, density was only 0.28 birds.km^{-1} (± 0.08). The most parsimonious GLM for the ERS section, included all the tested parameters (Table 5.2). Similar to the ES section, the effect of position (longitude/latitude) was illustrated by the increase in density, from 0.43 (± 0.17) to 8.95 (± 1.88) birds.km^{-1} as we approached the continental shelf break. The high density of birds in this section coincided with the highest values of chlorophyll-a (> 1.12 mg.m^{-3}). As in the ES section, the sea was uniformly covered in "giant" floes (>80% ice concentration) with birds remaining at the edge of narrow leads or water holes. Besides the large aggregations of Adélie penguins in the ES section, the only significant differences in density were between the WRS section (0.34 birds.km^{-1} ± 0.06, with a total count of 575 birds) and the TR section (WRST, $W=5851$, $P<0.05$), which had a total of 30 birds, or 0.05 birds.km^{-1} (± 0.01).

5.4.4 Volant sea birds

We observed throughout our surveys three different species of volant sea birds: snow petrels (*Pagodroma nivea nivea*), south polar skuas (*Catharacta maccormicki*) and

Antarctic petrels (*Thalassoica antarctica*).

From McMurdo station to the end of the ES section, snow petrels were a constant presence. We counted a total of 310 birds (Table 5.1). Seen frequently in pairs or in groups of up to 20 individuals (mean group size was 1.9 birds), snow petrels would typically circle the ship a few times at close range before continuing.

GLM modeling showed that *ice cover* and *ice type* best explained the density of snow petrels in the WRS section with birds preferring areas with 20-60% ice cover and "small" to "medium" size floes. In these areas, characterized by numerous leads, the density for this species was 0.16 birds.km^{-1} (± 0.04). In a more open seascape (<20 % cover) composed mainly of pancake ice we sighted fewer birds (0.03 birds.km^{-1} [± 0.004]). In areas with where leads were scarce (>80 % cover), the density was 0.06 birds.km^{-1} (± 0.007). For the ERS and ES sections, the most parsimonious GLMs comprised location variables *latitude* and *longitude*, and either *ice type* or *ice cover*. The relationship between sightings and ice characteristics should be taken with caution as both sections were almost entirely covered in pack ice (>80 % cover), which was uniform in structure, except for a small swath of open water with medium size bergs North of Cape Colbeck (Table 5.3).

Pair-wise comparisons showed that the WRS section, with 0.13 birds.km^{-1} (± 0.03), had a significantly higher density of snow petrels than the TR section (0.007 birds.km^{-1} [± 0.004]; WRST; W=6564.5 P<0.001) and the ES section (0.06 birds.km^{-1} [± 0.03]; WRST; W=3931 P<0.05). It was, however, not significantly different from the ERS section (0.1 birds.km^{-1} [± 0.03]). The density of snow petrels in the latter section was, in turn, not significantly different from the ES section but higher than the TR section (WRST; W=2028.5 P<0.001; Fig. 5.3 B).

The second most abundant bird (186 individuals) was the Antarctic petrel. It was seen everywhere except the WRS section (Figs. 5.3.B & 5.5). In a single sighting, on

Mar. 12th (TR section), we counted 120 birds, which were aggregated on the steep incline of a medium size berg.

The most parsimonious GLMs for the Antarctic petrel density data in the TR and ES sections included *ice type* and *chlorophyll-a*, with birds preferring new ice with "small" to "medium" size floes. For the ERS section, a GLM with only *chlorophyll-a* best explained the density of Antarctic petrels (Table 5.3). In the vicinity of the Antarctic Slope Front, where the highest concentrations of chlorophyll-a were measured (Fig. 5.2), the number of sightings of Antarctic petrels was an order of magnitude larger than above the continental shelf (0.48 [± 0.19] and 0.046 [± 0.03] birds.km^{-1}, respectively). Pair-wise comparisons between sections showed that the density of Antarctic petrels in the ERS section (0.13 birds.km^{-1} [± 0.04]) was significantly higher than in the TR section (0.18 birds.km^{-1} [± 0.17]; WRST; W=1924, P<0.001) and the ES section (0.04 birds.km^{-1} [±0.02]; WRST; W=1261.5, P<0.05), despite the large group of birds seen in the TR section (Fig. 5.5).

South polar skuas, with 116 birds, were not observed in the ES section (Table 5.1; Figs. 5.3.B & 5.5). With a few exceptions, skuas were seen alone or in company of 2 to 3 other birds. In one occasion we counted 12 skuas in a single sighting, in the WRS section.

The most parsimonious GLMs for the south polar skua data included, for both the WRS and the TR sections (the ERS, with only 3 birds, was discarded from the analysis), the variables *ice cover* and *ice type*. The highest densities were recorded in areas with wide leads, in new ice with 50-60% cover. A competing model for the TR section included *chlorophyll-a* (Table 5.3). There was no significant difference in density of skuas between the WRS and TR sections.

5.4.5 Whales

Antarctic minke whales and killer whales were the only cetaceans encountered

during our cruise (64 and 62 animals, respectively; Table 5.1).

The eastern sections (ERS and ES) accounted for 71% of all our minke whale sightings (45 individuals; Figs. 5.3.C & 5.6.A). Minke whales were generally seen alone or in pairs. Larger groups of 4 to 7 whales were seen traveling along narrow leads in the ES section, in dense multi-year pack ice (90-100% cover). During a weeklong stop at the Drygalski polynya (WRS section; Fig. 5.1 B) two minke whales were seen circling the ship.

Killer whales were most frequently observed in the WRS section (43 individuals, or 70% of all sightings), followed by the TR (13 whales) and ERS (6 whales) sections and no sightings in the ES section (Table 5.1; Figs. 5.3.C & 5.6.A). On Mar. 7th, we observed a group of 20-30 B-type killer whales in the WRS section (Fig. 5.6 A). The group was scattered into 3 to 4 subgroups over a large area (at least 1 km at either side of the ship) composed of pancake ice (50-60% ice cover) and "small" floes (20-100 m across). While one or more individuals checked the surface of a given floe by spyhopping, others circled it. This behavior was repeated many times until all floes in the vicinity had been inspected. We did not witness any predation event. Due to low sample sizes, we refrained from modeling the data or establishing comparisons of density of cetaceans between survey sections. Further along our survey, in the TR and ERS sections, killer whales were seen in dense pack ice (new ice and "big"- to "giant" floes, with 80-100% cover), spyhopping intermittently while traveling along leads. Overall, the density of minke and killer whales was 0.02 (± 0.004) and 0.02 (± 0.01) animals.km^{-1}, respectively (Table 5.1).

5.4.6 Seals

During our surveys we observed Weddell, crabeater and leopard seals, with only two sightings of the latter species (in the TR and the ERS sections; Fig. 5.6 B). Weddell

seals were the most frequently observed pinniped: a total of 230 animals in the WRS, TR and ERS sections (88, 68 and 74 seals, respectively), but no sightings in the ES section (Fig. 5.6 B). There was no significant difference in the density of Weddell seals between the other three sections (Fig. 5.3 D). The overall mean density was 0.07 seals.km^{-1} (± 0.01; Table 5.1). All Weddell seals we observed were hauled out, either alone or in small clusters of up to 5 animals. They were most frequently encountered in areas of new ice (30% of sightings) or "small" floes (21% of sightings) with 90-100% cover, and always near a lead or ice hole.

The GLM model that best explained the density of Weddell seals in the WRS section included *latitude* and *chlorophyll-a*, with most animals sighted in and nearby Terra Nova Bay (Fig. 5.6 B), a focal point for the other science teams due to the high levels of primary productivity; whereas for the TR and the ERS sections, the most parsimonious GLMs included all explanatory variables, except *chlorophyll-a* (Table 5.4). The highest densities of Weddell seals (0.17 seals.km^{-1} [± 0.04]) were found in areas with ice cover >80% and "big" to "giant" floes.

We counted 129 crabeater seals, divided as follows: 23 sightings in the WRS (0.01 seals.km^{-1} [± 0.04]); 2 in the TR (0.003 seals.km^{-1} [± 0.002]); 56 in the ERS (0.1 seals.km^{-1} [± 0.03]) and 48 in the ES sections (0.1 seals.km^{-1} [± 0.08]). The density of crabeaters was significantly higher in the ERS than in the ES (WRST; W=1281, P<0.05), TR (WRST; W=1933, P<0.001) and WRS (WRST; W=5338, P<0.001) sections, and there was no significant difference between those three less dense sections (Table 5.1; Fig. 5.3 D). Mean group sizes varied from 1 individual in the TR and WRS sections to 1.7 and 3.4 individuals in the ERS and ES sections, respectively. We observed groups of 10 to 17 seals in the ES section, in dense pack ice with 90-100% cover (Fig. 5.6 B).

The best GLM model for the crabeater sightings data in the WRS included *latitude*, *longitude* and *ice type*; whereas the most parsimonious GLM for the ERS section

contained *latitude*, *ice cover* and *ice type*. For the ES section, the best model contained *ice cover* and *ice-type* (Table 5.4). For both seal species, the relationship between ice-related parameters and density may be an artifact of increased visibility of the animals when hauled out, rather than active selection for specific ice type and/or ice cover. Due to the small sample size (n=2) we did not model data from the TR section. Crabeater seals were not seen as frequently as Weddell seals throughout our survey. However, they aggregated in larger groups of up to 17 animals (ES section), with several seals huddling within these groups (Fig. 5.6 B).

5.5 DISCUSSION

5.5.1 Overall route

Our surveys in the WRS were influenced by the scientific agenda of other researchers aboard *R/V NB Palmer*. As a result, many days were spent in waters where plankton blooms were occurring, skewing our data towards sightings in high chlorophyll-a areas. During the second part of the cruise, which included our transit to the eastern Ross Sea for work at Cape Colbeck, the ship traveled in a straight line through a relatively uniform seascape (same ice type and ice cover). This reduced boundary effects, giving, we believe, a realistic impression of the density of animals along the transect line. Further east (ERS and ES section), the ship traveled through heavy pack ice, seeking open water wherever possible. As animals tend to concentrate along ice edges, our survey violated a basic assumption of distance sampling that requires transect lines be selected randomly relative to the distribution of animals (Buckland 2001). For this reason we have refrained from making any inference of abundance of animals beyond the bounds of our transect, although we have no reason to suspect that the concentration of the various species would be dissimilar for a broad swath beyond the transect line. However, here we present a primarily qualitative description of the distribution of marine megafauna along the ship's

route, the intrinsic value of which lies in the novelty of the information. Our diurnal survey schedule coincided with the daytime foraging habits of penguins and seals (Lake *et al*. 1997, Bengtson *et al*. 2011). This may have caused us to miss individuals that were diving and thus invisible from the ship, resulting in an underestimation of the actual density of animals.

5.5.2 Emperor penguins

While most studies of emperor penguins have focused on behavior, ecology and physiology, there have been few attempts to describe the distribution of penguins away from high concentration areas, such as known colonies (Figs. 5.4.A & 5.4.B). Surveys carried out in the 1980's by Ainley, during or shortly after the chick-rearing season in December-January (Ainley 1985, Ainley & Jacobs 1981, Ainley *et al*. 1984), show the highest concentrations of birds is in the WRS, close to breeding colonies. Our survey, which began in late summer, paints a different picture, as it took place when chicks had fledged and adults have left the colonies to moult. Indeed, the WRS had the lowest density of emperor penguins, even in the vicinity of large colonies (we came within 26 km of Coulman Island and 3.5 km from Cape Washington; Fig. 5.4 A). While Kooyman *et al*. (2000, 2004) determined pre- and post-moult migration routes using satellite telemetry, prior to our study there had been no visual evidence of these movements in the Ross Sea. Although we were are not able to determine if our crossing of the Ross Sea occurred during a period of "peak flux" of emperor penguins migrating back from the ERS, our data and most parsimonious GLM for the TR section show that density increased and was significantly related to *longitude* as we traveled eastward. This suggests the existence of a migration front of birds traveling back from ERS moulting floes to breeding colonies located in the northwest and southwest Ross Sea. We give a detailed account on this section of our survey in a separate paper (Gearheart *et al*. 2014).

In the ERS, not far from Cape Colbeck and near a seasonally abandoned colony (Fig. 5.4 A), we found the highest concentrations of emperor penguins. As further north, in the ES section, the density was lower, we hypothesize we observed a "pre-migratory" aggregation of post-moult birds, or the early stages of a migratory front away from the ERS and bound for either the Cape Colbeck and WRS breeding colonies (breeding birds) or areas at the marginal ice zone where non-breeders and juveniles can forage throughout the winter twilight. The largest groups of birds (>100 individuals) were found at or in the vicinity of the continental shelf break. Coincident with these large aggregations of emperor penguins was an increase in our Adélie penguin sightings (the highest density for this species was recorded in the ES section). Large patches of red-colored guano, indicative of a krill-dominated diet (Kooyman *et al*. 2004), were seen along leads where Adélie penguins congregated. This is in contrast with the dark guano observed around emperor penguins above the continental shelf, in the TR and ERS sections, suggesting the main prey there is the Antarctic silverfish (Cherel & Kooyman 1998). The shift from a food-web dominated by Antarctic silverfish and crystal krill to one composed primarily of Antarctic krill occurs at the Antarctic Slope Front, which is located above the continental shelf break and characterized by high levels of primary productivity (Jacobs 1991, La Mesa *et al*. 2004). Our most parsimonious GLMs for the density of emperor and Adélie penguins in the ERS and the ES sections included the predictor variable *chlorophyll-a*, a proxy of primary productivity. At the Antarctic Slope Front, chlorophyll-a concentration was 1.54 $mg.m^{-3}$ (±0.08), considerably higher than above the continental shelf (0.89 $mg.m^{-3}$ [±0.05] in the TR section; Fig. 5.2). Hence, the high densities of birds recorded in the ERS, in the vicinity of the Antarctic Slope Front, may be the result of emperor penguins aggregating in high productivity areas to refuel before migrating either to breeding colonies in the WRS or northward to the marginal ice zone (Kooyman 2002). This area may thus serve as a "migratory hub" that offers sufficient amounts of prey

for emperor penguins to regain part, if not all, the weight lost during the moulting fast (Groscolas & Cherel 1992, Groscolas & Robin 2001, Kooyman *et al*. 2004). The lower density of emperor penguins beyond the Antarctic Slope Front (ES section) may be due to the fact that, compared to the numbers seen in the "hubs", a smaller proportion of birds migrate northward (i.e., non-breeders and juveniles).

5.5.3 Adélie penguins

The movement of Adélie penguins both above the continental shelf (ERS section) and beyond the Antarctic Slope Front (ES section), is related to primary productivity and follows a geographic pattern, i.e. away from the continent (*latitude* and *longitude* were significant predictor variables, along with *chlorophyll-a*). In the Ross Sea, all known colonies of Adélie penguins, an ice-obligate species that nests on land (Wilson *et al*. 2001), are located along the coast of Victoria Land and Ross Island (Taylor *et al*. 1990); see Fig. 5.4 B for the locations of main Ross Sea colonies). Thus, the high concentration of Adélie penguins observed in the ES section may be the result of birds from WRS colonies having crossed the central Ross Sea synchronously with the expanding sea ice (Figs. 5.1.A & 5.1.B). With no breeding sites in the vicinity of the Ross Ice Shelf and few in Marie Byrd Land, this migration front of Adélie penguins bypasses the ERS section. It could also be that during the summer months the melting pack ice concentrates Adélie penguin populations, grouping animals that were distributed throughout the eastern half of the Ross Sea into "pockets" of decreasing size. Once sea-ice starts reforming in late February, these pockets would become the starting points of their migration. Then, en route to winter feeding-grounds, they aggregate along leads where they can feed. The absence of sightings of Adélie penguins beyond 162ºW (March 21st, Fig. 5.4 B), while still in pack ice with 90% cover, suggests the pace of their migration is slower than the expansion rate of sea ice.

5.5.4 Volant sea birds

As seabirds seemed attracted by our ship, our observations may not give an adequate representation of their natural distribution (for example, behavioral traits such as their preference for certain pack ice habitats or tendency to fly above the center of leads, as reported by (Ainley *et al*. 1984), might have been influenced by our vessel). Rather, we assume that the attracted birds came from a relatively well-mixed assemblage, giving us a representation of the overall species composition in each of the four sections. In this context, it is not surprising that the least frequently sighted bird, the skua, is also the most uncommon of the three (Ainley *et al*. 1984). Ainley & Jacobs (1981) describe the rich avifauna associated with the Antarctic Slope Front. Our data does not show this trend, as in the ERS and ES sections petrels and skuas were not significantly more abundant than in the TR and WRS sections. This difference might be due to one or a combination of the following: (1) changes in primary productivity, (2) the thickening of the pack ice over the Antarctic Slope Front during February-March (Figs. 5.1.A & 5.1.B) making prey less accessible, (3) the tendency for birds to remain above leads and along ice edges (Ainley *et al*. 1984), which were more prevalent in the WRS. The potential effect of the onset of winter on the Ross Sea bird community is illustrated by changes in species diversity: while Ainley *et al*. (1984) recorded 18 species of volant sea birds during his summer surveys (spanning from December 15th to February 21st), we only saw 3 species during our February-March cruise. We propose the term “Saint Tropez effect” (in reference to the annual summer migration of north European tourists to the Mediterranean coastline) to describe this seasonal change in species diversity and abundance.

5.5.5 Seals

In the Amundsen and eastern Ross Seas, Weddell seals were 1-2 orders of

magnitude more abundant in fast ice than in pack ice (Bengtson *et al*. 2011). Our survey, which largely bypassed areas of fast-ice (we steamed along the Ross Ice-shelf for less than 24 hours, on Mar. 13th), showed Weddell seals were the most abundant pinniped. Satellite telemetry shows Weddell seals breed and moult during the summer in continental fast-ice, and then disperse in late summer throughout the Ross Sea (K. Goetz, unpubl. data). The main determining factor for their distribution is thought to be a combination of suitable haul-out habitat and the availability of prey. We observed Weddell seals in a range of pack-ice habitats, from 10-20% cover and "small" floes (in the WRS) to individuals hauled out near isolated cracks on "giant" floes (in the ERS). The animals could have been adults that just finished moulting and dispersed throughout the Ross Sea, possibly converging towards suitable foraging areas, or immature or non-breeding animals that remained in the pack ice during the summer. Additionally, the seasonal cycle of melting and freezing, which contracts and expands the area of pack ice, may act as a concentrator of seals (Bengtson 2011). This, combined with the higher levels of chlorophyll-a measured in the vicinity of the Antarctic Slope Front (Fig. 5.2), may explain the higher densities of Weddell and crabeater seals in the stable pack ice of the eastern Ross Sea section. Crabeater seals were more abundant on the northern edges of the continental shelf and over the continental slope (ERS and ES sections; Fig. 5.6 B), a pattern similar to that found by Bengtson *et al*. (2011) in the Amundsen and eastern Ross Seas, and possibly caused by the higher densities of Antarctic krill found in these areas (the most parsimonious GLMs included ice characteristics and *chlorophyll-a*). The average group size of 3.4 individuals was larger than that reported by Bengtson *et al*. (2011) for the Amundsen and eastern Ross Seas (1.67 individuals). Groups of 10 to 17 individuals along leads may indicate local primary productivity hotspots as beyond the slope front and above deep waters crabeater seals may not rely on the prey concentrating effect caused by an irregular, shallow bathymetry characteristic of the continental shelf

(Burns *et al*. 2004).

5.5.6 Whales

In contrast to most cetaceans that forage in Antarctic waters and migrate to lower latitudes in autumn, part of the minke and killer whale populations overwinter in the pack ice of Antarctica (Friedlaender *et al*. 2009, Gill & Thiele 1997, Pitman & Ensor 2003, Thiele *et al*. 2004). Ecotype-B killer whales, which feed primarily on seals, are the most common form of killer whale in the pack ice of the Ross Sea (Pitman & Ensor 2003). This is in line with our observations, as 45 of a total of 62 animals were positively identified as B-types. The behavior of the largest group of whales, 20 to 30 individuals we observed in the WRS section, was consistent with seal hunting (Pitman & Ensor 2003), with Weddell seals being the most abundant in that section. Pitman & Durban (2010) described that, off the western Antarctic Peninsula, B-type killer whales (and possibly A-types) consume gentoo (*Pygocelis papua*) and chinstrap (*Pygocelis antarctica*) penguins, in addition to seals. B-types have also been tracked to WRS emperor penguin colonies during the breeding season (Andrews *et al*. 2008). However, despite speculation that (A-type) killer whales may be responsible for the decline of entire emperor penguin colonies (Ainley *et al*. 2007), there have been no direct observations of killer whales eating, or killing emperor penguins. Prévost (1961) states “one has found an entire emperor penguin in the stomach of a killer whale [of unspecified ecotype]”, but in a later publication that statement is replaced by: “orcas probably consume a certain number of adult emperor penguins” (Prévost & Sapin-Jaloustre 1965). Supporting this hypothesis, Gerald Kooyman, who spent over 10 seasons at the Cape Washington colony, describes how the higher-than-normal leaps made by penguins upon exiting the water are a telltale sign of killer whales swimming nearby (G. Kooyman, pers. comm.). Interestingly, in McMurdo Sound, where killer whales are predominantly of the fish-eating C-ecotype,

emperor penguins do not display fear in their presence (G. Kooyman, pers. comm.). A dedicated study is needed to confirm whether or not emperor penguins are prey to killer whales. Adélie penguins do not seem to be a common prey item for B-type killer whales, despite reports of whales harassing or attacking them close to colonies (Lauriano *et al*. 2007, Pitman & Durban 2010). A hotspot for migrating Adélie penguins, the ES section also had the second highest density of crabeater seals, but neither Weddell seals nor killer whales were observed there. This may be an indication that Weddell seals are the preferred prey species, so that the distribution of B-type killer whales in the Ross Sea follows that of Weddell seals rather than crabeater seals (Smith *et al*. 1981, Visser *et al*. 2008). Again, the limited spatiotemporal coverage of our survey may have caused us to miss killer whales in the ES section. The high density of minke whales in the ES section may be due to the presence of Antarctic krill, its main prey off the continental shelf.

5.6 CONCLUSIONS

Our survey reveals a very different picture of the Ross Sea from the more common "summer" perspective. To illustrate the need to consider the seasonal effect of the Antarctic climate on the distribution and habitat use of megafauna species, we give the example of Ballard et al.'s (2012) work on the spatial distribution of nine mesopredators in the Ross Sea. The goal of this study was to inform the designation of Marine Protected Areas (MPAs). In their emperor penguin distribution model, the weakest contributing variable was *chlorophyll a*. Our GLM analyses suggests otherwise, especially in the vicinity of the continental shelf. The discrepancy may originate from the fact that the historical data used by the authors was exclusively collected during the summer, when emperors are congregated at the colonies tending to their chicks. In this case, breeding site philopatry is the determining factor for their distribution rather than the nearby presence of high levels of productivity; hence the weak relationship

found by Ballard et al. A few months later, in early March, emperor penguins are in the eastern Ross Sea, finishing their moult. Weakened by a long fast, they need to gain weight quickly. The availability of abundant prey nearby the molting floes is of crucial importance (Kooyman et al., 2004) as the animals are too weak to carry out long foraging trips. It is therefore not surprising we found *chlorophyll-a* as being a significant predictor variable. When considering the need of protecting the Ross Sea, and therewith designating adequate MPA boundaries, one can easily see the implications of an incomplete understanding of the seasonal distribution patterns of its fauna.

5.7 ACKNOWLEDGEMENTS

Chapter 5, in full, has been submitted for publication as:
Gearheart, G., Kooyman, G.L., Goetz, K.T. and McDonald, B.I. (2014). Autumn distribution of seabirds, seals and whales in the Ross Sea, Antarctica: the “St. Tropez” effect. Submitted to: *PlosONE*

The dissertation author was the primary investigator and author of this paper. Research was funded by National Science Foundation grant NSF ANT-1043454 to G. Kooyman, (UCSD). We thank the crew of the R/V N. B. Palmer and ASC personnel for logistical support. Brandon Bell and Gianluca Paglia helped collect field data; Joshua E. Meyer (MathWorks) provided Matlab code. Thanks to Jonathan Shurin (UCSD) for reviewing, Jay Barlow (NOAA) for reviewing and statistical insight, and Elizabeth Johnstone (SIO) for help with GIS and figures.

5.8 REFERENCES

Ackley, S.F., Bengtson, J.L., Boveng, P., Castellini, M., Daly, K.L., Jacobs, S., Kooyman, G.L., Laake, J., Quetin, L., Ross, R., Siniff, D.B., Stewart, B.S., Stirling, I., Torres, J., & Yochem, P.K. 2003. A top-down, multidisciplinary study of the structure and function of the pack-ice ecosystem in the eastern Ross Sea, Antarctica. *Polar Record,* 39(210).

Ainley, D., Ballard, G., Ackley, S., Blight, L.K., Eastman, J.T., Emslie, S.D., Lescroël, A., Olmastroni, S., Townsend, S.E., & Tynan, C.T. 2007. Paradigm lost, or is top-down forcing no longer significant in the Antarctic marine ecosystem? *Antarctic Science-Institutional Subscription,* 19(3), 283-290.

Ainley, D.G. 1985. Biomass of birds and mammals in the Ross Sea Antarctica. *Siegfried, W. R., P. R. Condy and R. M. Laws (Ed.). Antarctic Nutrient Cycles and Food Webs; 4th Scar (Scientific Committee on Antarctic Research) Symposium on Antarctic Biology, Wilderness, South Africa, Sept. 12-16, 1983. Xiv+700p. Springer-Verlag: New York, N.Y., USA; Berlin, West Germany. Illus. Maps*, 498-515.

Ainley, D.G., & Jacobs, S.S. 1981. Sea-bird affinities for ocean and ice boundaries in the Antarctic. *Deep-Sea Research Part a-Oceanographic Research Papers,* 28(10), 1173-1185.

Ainley, D.G., O'Connor, E.F., & Boekelheide, R.J. 1984. The marine ecology of birds in the Ross Sea, Antarctica. *Ornithological Monographs*, 1-97.

Andrews, R.D., Pitman, R.L., & Ballance, L.T. 2008. Satellite tracking reveals distinct movement patterns for Type B and Type C killer whales in the southern Ross Sea, Antarctica. *Polar Biology,* 31(12).

Ballard, G., Jongsomjit, D.,Veloz, S.D., & Ainley, D.G. (2012) Coexistence of mesopredators in an intact polar ocean ecosystem: the basis for defining a Ross Sea marine protected area. *Biol Conserv* 156, 72-82.

Bengtson, J.L., Laake, J.L., Boveng, P.L., Cameron, M.F., Hanson, M.B., & Stewart, B.S. 2011. Distribution, density, and abundance of pack-ice seals in the Amundsen and Ross Seas, Antarctica. *Deep-Sea Research Part II-Topical Studies in Oceanography,* 58(9-10), 1261-1276.

Blix, A.S., & Nordøy, E.S. 2007. Ross seal (Ommatophoca rossii) annual distribution, diving behaviour, breeding and moulting, off Queen Maud Land, Antarctica. *Polar Biology,* 30(11), 1449-1458.

Buckland, S.T., Anderson, D.R., Burnham, K.P., Laake, J.L., Borchers, D.L. and Thomas, L. 2001. Introduction to Distance Sampling. *In* Oxford University Press, Oxford, 432pp.

Burnham, & Anderson. 2002. Model selection and multimodel inference: a practical information-theoretic approach. *In* New York, New York, USA: Springer.

Burns, J.M., Castellini, M.A., & Testa, J.W. 1999. Movements and diving behavior of weaned Weddell seal (Leptonychotes weddellii) pups. *Polar Biology,* 21(1), 23-36.

Burns, J.M., Costa, D.P., Fedak, M.A., Hindell, M.A., Bradshaw, C.J.A., Gales, N.J., McDonald, B., Trumble, S.J., & Crocker, D.E. 2004. Winter habitat use and foraging behavior of crabeater seals along the Western Antarctic Peninsula. *Deep-Sea Research Part II-Topical Studies in Oceanography,* 51(17-19), 2279-2303.

Burns, J.M., & Kooyman, G.L. 2001. Habitat use by Weddell seals and emperor penguins foraging in the Ross Sea, Antarctica. *American Zoologist,* 41(1).

Cherel, Y., & Kooyman, G.L. 1998. Food of emperor penguins (Aptenodytes forsteri) in the western Ross Sea, Antarctica. *Marine Biology,* 130(3).

Davis, L.S., Harcourt, R.G., & Bradshaw, C.J.A. 2001. The winter migration of Adelie penguins breeding in the Ross Sea sector of Antarctica. *Polar Biology,* 24(8).

Davis, L.S., & Miller, G.D. 1992. Satellite tracking of Adélie penguins. *Polar Biology,* 12(5), 503-506.

ESRI. 2011. ArcGIS Desktop: Release 10. *In* Redlands, CA: Environmental Systems

Research Institute.

Friedlaender, A.S., Lawson, G.L., & Halpin, P.N. 2009. Evidence of resource partitioning between humpback and minke whales around the western Antarctic Peninsula. *Marine Mammal Science,* 25(2), 402-415.

Gearheart, G., Kooyman, G.L., Goetz, K.T., & McDonald B.I. 2014. Migration front of post-moult emperor penguins. *Polar Biology*, 1-5.

Gill, P.C., & Thiele, D. 1997. A winter sighting of killer whales (Orcinus orca) in Antarctic sea ice. *Polar Biology,* 17(5), 401-404.

Groscolas, R., & Cherel, Y. 1992. How to molt while fasting in the cold - the metabolic and hormonal adaptations of emperor and king penguins. *Ornis Scandinavica,* 23(3), 328-334.

Groscolas, R., & Robin, J.P. 2001. Long-term fasting and re-feeding in penguins. *Comparative Biochemistry and Physiology a-Molecular and Integrative Physiology,* 128(3), 645-655.

Hill, S.E. 1987. Reproductive ecology of Weddell seals (Leptonychotes weddellii) in McMurdo Sound, Antarctica. *In* Ph.D. Diss., University of Minnesota, Minneapolis, MN.

Jacobs, S.S. 1991. On the nature and significance of the Antarctic slope front. *Marine Chemistry,* 35(1-4), 9-24.

Jacobs, S.S., & Comiso, J.C. 1989. Sea ice and oceanic processes on the Ross Sea continental-shelf. *Journal of Geophysical Research-Oceans,* 94(C12), 18195-18211.

Kerry, K.R., Clarke, J.R., & Else, G.D. 1996. The foraging range of Adélie penguins at Béchervaise Island, Mac. Robertson Land, Antarctica as determined by satellite telemetry. *The penguins: Ecology and management*, 216-243.

Kooyman, G.L. 1993. Breeding habitats of emperor penguins in the western Ross Sea. *Antarctic Science,* 5(2).

Kooyman, G.L. 2002. Evolutionary and ecological aspects of some Antarctic and sub-Antarctic penguin distributions. *Oecologia,* 130(4), 485-495.

Kooyman, G.L., Hunke, E.C., Ackley, S.E., van Dam, R.P., & Robertson, G. 2000. Moult of the emperor penguin: travel, location, and habitat selection. *Marine Ecology Progress Series,* 204, 269-277.

Kooyman, G.L., & Ponganis, P.J. 2007. The initial journey of juvenile emperor penguins. *Aquatic Conservation-Marine and Freshwater Ecosystems,* 17.

Kooyman, G.L., Siniff, D.B., Stirling, I., & Bengtson, J.L. 2004. Moult habitat, pre- and post-moult diet and post-moult travel of Ross Sea emperor penguins. *Marine Ecology Progress Series,* 267, 281-290.

La Mesa, M., Eastman, J.T., & Vacchi, M. 2004. The role of notothenioid fish in the food web of the Ross Sea shelf waters: a review. *Polar Biology,* 27(6), 321-338.

Lake, S.E., Burton, H.R., & Hindell, M.A. 1997. Influence of time of day and month on Weddell seal haul-out patterns at the Vestfold Hills, Antarctica. *Polar Biology,* 18(5), 319-324.

Lauriano, G., Vacchi, M., Ainley, D., & Ballard, G. 2007. Observations of top predators foraging on fish in the pack ice of the southern Ross Sea. *Antarctic Science,* 19(4).

Nordøy, E., & Blix, A. 2009. Movements and dive behaviour of two leopard seals (Hydrurga leptonyx) off Queen Maud Land, Antarctica. *Polar Biology,* 32(2), 263-270.

Pitman, R.L., & Durban, J.W. 2010. Killer whale predation on penguins in Antarctica. *Polar biology,* 33(11), 1589-1594.

Pitman, R.L., & Ensor, P. 2003. Three forms of killer whales (Orcinus orca) in Antarctic waters. *Journal of Cetacean Research and Management,* 5(2), 131-139.

Prévost, J. 1961. Ecologie du manchot empereur. Paris: Hermann.

Prévost, J., & Sapin-Jaloustre, J. 1965. Ecologie des manchots antarctiques. *In Biogeography and ecology in Antarctica.* The Hague: Dr. W. Junk, 634.

R Development Core Team. 2010. R: A language and environment for statistical computing. *In* R Foundation for Statistical Computing, Vienna, Austria. .

Richards, S.A. 2008. Dealing with overdispersed count data in applied ecology. *Journal of Applied Ecology,* 45(1), 218-227.

Smith, O.P. 2007. Observer's guide to sea ice. *In* National Oceanic and Atmospheric Administration NOAA Ocean Service, 28pp.

Smith, T.G., Siniff, D.B., Reichle, R., & Stone, S. 1981. Coordinated behavior of killer whales, Orcinus orca, hunting a crabeater seal, Lobodon carcinophagus. *Canadian Journal of Zoology,* 59(6), 1185-1189.

Smith, W.O., Jr., Ainley, D.G., & Cattaneo-Vietti, R. 2007. Trophic interactions within the Ross Sea continental shelf ecosystem. *Royal Society Philosophical Transactions Biological Sciences,* 362(1477).

Southwell, C., Kerry, K., Ensor, P., Woehler, E.J., & Rogers, T. 2003. The timing of pupping by pack-ice seals in East Antarctica. *Polar Biology,* 26(10), 648-652.

Southwell, C., & Low, M. 2009. Black and white or shades of grey? Detectability of AdElie penguins during shipboard surveys in the Antarctic pack-ice. *Journal of Applied Ecology,* 46(1).

Spreen, G., Kaleschke, L. & Heygster, G. 2008. Sea ice remote sensing using AMSR-E 89 GHz channels. *Journal of Geophysical Research: Oceans (1978-2012),* 113-C2.

Symonds, M.R.E., & Moussalli, A. 2011. A brief guide to model selection, multimodel inference and model averaging in behavioural ecology using Akaike's information criterion. *Behavioral Ecology and Sociobiology,* 65(1), 13-21.

Taylor, R.H., Wilson, P.R., & Thomas, B.W. 1990. Status and trends of Adélie penguin populations in the Ross Sea region. *Polar Record,* 26(159), 293-304.

Testa, J.W. 1994. Over-winter movements and diving behavior of female Weddell seals (*Leptonychotes weddellii*) in the southwestern Ross Sea, Antarctica. *Canadian Journal of Zoology-Revue Canadienne De Zoologie,* 72(10), 1700-1710.

Testa, J.W., & Siniff, D.B. 1987. Population-dynamics of Weddell seals (*Leptonychotes weddellii*) in McMurdo Sound, Antarctica. *Ecological Monographs,* 57(2), 149-165.

Thiele, D., Chester, E.T., Moore, S.E., Širovic, A., Hildebrand, J.A., & Friedlaender, A.S. 2004. Seasonal variability in whale encounters in the Western Antarctic Peninsula. *Deep Sea Research part II: topical studies in Oceanography,* 51(17), 2311-2325.

van Dam, R.P., & Kooyman, G.L. 2003. Latitudinal distribution of penguins, seals and whales observed during a late autumn transect through the Ross Sea. *Antarctic Science,* 16(3).

Visser, I.N., Smith, T.G., Bullock, I.D., Green, G.D., Carlsson, O.G., & Imberti, S. 2008. Antarctic peninsula killer whales (Orcinus orca) hunt seals and a penguin on floating ice. *Marine Mammal Science,* 24(1), 225-234.

Wilson, P.R., Ainley, D.G., Nur, N., Jacobs, S.S., Barton, K.J., Ballard, G., & Comiso, J.C. 2001. Adelie penguin population change in the pacific sector of Antarctica: relation to sea-ice extent and the Antarctic Circumpolar Current. *Marine Ecology Progress Series,* 213.

Wilson, R.P., Puetz, K., Bost, C.A., Culik, B.M., Bannasch, R., Reins, T., & Adelung, D. 1993. Diel dive depth in penguins in relation to diel vertical migrtion of prey - whose dinner by candlelight. *Marine Ecology Progress Series,* 94(1), 101-104.

Table 5.1: Results of megafauna surveys for the western Ross Sea (WRS), transit (TR), eastern Ross Sea (ERS) and east of shelf (ES) sections, as well as for the entire survey. Section lengths (kilometers of on-effort surveys) are given in parenthesis. Number of animals (*n*) and density (animals/km along the transect line, ± standard error) are given for the following species: Adélie penguin (ade), emperor penguin (emp), killer whale (kil), minke whale (min), leopard seal (leo), crabeater seal (cra), Weddell seal (wed), south polar skua (sku), Antarctic petrel (ape), snow petrel (spe), unknown cetacean (uce), unknown penguin (upe), unknown seabird (usb), unknown seal (use)

	Entire survey (3427 km)		WRS (1873 km)		TR (613 km)		ERS (519 km)		ES (422 km)	
Species	*n*	animals/km (±SE)	*n*	animals/km (±SE)	*n*	animals/km (±SE)	*n*	animals/km (±SE)	*n*	animals/km (±SE)
ade	5332	1.7±.34	575	.34±.06	30	.05±.01	279	.53±.29	4448	10.8±2.13
emp	1315	.41±.08	90	.05±.02	196	.33±.17	896	1.7±.39	133	.32±.09
kil	62	.02±.01	43	.02±.01	13	.022±.02	6	.01±.01	0	-
min	64	.02±.004	14	.008±.003	5	.008±.004	19	.03±.01	26	.06±.02
leo	2	$6X10^{-4}$±$4X10^{-4}$	0	-	1	.002±.002	1	.002±.002	0	-
cra	129	.04±.01	23	.01±.004	2	.003±.002	56	.1±.03	48	.1±.08
wed	230	.07±.01	88	.05±.01	68	.11±.03	74	.14±.04	0	-
sku	116	.04±.005	85	.05±.007	26	.04±.01	3	.006±.004	0	-
ape	186	.06±.01	0	-	104	.18±.17	67	.13±.04	15	.04±.02
spe	310	.1±.02	227	.13±.03	4	.007±.004	53	.1±.03	26	.06±.03
uce	14	.004±.002	7	.004±.001	7	.012±.009	0	-	0	-
upe	36	.01±.004	12	.007±.003	4	.007±.005	10	.02±.02	10	.02±.01
usb	2	$6X10^{-4}$±$4X10^{-4}$	2	.001±$8X10^{-4}$	0	-	0	-	0	-
use	164	.05±.01	37	.02±.007	56	.09±.04	68	.13±.03	3	.007±.004

Table 5.2: Most parsimonious quasi-poisson GLM models for emperor (emp) and Adélie penguin (ade) density, in the western Ross Sea (WRS), transit (TR), eastern Ross Sea (ERS) and east of shelf (ES) sections. ΔQAIC=difference between QAIC of best and QAIC of next best model. All models with similar explanatory power (ΔQAIC≤2) are given; otherwise, the next best model (ΔQAIC>2) is noted as a means of comparison. Explanatory variable names are: *lat*=latitude, *long*=longitude, *icecov*=percent ice cover, *icetyp*=ice type, *chla*=chlorophyll-a concentration. DF=degrees of freedom, ϕ= dispersion parameter.

emperor penguins

Section	GLM model	DF	ϕ	ΔQAIC
WRS	**emp**~ *icecov*	166	14.55	0
	emp~ *lat* + *icecov* + *icetyp*	164	13.86	2.1
TR	**emp**~ *long*	44	3.13	0
	emp~ *lat* + *long* + *icetyp*	42	3.19	5.4
ERS	**emp**~ *lat* + *icecov* + *icetyp* + *chla*	47	47.74	0
	emp~ *icecov* + *icetyp*	47	37.8	3.9
ES	**emp**~ *lat* + *icecov* + *icetyp* + *chla*	17	8.71	0
	emp~ *lat* + *icecov* + *icetyp*	17	8.88	2.46

Adélie penguins

Section	GLM model	DF	ϕ	ΔQAIC
WRS	**ade**~ *long* + *icecov* + *chla*	167	30.25	0
	ade~ *lat* + *icetyp* + *icecov* + *chla*	167	26.72	5.1
TR	**ade**~ *icecov* + *icetyp*	58	3.23	0
	ade~ *icetyp*	58	3.28	2
ERS	**ade**~ *lat* + *long* + *icetyp* + *icecov* + *chla*	51	30.09	0
	ade~ *lat*+ *long* + *icetyp* + *icecov*	51	8.59	2.9
ES	**ade**~ *lat*+ *long* + *icetyp* + *icecov* + *chla*	21	65.38	0
	ade~ *lat* + *long* + *icetyp* + *icecov*	21	74.00	0.4

Table 5.3: Most parsimonious quasi-poisson GLM models for South Polar skua (sku), snow petrel (spe) and Antarctic petrel (ape) density, in the western Ross Sea (WRS), transit (TR), eastern Ross Sea (ERS) and east of shelf (ES) sections. ΔQAIC=ΔQAIC between best and next to best model. All models with similar explanatory power (ΔQAIC≤2) are given; otherwise, the next best model (ΔQAIC>2) is noted as a means of comparison. Explanatory variable names are: *lat*=latitude, *long*=longitude, *icecov*=percent ice cover, *icetyp*=ice type, *chla*=chlorophyll-a concentration. DF=degrees of freedom, ϕ= dispersion parameter.

South polar skuas

Section*	GLM model	DF	ϕ	ΔQAIC
WRS	**sku**~ *icecov* + *icetyp*	167	5.53	0
	sku~ *lat* + *long* + *icetyp*	167	4.42	1.28
TR	**sku**~ *icecov* + *icetyp*	58	2.14	0
	sku~ *icetyp* + *chla*	58	2.34	0.88

Antarctic petrels

Section***	GLM model	DF	ϕ	ΔQAIC
TR	**ape**~ *icetyp* + *chla*	58	81.54	0
	ape~ *icetyp*	58	61.24	7.46
ERS	**ape**~ *chla*	51	11.22	0
	ape~ *icetyp*+ *chla*	51	10.05	0.36
ES	**ape**~ *icetyp*+ *chla*	21	10.81	0
	ape~ *icecov*	21	6.55	6.39

snow petrels

Section**	GLM model	DF	ϕ	ΔQAIC
WRS	**spe**~ *icecov* + *icetyp*	167	25.42	0
	spe~ *icecov*	167	21.62	10.39
ERS	**spe**~ *lat* + *long* + *icecov*	51	5.21	0
	spe~ *long* + *icecov*	51	5.14	3.51
ES	**spe**~ *lat* + *long* + *icetyp*	21	6.37	0
	spe~ *lat* + *long* + *chla*	21	5.98	0.74

*sample size too small in ERS, no sightings in ES
**sample size too small in TR
***no sightings in West RS section

Table 5.4: Most parsimonious quasi-poisson GLM models for crabeater (cra) and Weddell (wed) seal density, in the western Ross Sea (WRS), transit (TR), easte Ross Sea (ERS) and east of shelf (ES) sections. ΔQAIC=difference between QAIC of best and QAIC of next best model. All models with similar explanatory power (ΔQAIC≤2) are given; otherwise, the next best model (ΔQAIC>2) is noted as a means of comparison. Explanatory variable names are: *lat*=latitude, *long*=longitude, *icecov*=percent ice cover, *icetyp*=ice type, *chla*=chlorophyll-a concentration. DF=degrees of freedom, ϕ= dispersion parameter.

crabeater seals

Section*	GLM model	DF	ϕ	ΔQAIC
WRS	**cra**~ *lat*+ *long* + *icetyp*	167	2.52	0
	cra~ *lat* + *long* + *chla*	167	2.37	7
ERS	**cra**~ *lat* + *icecov* + *icetyp*	51	5.47	0
	cra~ *icetyp*	51	7.20	2.9
ES	**cra**~ *icecov* + *icetyp*	21	3317	0
	cra~ *lat* + *icecov* + *icetyp* + *chla*	21	37.53	1.55

Weddell seals

Section**	GLM model	DF	ϕ	ΔQAIC
WRS	**wed**~ *lat* + *chla*	286	6.67	0
	wed~ *lat* + *long* + *chla*	286	5.99	4.01
TR	**wed**~ *lat* + *long* + *icecov* + *icetyp*	58	99.8	0
	wed~ *long* + *icecov* + *icetyp*	58	6.70	38.17
ERS	**wed**~ *long* + *icecov* + *icetyp*	51	5.51	0
	wed~ *icetyp* + *chla*	51	6.59	3.59

*no sightings in TR
**no sightings in ES

Figure 5.1: Part A: Advanced Microwave Scanning Radiometer (AMSR 2) satellite image of sea ice concentration taken on 02/14/2013 (Spreen *et al*. 2008), when surveys were carried out in the western Ross Sea (WRS) section, delimited by the white frame. This period corresponds to the minimum ice extent in the Ross Sea. The stable pack ice in the eastern Ross Sea remains well developed. Part B: AMSR 2 sea ice image taken one month later (03/14/2013), when surveys were carried out in the transit (TR), eastern Ross Sea (ERS) and east of shelf (ES) sections. Note the rapid expansion of sea ice, marking the onset of winter. The "on-effort" survey lines are given along with the ship's track. Abbreviations: TNB=Terra Nova Bay, CW=Cape Washington, CI=Coulman Island, DIT=Drygalski Ice Tongue, DP=Drygalski polynya, CC=Cape Colbeck, BoW=Bay of Whales.

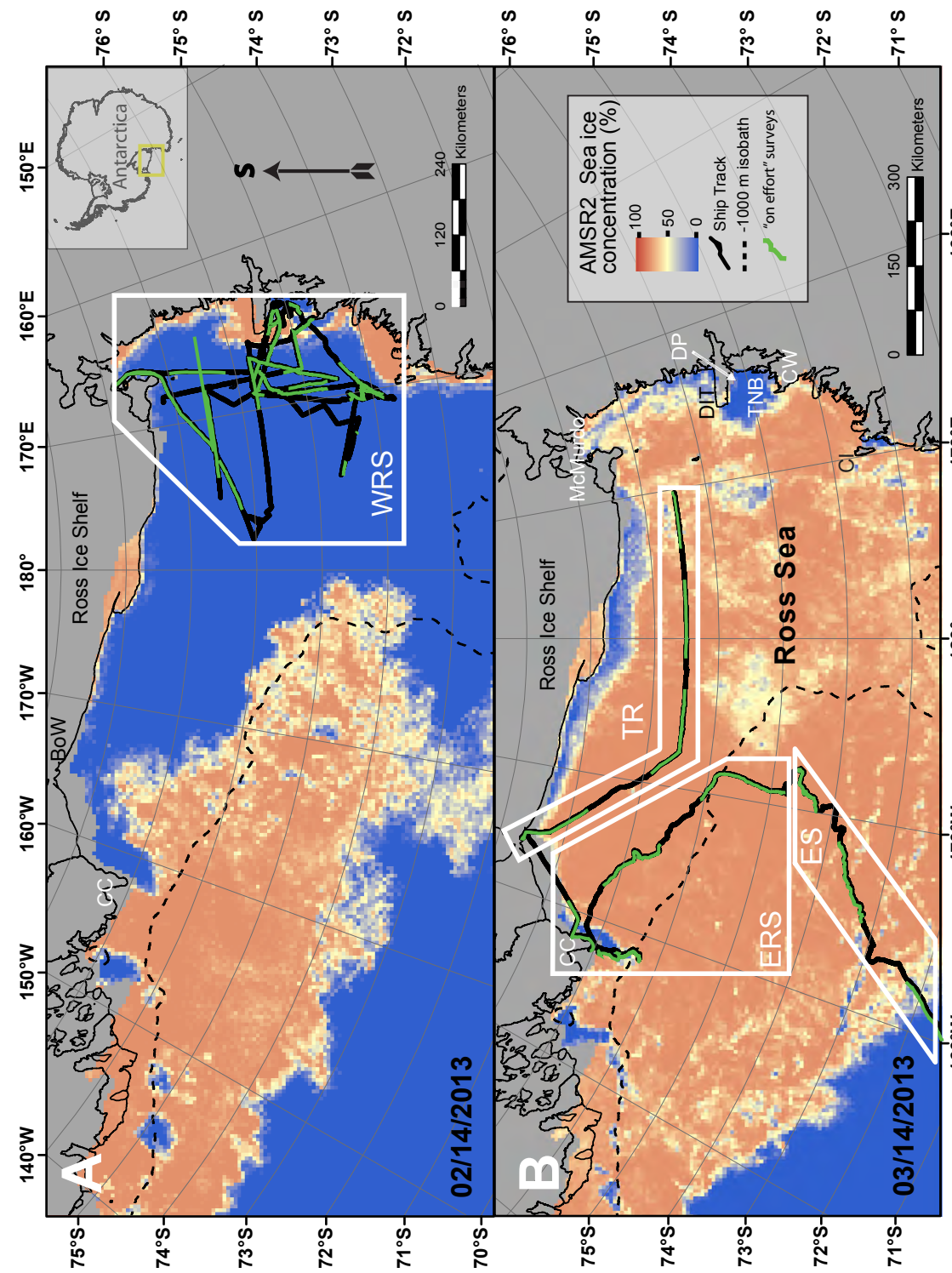
A
B
02/14/2013
03/14/2013
Ross Ice Shelf
Ross Sea
BoW
CC
WRS
TR
ERS
ES
DP
DIT
TNB
CW
CI
McMurdo
Antarctica
AMSR2 Sea ice concentration (%)
100
50
0
Ship Track
-1000 m isobath
"on effort" surveys
Kilometers
0
120
240
150
300
140°W
150°W
160°W
170°W
180°
170°E
160°E
150°E
76° S
75° S
74° S
73° S
72° S
71° S
70°S
75°S
74°S
73°S
72°S
71°S

Figure 5.2: Chlorophyll-a (Chl-a) concentration ($mg.m^{-3}$) measured on the on-effort survey lines by the ship's flow-trough fluorometer. A clear increase in Chl-a was measured above the continental shelf break, indicated by the -1000 m isobath, at the end of the ERS section. The ES section, maintained these higher values up to approximately 72°S, possibly the end of the Antarctic Slope Front. The high Chl-a concentrations measured in the WRS section are caused by phytoplankton blooms in Terra Nova Bay and the Drygalski polynya.

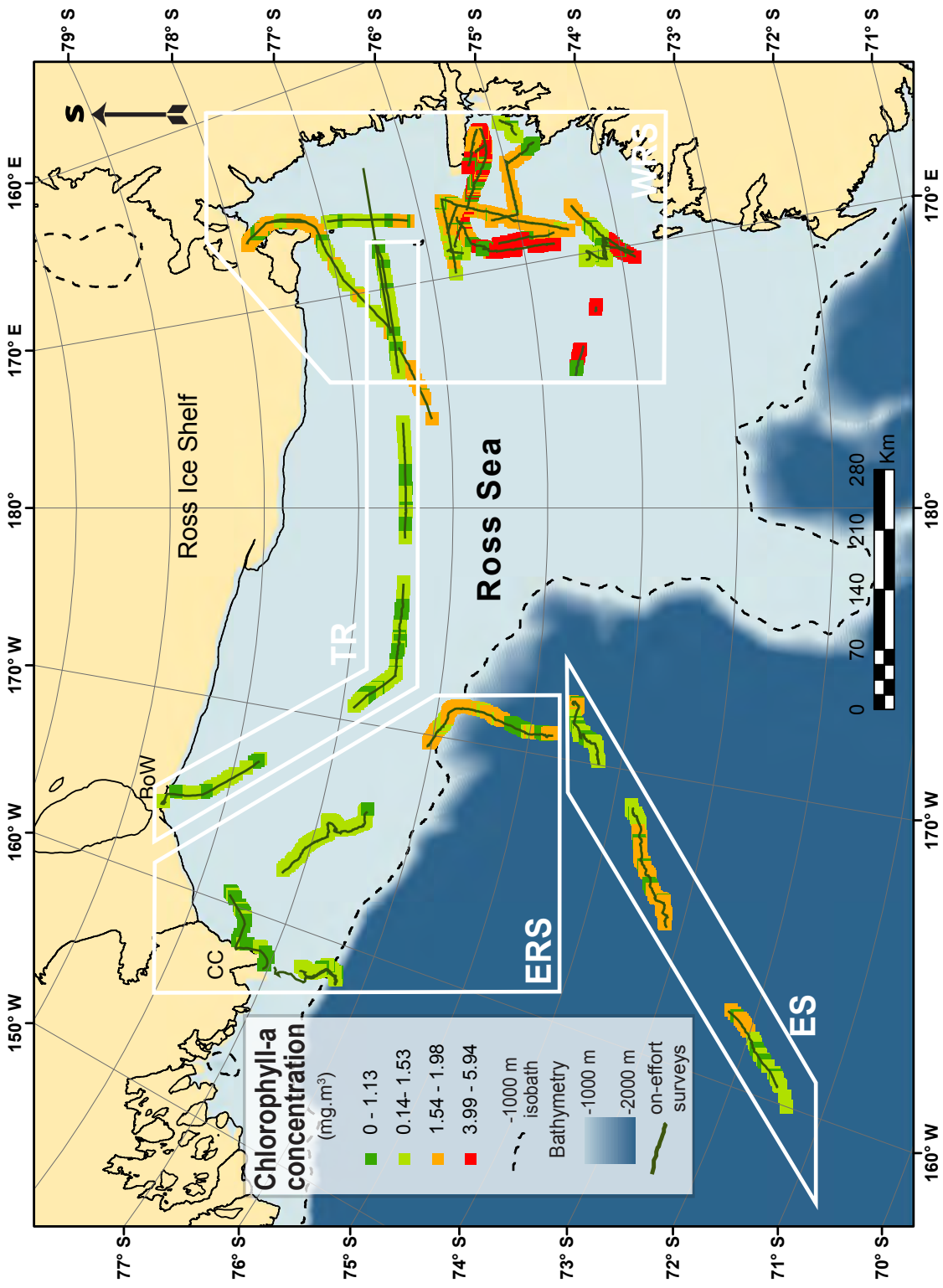
Ross Ice Shelf
Ross Sea
RoW
CC
TR
ERS
ES
WRS
Chlorophyll-a concentration (mg.m³)
0 - 1.13
0.14- 1.53
1.54 - 1.98
3.99 - 5.94
-1000 m isobath
Bathymetry
-1000 m
-2000 m
on-effort surveys
0 70 140 210 280 Km
S
79° S
78° S
77° S
76° S
75° S
74° S
73° S
72° S
71° S
70° S
160° E
170° E
180°
170° W
160° W
150° W

Figure 5.3: Density, expressed as the number of animals per kilometer along the transect line, of: A) emperor (emp) and Adélie (ade) penguins; B) South Polar skua (sku), snow petrel (spe) and Antarctic petrel (ape); C) killer (kil) and minke (min) whales; and D) crabeater (cra) and Weddell (wed) seals, for the western Ross Sea (WRS), transit (TR), eastern Ross Sea (ERS) and east of shelf (ES) sections. Error bars are ± SE.

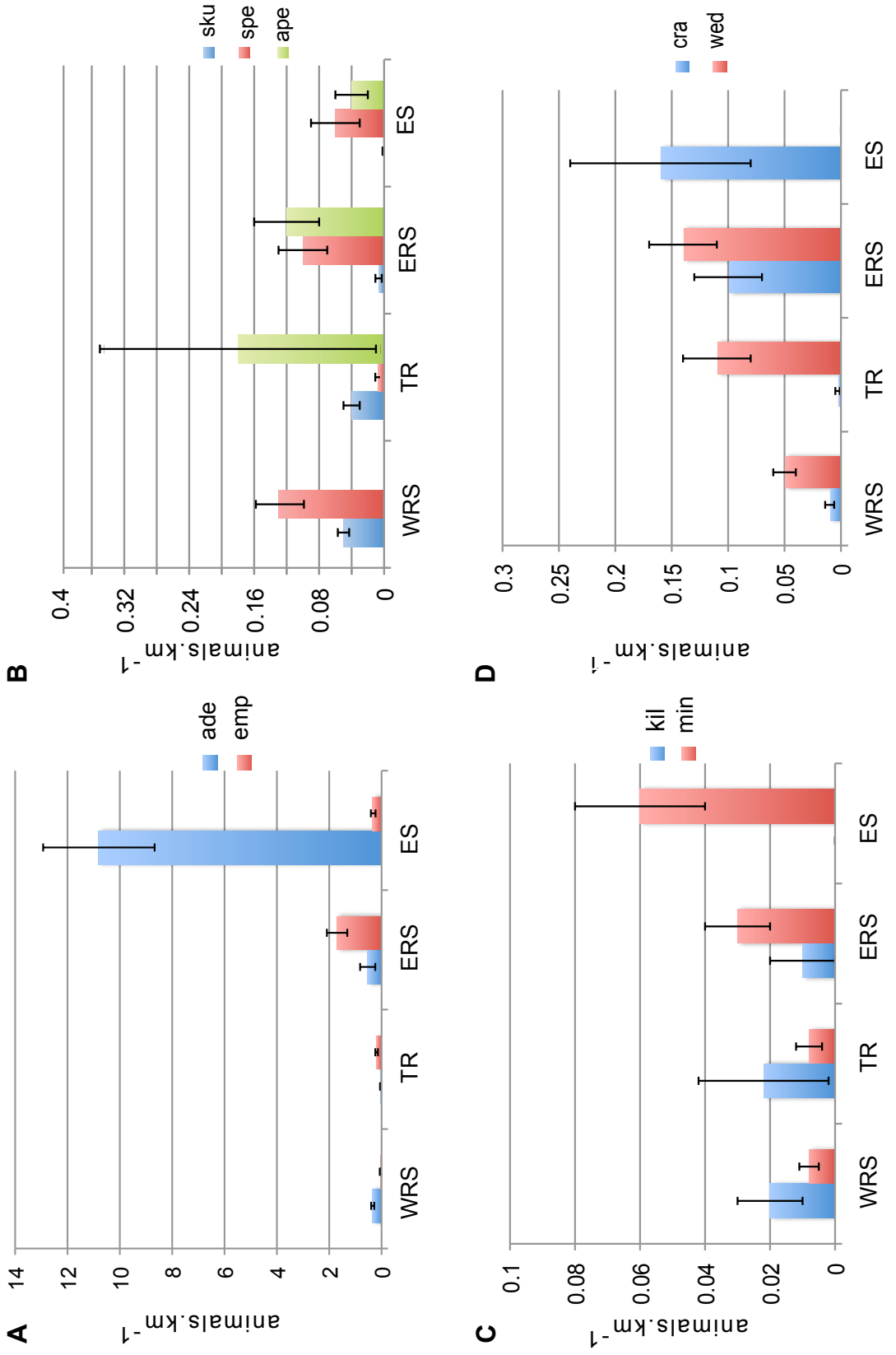
A
animals.km-1
14
12
10
8
6
4
2
0
ade
emp
WRS
TR
ERS
ES
B
animals.km-1
0.4
0.32
0.24
0.16
0.08
0
sku
spe
ape
WRS
TR
ERS
ES
C
animals.km-1
0.1
0.08
0.06
0.04
0.02
0
kil
min
WRS
TR
ERS
ES
D
animals.km-1
0.3
0.25
0.2
0.15
0.1
0.05
0
cra
wed
WRS
TR
ERS
ES

Figure 5.4: On-effort sightings of penguins in the four survey sections. Part A: the highest abundance of emperor penguins was in the ERS section, above the continental shelf break (-1000 m isobath) and beyond, in the Antarctic Slope Front. Ross Sea breeding colonies are indicated: Cape Colbeck, Cape Crozier, Beaufort Island (BI), Franklin Island (FI), Cape Washington (CW) and Coulman Island (CI). The seventh, Cape Roget, is shown in part b. Part B: Sightings of Adélie penguins in the ES section outnumbered that of all other animals by one order of magnitude. Main Adélie penguin breeding colonies (50,000-200,000 breeding pairs) as shown by Taylor *et al*. (1990), are indicated: CH=Cape Hallett, PI=Possession Isl.; CA=Cape Adare, FI=Franklin Isl. BI=Beaufort Isl. CC=Cape Crozier. Cape Roget (CR) is an emperor penguin colony.

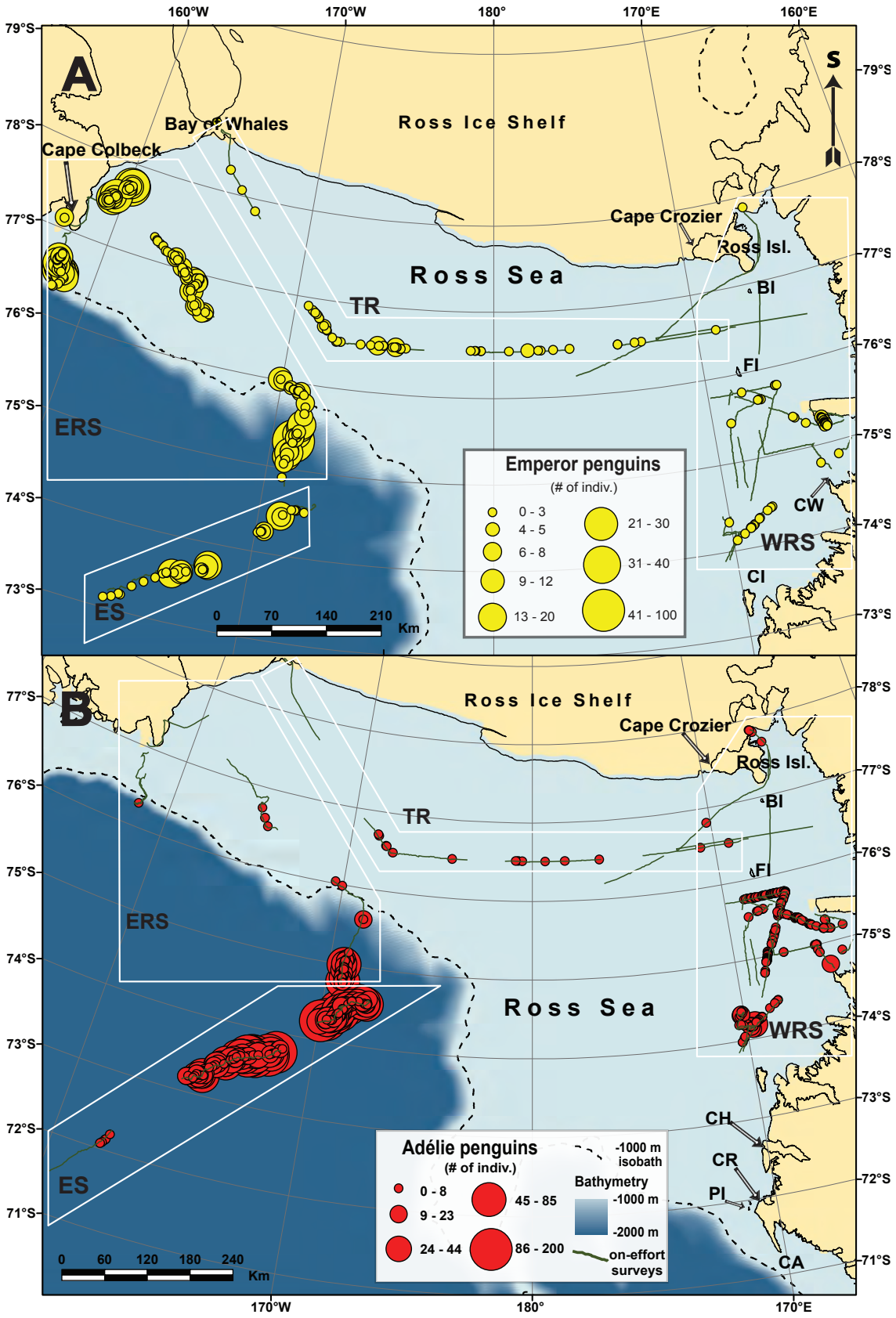
A
B
Ross Ice Shelf
Bay of Whales
Cape Colbeck
Ross Sea
Cape Crozier
Ross Isl.
BI
FI
TR
ERS
ES
CW
WRS
CI
CH
CR
PI
CA
S
160°W
170°W
180°
170°E
160°E
79°S
78°S
77°S
76°S
75°S
74°S
73°S
72°S
71°S
Emperor penguins
(# of indiv.)
0 - 3
4 - 5
6 - 8
9 - 12
13 - 20
21 - 30
31 - 40
41 - 100
0 70 140 210 Km
Adélie penguins
(# of indiv.)
0 - 8
9 - 23
24 - 44
45 - 85
86 - 200
-1000 m isobath
Bathymetry
-1000 m
-2000 m
on-effort surveys
0 60 120 180 240 Km

Figure 5.5: On-effort sightings of volant sea birds in the four survey sections. Abbreviations are: sku=South Polar skua, ape=Antarctic petrel, spe=snow petrel. Snow petrels were seen in all sections, while skuas were absent in the ES section. Antarctic petrels were seen everywhere except in the WRS section.

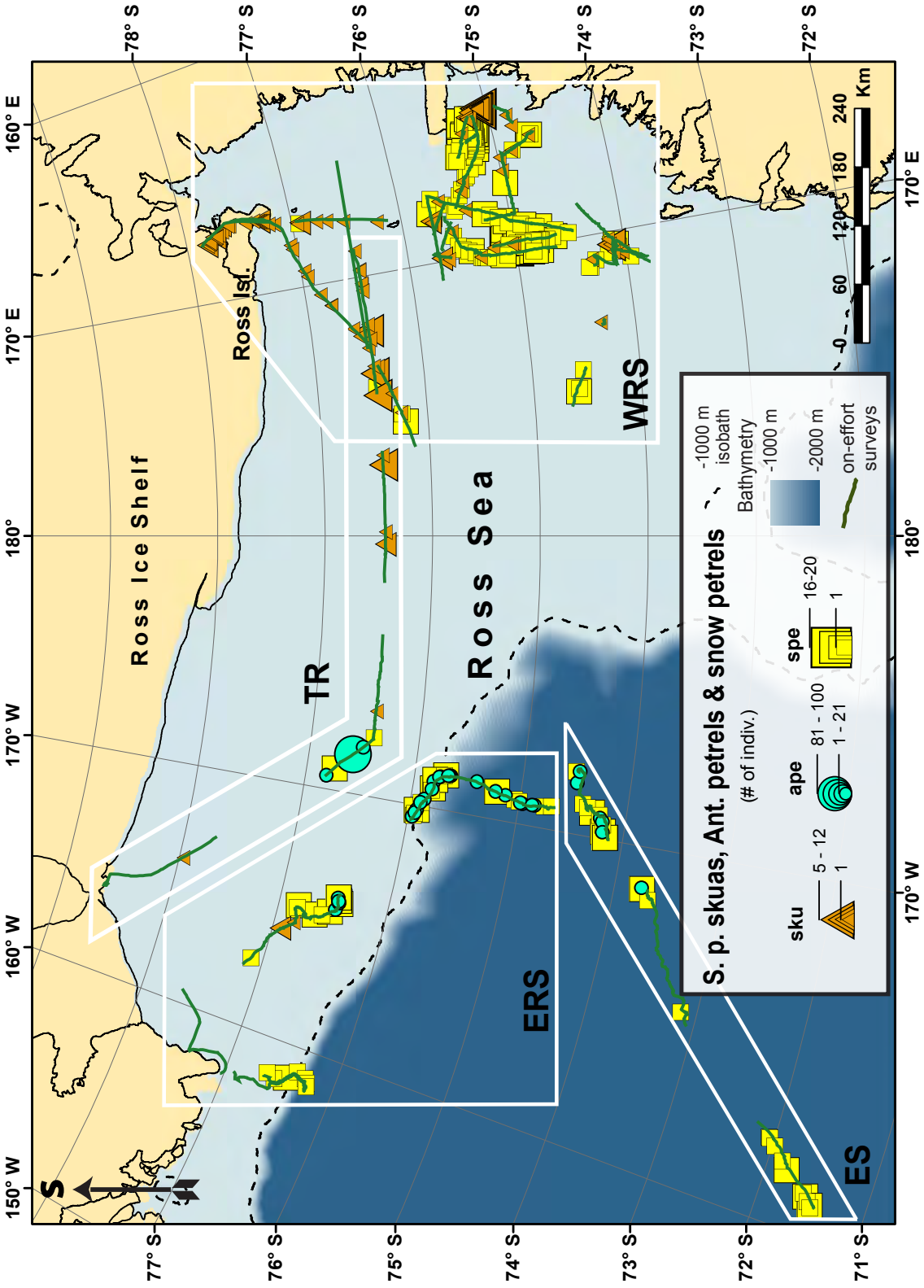
Ross Ice Shelf
Ross Isl.
Ross Sea
TR
WRS
ERS
ES
S. p. skuas, Ant. petrels & snow petrels
(# of indiv.)
sku
5 - 12
1
ape
81 - 100
1 - 21
spe
16-20
1
-1000 m isobath
Bathymetry
-1000 m
-2000 m
on-effort surveys
0
60
120
180
240
Km
78° S
77° S
76° S
75° S
74° S
73° S
72° S
71° S
150° W
160° W
170° W
180°
170° E
160° E

Figure 5.6: Part A: On-effort sightings of minke and killer whales in the four survey sections. Killer whales were most abundant in the WRS and were not observed in the ES section, while minke whales were more abundant in the ES section.
Part B: On-effort sightings of seals in the four survey sections. Note the absence of Weddell seal sightings in the ES section. Crabeater seals were seen in all sections but were most abundant at the end of the ERS and in the ES sections, possibly due to higher concentrations of krill near the Antarctic Slope Front. Abbreviations are: wed=Weddell seal, cra=crabeater seal, leo=leopard seal.

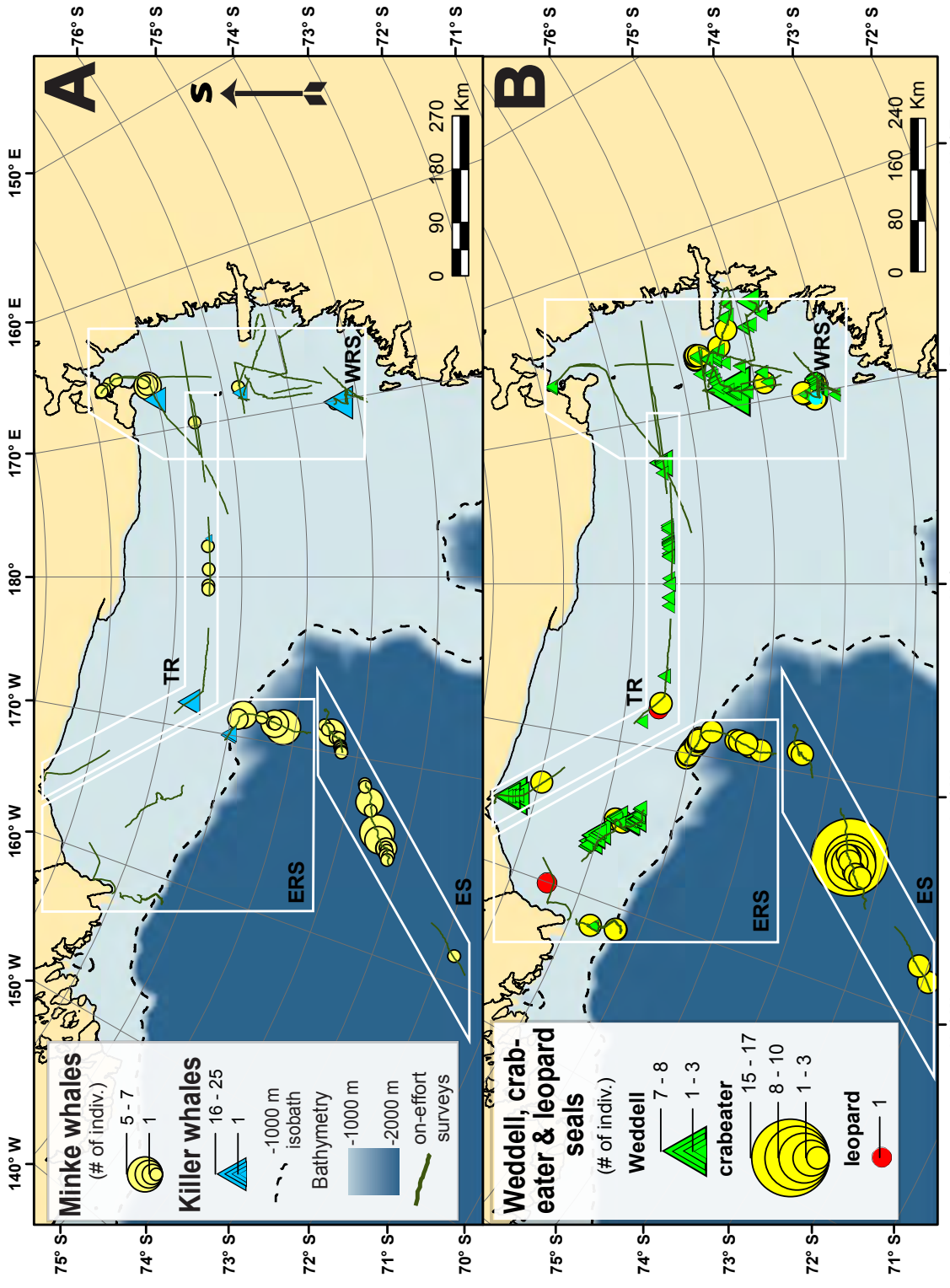
A
B
N
0 90 180 270 Km
0 80 160 240 Km
TR
WRS
ERS
ES
Minke whales
(# of indiv.)
5 - 7
1
Killer whales
16 - 25
1
-1000 m isobath
Bathymetry
-1000 m
-2000 m
on-effort surveys
Weddell, crab-eater & leopard seals
(# of indiv.)
Weddell
7 - 8
1 - 3
crabeater
15 - 17
8 - 10
1 - 3
leopard
1
140° W
150° W
160° W
170° W
180°
170° E
160° E
150° E
76° S
75° S
74° S
73° S
72° S
71° S
70° S